

AD-A257 718



DTIC  
ELECTE  
DEC 2 1992  
S C D

ABSTRACTS OF PAPERS  
PRESENTED AT THE  
FORTY-SIXTH ANNUAL  
MEETING OF THE SOCIETY  
OF GENERAL PHYSIOLOGISTS

Marine Biological Laboratory  
Woods Hole, Massachusetts  
10-13 September 1992

DISTRIBUTION STATEMENT A  
Approved for public release  
Distribution Unlimited

82 11 16 015

92-29577



8098

ABSTRACTS OF PAPERS  
PRESENTED AT THE  
FORTY-SIXTH ANNUAL  
MEETING OF THE SOCIETY  
OF GENERAL PHYSIOLOGISTS

Marine Biological Laboratory  
Woods Hole, Massachusetts  
10-13 September 1992

Accession For	
NTIS	<input checked="" type="checkbox"/>
DTIC	<input type="checkbox"/>
Unannounced	<input type="checkbox"/>
Justification	
By	
Distribution/	
Availability Codes	
Dist	Avail and/or Special
A-1	

DTIC QUALITY INSPECTED 2

## KEYNOTE ADDRESS

1. The Lactose Permease of *Escherichia coli*: A Paradigm for Membrane Transport Proteins H. R. KABACK, *Howard Hughes Medical Institute, Departments of Physiology and Microbiology & Molecular Genetics, Molecular Biology Institute, University of California Los Angeles, Los Angeles, California*

$\beta$ -Galactoside accumulation against a concentration gradient in *Escherichia coli* is dependent on the lactose (lac) permease, a hydrophobic, polytopic cytoplasmic membrane protein that catalyzes the coupled translocation of  $\beta$ -galactosides and  $H^+$  with a stoichiometry of unity. Encoded by the *lacY* gene, the permease has been solubilized from the membrane, purified to homogeneity, and reconstituted into phospholipid vesicles in a fully functional state. Based on circular dichroic measurements demonstrating that purified permease is  $\sim 80\%$  helical and hydropathy analysis of the deduced amino-acid sequence, a secondary structure was proposed in which the protein is predicted to have 12 hydrophobic domains in  $\alpha$ -helical conformation which traverse the membrane in zig-zag fashion connected by hydrophilic loops. Evidence confirming the general features of the model and demonstrating that the  $NH_2$  and  $COOH$  termini are on the cytoplasmic surface of the membrane has been obtained from other spectroscopic techniques, chemical modification, limited proteolysis, and immunological studies. Moreover, studies on an extensive series of lac permease-alkaline phosphatase fusion proteins provide strong exclusive support for the topological predictions of the 12-helix model (Calamia and Manoil, 1990. *Proc. Natl. Acad. Sci. USA.* 87:4937). More than 200 site-directed amino acid replacements have been made in lac permease, and  $>90\%$  of the mutants retain significant activity. On the other hand, Arg302 (putative helix IX) and Lys319, His322, and Glu325 (putative helix X) are critically involved in active lac transport and/or substrate binding and recognition. The properties of some of the mutants and molecular modeling studies, which suggest that the four residues may be sufficiently close to form an H-bond network, have led to the suggestion that a type of  $H^+$  relay may be involved in the mechanism. However, if  $H^+$ - and  $Na^+$ -coupled transport occurs by similar mechanisms, it is unlikely that a  $H^+$  relay is directly involved. In addition, experiments on the insertion of lac permease into the membrane, its stability and topology, and the ability of certain deletion mutations to complement functionally will be discussed.

## INVITED PAPERS

2. Dimerization of Glycophorin A Transmembrane Helices: Mutagenesis and Modeling D. M. ENGELMAN,\* B. D. ADAIR,\* A. BRÜNGER,\* J. M. FLANAGAN,\* M. A. LEMMON,\* H. TREUTLEIN,\* and J. ZHANG,\* *Department of Molecular Biophysics and Biochemistry, Yale University, New Haven, Connecticut*

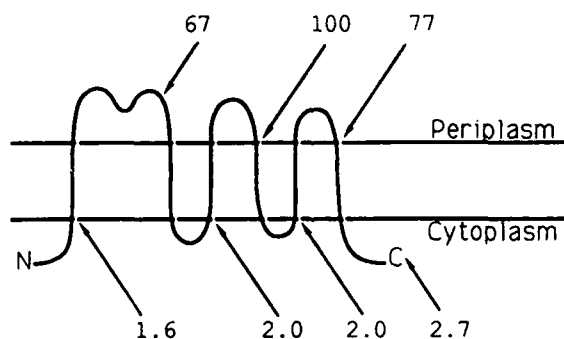
The human erythrocyte sialoglycoprotein, glycophorin A (GpA), forms dimers that are stable under the conditions of SDS-PAGE, and the interactions of its single transmembrane domain drive the association. We have studied the properties of the GpA transmembrane domain by genetically fusing it to the carboxy terminus of staphylococcal nuclease (Lemmon et al. 1992. *J. Biol. Chem.* 267:7683).

Asterisks indicate authors who are not members of the Society of General Physiologists.

The resulting chimera forms a dimer in SDS, which is disrupted upon addition of a peptide corresponding to the transmembrane domain of GpA, but not by addition of transmembrane domains from the EGF receptor, *neu* oncogene, or bacteriorhodopsin. Deletion mutagenesis has been used to define the boundaries of the transmembrane domain responsible for dimerization, and site-specific mutagenesis has been used to explore the properties of the interactions in the dimer. More than 300 mutants in the 23 amino acid transmembrane domain have been analyzed, and several striking features are apparent. First, the interaction is highly specific: relatively conservative changes (e.g., V-L or L-A) have marked effects on the dimerization reaction. Second, there is a periodicity in the mutant effects, suggesting a number of points of interaction between the helices, as would be the case in a coiled-coil. To understand the mutants, we have undertaken molecular modeling experiments using molecular dynamics simulations and global searches of helix-helix interactions. These efforts have been productive, and suggest that the interaction can be well predicted as a right-handed supercoil with a closely packed dimeric interface. The agreement of our experimental data with independent, *a priori* computational modeling is highly encouraging. It suggests that it may be possible to understand the folding of membrane proteins in chemical terms and to predict structures on the basis of amino acid sequence information alone. [Supported by grants from the NIH, NSF, and National Foundation for Cancer Research.]

3. Analysis of Membrane Protein Topology by Gene Fusion DANA BOYD,\* BETH TRAXLER,\* GEORG JANDER,\* CATHY LEE,\* and JON BECKWITH.\* *Department of Microbiology and Molecular Genetics, Harvard Medical School, Boston, Massachusetts*

Fusions of *Escherichia coli* alkaline phosphatase (AP) allow the determination of the topology of bacterial cytoplasmic membrane proteins. Fusions to periplasmic (external) domains of a membrane protein give high AP enzymatic activity, while fusions to cytoplasmic domains give low activity. The figure below shows an AP fusion-based topological analysis of the MalG protein, a membrane component of the *E. coli* maltose transport system (Boyd, D., B. Traxler, and J. Beckwith, manuscript in preparation).



In AP fusions, the carboxy-terminal regions of a membrane protein are replaced with AP. If carboxy-terminal sequences affect the topological assembly of upstream regions, then the absence of these sequences could lead to false conclusions. This eventuality has been observed. Some AP fusions to cytoplasmic domains of membrane proteins exhibited quite high activity, due to translocation of AP across the cytoplasmic membrane. We have shown that basic amino acids in the cytoplasmic domains are essential topological signals for the retention of those domains in the cytoplasm (Boyd and Beckwith, 1989, *Proc. Natl. Acad. Sci. USA*, 86:9446). Fusions missing these signals do not efficiently retain AP in the cytoplasm. We also showed that the AP moiety in different fusions is translocated at different rates (Traxler et al. 1992, *J. Biol. Chem.* 267:5339). The anomalous fusions to cytoplasmic domains described above exhibited a far slower transfer of AP across the membrane than fusions to periplasmic domains. However, one fusion to a periplasmic domain of MalF also exhibited slow

kinetics of export. In this fusion, AP follows a hydrophobic export signal that appears weaker than other such signals in the protein since it contains one basic amino acid. We have developed a direct gene fusion test for the kinetics of export of hydrophilic domains of a membrane protein (Jander, G., and J. Beckwith, unpublished results). It involves the use of a fragment of the gene for the biotinylatable enzyme, acetylCoA carboxylase. This cytoplasmic protein and the fragment are normally biotinylated, but when the fragment is fused to an efficiently exported protein, it escapes modification. We have fused this fragment to different positions in the MalF protein. Fusions of the fragment to certain periplasmic domains do not yield biotinylated protein, but fusions to cytoplasmic domains, even those that precede the basic amino acids, are heavily biotinylated. Thus, this type of fusion can provide a sensitive measure of the kinetics of export of different domains of a membrane protein.

4. The High-Resolution 3-D Structure of a Membrane Protein JOHANN DEISENHOFER,\* *Howard Hughes Medical Institute and Department of Biochemistry, University of Texas Southwestern Medical Center, Dallas, Texas*

The photosynthetic reaction center (RC) from the purple bacterium *Rhodospseudomonas viridis* was the first integral membrane protein whose 3-D structure was determined to atomic resolution. It catalyzes the primary reaction in photosynthesis (light-driven charge separation across the bacterial inner membrane from a pair of bacteriochlorophylls to quinone acceptors) and consists of four different protein subunits and 14 cofactors with a total molecular weight of ~140,000. The structure analysis was done with the methods of x-ray crystallography (Deisenhofer and Michel, 1989. *EMBO J. [Eur. Mol. Biol. Organ.]* 8:2149, and references therein). The RC complex has an elongated shape with a longest dimension of 130 Å. Its central part is formed by the subunits L and M, which are arranged with an approximate twofold symmetry with the symmetry axis perpendicular to the membrane plane. Each of these subunits has five transmembrane helices. On either side of the membrane-spanning region a peripheral subunit is attached to the L-M complex: the cytochrome on the periplasmic side, and the H subunit on the cytoplasmic side. The H subunit has a single transmembrane helix near its NH<sub>2</sub> terminus. The membrane-spanning region of the RC complex can be easily recognized by unusual structural features: The molecular surface in the central region of the model contains an extremely hydrophobic zone of 30 Å thickness with sharp boundaries to the peripheral parts of the complex. In the crystal this hydrophobic surface is covered by detergent (Roth et al. 1989. *Nature [Lond.]* 340:659). Also, the membrane-spanning region of the RC is completely free of charged residues, and includes only a few tightly bound water molecules. In contrast, the distribution of charged and polar residues and of bound water molecules in the peripheral parts of the RC resembles that found in water-soluble proteins.

5. Membrane Insertion by Proteins Lacking Typical Hydrophobic Sequences: Linkage of Partial Unfolding to Hydrophobic Behavior ERWIN LONDON,\* *Department of Biochemistry and Cell Biology, State University of New York at Stony Brook, Stony Brook, New York*

Several A-B type protein toxins can cross membranes even though they contain few or no obviously hydrophobic sequences. Diphtheria toxin membrane insertion and translocation into the cytoplasm is triggered in vivo by its exposure to the low pH within the lumen of endocytic vesicles. We have found that low pH triggers the switch of both the B and relatively hydrophilic A domains of the toxin from a soluble to a membrane-inserting form by inducing partial unfolding. Upon exposure to neutral pH and reduction of the A-B disulfide link, the catalytic A domain is released from the membrane and refolds. Linkage of unfolding to hydrophobic behavior and membrane insertion also occurs in *Pseudomonas* exotoxin A. It appears that a cycle of unfolding and refolding plays a central role in the translocation of these toxins across membranes. This behavior may not be restricted to protein toxins. SecA plays a critical role in the translocation of proteins across membranes in *Escherichia coli*. In collaboration with the laboratory of D. B. Oliver (Wesleyan University), we have found that SecA has an ability to insert into membrane bilayers that is closely linked to its partial unfolding. It is not clear

whether these proteins form transmembrane  $\alpha$ -helices or  $\beta$ -sheets, as found in other membrane proteins, or some other structure. Their properties under membrane-inserting conditions are similar to those of proteins in the partially unfolded molten globule conformation. It is possible that partial unfolding exposes the core of these proteins, where noncontiguous hydrophobic residues may be clustered at the level of tertiary structure. To define the structure of the membrane-inserted form of these proteins, fluorescence quenching by spin-labeled phospholipids is being utilized. Algebraic expressions have been developed that allow the membrane location of a fluorescent group on a protein to be calculated when its quenching by spin labels at shallow and deep positions within the membrane is measured. Quenching studies with fluorescent fatty acids and proteins show the sensitivity and accuracy of this approach.

6. Two-dimensional Crystals Assembled from Proteins: Could They Be Used for Direct Assessments of Structure and Function? ANDREAS ENGEL,\* *Maurice E. Müller-Institute, Biocenter, Basel, Switzerland*

Suitable detergents are now available to solubilize membrane proteins and to isolate them using standard techniques. High purity and conformational homogeneity, prerequisites for crystallization experiments, may thus be achieved. Conditions have also been established to reconstitute the isolated membrane protein in the lipid bilayer and to reestablish the functional state. A wealth of functional studies is reported (e.g., studies on channel-forming proteins), but in general their structure needs to be derived from sequence data by the use of structure prediction techniques. Two-dimensional (2-D) crystals assembled from membrane proteins and lipids may open some novel avenues to elucidate not only the structure but also the relationship between structure and function. Electron crystallography, in a process of steady progress, has demonstrated near atomic scale resolution (Henderson et al. 1990. *J. Mol. Biol.* 213:899). New types of scanning probe microscopes allow surfaces of proteins and lipids to be imaged in their native aqueous environment at 1–3-nm resolution. Even biological processes may be directly followed by such techniques at molecular resolution (Drake et al. 1989. *Science (Wash. DC)*. 243:1586). In 2-D crystals the protein is embedded in its native environment and is therefore expected to exhibit native functionality. *A priori* knowledge of position and orientation of the subunits constituting the crystal appears to make the detection of small conformational changes possible. This could be achieved either by preserving a functional state during specimen preparation for electron microscopy, or by directly observing function-related structural rearrangements using scanning probe microscopy. This approach may provide exciting new data hitherto not directly accessible. [Supported by the Swiss National Foundation for Scientific Research, 31-25684.88 and the M. E. Müller-Foundation of Switzerland.]

7. The Retinal Protein Family of Halobacteria as a Paradigm for Other 7-Transmembrane Helical Proteins D. OESTERHELT, *Max Planck Institute of Biochemistry, Martinsried, Germany*

Hydropathy analysis of an increasing number of cDNAs coding for membrane-bound receptors from eukaryotes and prokaryotes revealed the topographic feature of 7-transmembrane (7-TM) helices as a common secondary structural motif. The function of these proteins is reception of signals from hormones, peptide neurotransmitters, olfactory substances, and light. Most of them are G protein-coupled receptors which upon ligand binding initiate a signal transduction cascade through interaction with G proteins. Halobacteria, as members of the archaeobacterial kingdom also possess 7-TM helical proteins which function as light-driven proton or chloride pumps (bacteriorhodopsin and halorhodopsin) or as sensors (sensory rhodopsin I and II). Like visual pigments these retinal proteins photoisomerize, but instead of the agonistic all-*trans* configuration in rhodopsins, the halobacterial proteins isomerize to 13-*cis*. Furthermore, this state is transient and lives for only 10 ms in the pumps and for ~1 s in the sensors. The signal transduction cascade triggered by the visual pigment has been elucidated in detail, including G protein coupling. In contrast, the halobacterial retinal proteins apparently do not interact. The only protein structure of the 7-TM superfamily

available as a molecular model is that of bacteriorhodopsin, and the mechanism of vectorial ion transport and the molecular changes necessary for the transition from an ion pump to a sensory receptor will be a focus of this presentation. In retinal proteins the seven helices are arranged in a circular way with short connections between the helices. The extended retinal molecule is bound to the seventh helix and spans the pore formed by the helices. This arrangement is crucial for function. It is unclear why 7-TM helices are necessary for the nonretinal proteins of the family. The molecular weights and therefore the interhelical connections are much larger than in the halobacterial proteins. Ligand binding in some cases has been shown to occur in the area of the seventh helix, and G protein binding, at least in rhodopsin, requires the concerted action of several helix connecting loops. Therefore, the 7-TM motif might have an important role in the determination of the spatial disposition of the loops for optimal molecular interaction.

8. Molecular Analysis of "12-Helix" Sugar Transport Proteins PETER J. F. HENDERSON, JEFFREY K. GRIFFITH, GILES E. M. MARTIN, ADRIAN R. WALMSLEY, TERRY P. McDONALD, WEI-JUN LIANG, and FRANK J. GUNN, *Department of Biochemistry, University of Cambridge, Cambridge, United Kingdom*

In *Escherichia coli* there are transport proteins for galactose (GalP), arabinose (AraE), and xylose (XylE) that are 21–64% identical in amino acid sequence to each other and to sugar transporters from diverse organisms, including the human glucose transporters (Henderson et al. 1992, *Int. Rev. Cytol.* 137A:149). Statistical comparisons of the amino acid sequences of 58 transport proteins suggest the existence of at least four related families: one for the sugar transporters; one containing transporters for citrate, oxoglutarate, bialaphos, and proline; one containing transporters for antibiotics or antiseptics such as methylenomycin, actinorhodin, and quaternary ammonium compounds; and one for antibiotics such as quinolones, tetracyclines, and chloramphenicol. The hydrophobic profiles of these proteins indicate that the majority contain 12 membrane-spanning  $\alpha$ -helices, and occasionally 13 or 14. This 12-helix theme also applies to other transport proteins of apparently unrelated sequences, including those for lactose (LacY), fucose (FucP), and glucuronides (GusB) in *E. coli* and the glucose/ $\text{Na}^+$  transporters in mammals (Hediger et al. 1989, *Proc. Natl. Acad. Sci. USA.* 86:5748). We have amplified expression of each of the *E. coli* GalP, AraE, XylE, and FucP transporters so they constitute 8–66% of the inner membrane protein. These levels permit molecular analysis of the structure–function relationship by combining techniques such as stopped-flow fluorescence spectroscopy, quantitative measurement of cytochalasin B binding, reaction with *N*-ethylmaleimide, directed mutagenesis of individual amino acids, homologous recombination, and fusions to topological probes such as  $\beta$ -lactamase and  $\beta$ -galactosidase. The results are described and interpreted in terms of a unifying model of the structure of many transport proteins. [Supported by SERC, MRC, and the Wellcome Trust.]

9. Function and Biosynthesis of Erythroid and Nonerythroid Anion Exchangers STEPHAN RUETZ\* and RON R. KOPITO, *Department of Biological Sciences, Stanford University, Stanford, California*

AE1 and AE2 are tissue-specific, cation-independent anion exchange proteins. Transient expression of AE2 cDNA in human embryonic kidney (HEK) cells increased stilbene-inhibitable whole cell  $^{35}\text{SO}_4^{2-}$  efflux consistent with its function as a plasma membrane anion exchanger. No such increased transport activity was observed in AE1 transfectants, despite the fact that AE1 and AE2 accumulated to approximately equal steady-state levels. In contrast, both AE1 and AE2 expression resulted in a significant increase in  $\text{Cl}^-/\text{SO}_4^{2-}$  exchange in crude microsomes from transfected cells, demonstrating that both AE1 and AE2 cDNAs encode functional proteins. Immunofluorescence and pulse-chase experiments of transfected HEK cells revealed that, while 60% of AE2 was processed to the cell surface of transfectants, AE1 was restricted to the endoplasmic reticulum (ER). Crude microsomes from transfected cells were fractionated into plasma membrane- and ER-derived vesicles by concanavalin A affinity chromatography. Transport studies on these fractions confirmed that almost

100% of the total AE1 transport activity was recovered in the ER fraction, while AE2 activity was divided roughly equally between the two populations of vesicles. We conclude that both anion exchangers, which are normally localized and functioning at the plasma membrane, are potentially active at the earliest detectable stage of their biosynthesis. [Supported by NIH grant GM-38543, the Lucille P. Markey Charitable Trust, and the Forschungskommission der Universität Zürich (Switzerland).]

10. Mitochondrial Carrier Family MARTIN KLINGENBERG, *Institute of Physical Biochemistry, University of Munich, Munich, Germany*

Mitochondria contain ~15 solute carriers, 8 of which have been isolated. The primary sequence of four carriers has been determined. The two best characterized are that for ADP/ATP, ubiquitous in all mitochondria, and that for  $H^+/OH^-$  (uncoupling protein), occurring only in mitochondria from mammalian brown adipose tissue cells. All four known sequences have the same design: i.e., they are made up of three similar domains of ~100 residues. Although the internal and inter-carrier repeats have only 20–30% similarity, structurally critical residues (e.g., those confining the hydrophobic trans-membrane helices) are conserved throughout. Each repeat is suggested to contain two trans-membrane helices, the first more hydrophobic, the second more amphiphilic. The two helices are separated by ~50-residue-long intradomain polar regions. With a total of six trans-membrane helices both the COOH and  $NH_2$  terminals are directed to the cytosolic side, as shown by various data. Thus the intradomain polar central sections are on the matrix side. However, with membrane-impermeant reagents, accessibility of these regions from the cytosolic side is also shown. Further, azido-ATP added from outside labeled the intradomain regions. These data indicate that portions of these regions fold through the membrane toward the cytosolic side. They are visualized to line the translocation channel. Data on structure-function relationships by site-directed mutagenesis of the ADP/ATP carrier will be presented. For the uncoupling protein the mechanism of  $H^+/OH^-$  translocation will also be elucidated in terms of the structural models and its regulation by fatty acids. The nucleotide binding region and the nucleotide interaction with the  $H^+/OH^-$  transport from a site that is separated from the transport channel will be demonstrated. The participation of cationic and anionic residues in the nucleotide-induced conformation change will be elaborated.

11. Molecular Analysis of STE6, the Yeast  $\alpha$ -Factor Transporter CAROL BERKOWER\* and SUSAN MICHAELIS,\* *Department of Cell Biology and Anatomy, The Johns Hopkins University School of Medicine, Baltimore, Maryland* (Sponsor: William B. Guggino)

The STE6 protein of *Saccharomyces cerevisiae* mediates export of the  $\alpha$ -factor mating pheromone. STE6 is composed of two homologous halves, each containing six membrane-spanning segments and one putative ATP binding domain. STE6 belongs to a superfamily of transport proteins designated the ATP binding cassette (ABC) proteins, which share significant overall structure. ABC family members include MDR1, the mammalian multidrug resistance protein, and CFTR, the protein defective in patients with cystic fibrosis. The STE6, CFTR, and MDR1 proteins are each encoded by a single large polypeptide. Other family members, such as the bacterial histidine and oligopeptide permeases, differ from STE6 in that individual domains of a single transporter may be encoded by separate genes, reflecting the modular organization of these pumps. To examine structure-function relationships in STE6, we severed the coding region of the STE6 gene between its two homologous halves, and showed that the resulting half-molecules could regenerate a functional transporter (Berkower and Michaelis, 1991, *EMBO [Eur. Mol. Biol. Organ.] J.* 10:3777). More recent experiments have involved generating one-quarter and three-quarter molecules. The first-quarter molecule, containing six predicted membrane spans, is able to reassemble with the remaining three-quarter molecule (which lacks transport activity on its own) to generate a functional transporter. This suggests that the first membrane-spanning domain of STE6 has an essential role, which it can fulfill even when it is not covalently linked to the rest of the transporter. However, in contrast to several bacterial permeases, whose four domains are all encoded independently, our results suggest that an isolated ATP binding domain of STE6 cannot reassemble with the rest of the protein to reconstitute a

functional transporter. Studies are underway to examine the significance of sequence divergence between the two homologous halves of STE6 by swapping these halves (or smaller subdomains thereof) within STE6. [Supported by grants from the NIH, the CF Foundation, and the March of Dimes.]

12. Structural Analysis of Monoamine Neurotransmitter Transporters RANDY D. BLAKELY,\* KIM MOORE, and HALEY BERSON.\* *Department of Anatomy and Cell Biology, Emory University, Atlanta, Georgia* (Sponsor: T. Parsons)

The identification of a cDNA encoding the human norepinephrine (NE) transporter (Pacholczyk et al. 1991. *Nature [Lond.]*. 350:350) revealed significant sequence similarity (~46% amino acid identity) to the cloned  $\gamma$ -aminobutyric acid (GABA) transporter. Functional NE and GABA carriers are encoded by single RNAs with the inferred amino acid sequence predicting proteins containing ~12 hydrophobic domains capable of spanning the plasma membrane. Sequence identity among these carriers has permitted the identification of additional catecholamine, indoleamine, and amino acid transporters. The cloned rat brain serotonin (5HT) transporter (Blakely et al. 1991. *Nature [Lond.]*. 354:66) expressed in HeLa cells exhibits sodium-dependent, high-affinity 5HT transport and is antagonized by nanomolar concentrations of the 5HT transport-selective inhibitors paroxetine and citalopram. Both the NE and 5HT transporters are antagonized by cocaine and tricyclic antidepressants. By deletion and site-directed mutagenesis, and through the generation of transporter chimeras, we have begun to examine regions of the highly related monoamine transporters which are required for function and which define pharmacologic specificity. Hydrophilic  $\text{NH}_2$  and  $\text{COOH}$  termini of these carriers are presumed to lie in the cytoplasm. A deletion of 5HT transporter cDNA encoding the inferred amino terminus exposes an in-frame methionine two amino acids from the first putative transmembrane domain. Expression of this clone results in high-affinity 5HT transport, suggesting that most of the  $\text{NH}_2$ -terminal 87 amino acids are not required for expression. In preliminary studies, NE transporter chimeras containing 5HT sequences from transmembrane domain 5 or 7 to the  $\text{COOH}$  terminus fail to express either NE or 5HT transport, either by disrupting cell surface expression or by interactions among transmembrane domains. [Supported by NIDA grant DA 07390-01 and a Mallinckrodt award to R. D. Blakely.]

13. Transport of ATP and Biogenic Amines into Chromaffin Granule Ghosts LAURIE A. BANKSTON and GUIDO GUIDOTTI, *Department of Biochemistry and Molecular Biology, Harvard University, Cambridge, Massachusetts*

Chromaffin granules of adrenal medullary cells contain high concentrations of catecholamines and ATP (Hillarp. 1958. *Acta Physiol. Scand.* 42:321). Vesicles derived from the chromaffin granules (chromaffin granule ghosts) concentrate catecholamines and indoleamines in the presence of ATP, which is used by a membrane-bound proton pump to generate an electrochemical gradient of protons (Phillips. 1974. *Biochem. J.* 170:673; Phillips. 1978. *Biochem. J.* 192:273). Analysis of the amount of proton and serotonin transport into chromaffin granule ghosts in solvents containing ATP as the only anion revealed that the majority of the cations must be accompanied by an anion, presumably ATP, in order to achieve charge neutralization. We show that ATP is in fact transported into these vesicles in a time- and concentration-dependent fashion, and that this transport depends on the presence of the membrane potential. The linkage between amine uptake and ATP metabolism in the chromaffin granule ghosts is reminiscent of the transport properties of the multiple drug resistance (MDR) protein. Both systems interact with ATP and transport a variety of positively charged, planar hydrophobic solutes (Endicott and Ling. 1989. *Annu. Rev. Biochem.* 58:137). To elucidate further the properties of the amine transporter of chromaffin granule ghosts, we examined the effect of inhibitors of the MDR protein on serotonin uptake. Verapamil and quinidine, inhibitors of the MDR protein (Horio et al. 1988. *Proc. Natl. Acad. Sci. USA.* 85:3580), are noncompetitive inhibitors of serotonin uptake, with  $K_i$ 's of 25 and 100  $\mu\text{M}$ , respectively. In addition, reserpine, a well-known competitive inhibitor of serotonin uptake (Kirshner. 1962. *J. Biol. Chem.* 237:2311), inhibits transport through the

MDR protein (Pearce et al. 1989. *Proc. Natl. Acad. Sci. USA*. 86:5128). The conclusion is that there are similarities between the two transport systems. [Supported by NIH training grant GM-07598-14 and grant HL-08893.]

14. Cloning, Functional Characterization, and Tissue Distribution of the Thiazide-sensitive  $\text{Na}^+:\text{Cl}^-$  Cotransporter of the Winter Flounder (*Pseudopleuronectes americanus*) Urinary Bladder GERARDO GAMBA,\* AKIHIKO MIYANOSHITA,\* MICHAEL LOMBARDI,\* and STEVEN C. HEBERT,\* *Renal Division, Brigham and Women's Hospital and Harvard Medical School, Boston, Massachusetts* (Sponsor: Barry M. Brenner)

Using an expression cloning strategy in *Xenopus laevis* oocytes, we have cloned the thiazide-sensitive  $\text{Na}^+:\text{Cl}^-$  cotransporter (TSC) from winter flounder urinary bladder. Oocytes injected with poly(A)<sup>+</sup>RNA from the urinary bladder expressed a 15-fold higher  $^{22}\text{Na}^+$  uptake that was  $\text{Cl}^-$  dependent and completely inhibited by  $10^{-4}$  M of metolazone; water-injected oocytes did not express any TSC activity. A cDNA library was constructed in the plasmid, pSPORT1, from the size-fractionated poly(A)<sup>+</sup>RNA (3.5–4.0 kb) that elicited a  $\text{Cl}^-$ -dependent  $^{22}\text{Na}^+$  uptake when injected into oocytes. The library was screened for functional TSC expression until a single clone was isolated (TSC<sub>fl</sub>). Oocytes injected with 12.5 ng of cRNA transcribed from the TSC<sub>fl</sub> clone expressed a  $^{22}\text{Na}^+$  uptake that was 250-fold higher than control oocytes and exhibited: (a) interdependence of  $\text{Na}^+$  and  $\text{Cl}^-$  with a stoichiometry of 1:1; (b)  $K_m$  values for  $\text{Na}^+$  and  $\text{Cl}^-$  of  $25.0 \pm 0.4$  and  $13.6 \pm 0.2$  mM, respectively; (c) sensitivity to thiazide diuretics; and (d) insensitivity to ouabain, furosemide, bumetanide, amiloride, acetazolamide, and EIPA. The TSC<sub>fl</sub> cDNA sequence is 3.7 kb long with an open reading frame of 3,069 bp that predicts a protein of 1,023 amino acids with a calculated mass of 112 kD and three potential N-glycosylation sites. Hydropathy analysis revealed 12 putative membrane-spanning domains and a long nonhydrophobic COOH terminus of 450 amino acid residues. The molecular mass and glycosylation were confirmed by SDS-PAGE of in vitro translation products. Northern blot analysis using a full-length riboprobe at high stringency showed a single band of 3.7 kb in the urinary bladder and a single band of 3.0 kb on gonad, intestine, skeletal muscle, eye, brain, and kidney.

15. Identification of a New Family of Proteins Involved in Amino Acid Transport MATTHIAS A. HEDIGER, YOSHIKATSU KANAI, WEN-SEN LEE, and REBECCA G. WELLS, *Department of Medicine, Renal Division, Brigham and Women's Hospital and Harvard Medical School, Boston, Massachusetts*

Transport of amino acids across epithelial cells of the kidney and the small intestine is believed to be mediated by brush border and basolateral specific transporters with distinct substrate specificities. We have used expression cloning with *Xenopus* oocytes to study the molecular basis of these transporters. Screening a rat renal expression library for [ $^{14}\text{C}$ ]cystine uptake resulted in the isolation of the kidney- and intestine-specific clone D2 (Wells and Hediger. 1992. *Proc. Natl. Acad. Sci. USA*. In press). Using *Xenopus* oocytes injected with in vitro transcribed cRNA, we demonstrated that D2 induces the  $\text{Na}^+$ -independent high affinity transport of dibasic, and, surprisingly, neutral amino acids. The D2 amino acid sequence shows significant sequence identity (29%) to that of the 4F2 antigen heavy chain. This cell surface protein is induced during the process of cellular activation and is expressed widely in mammalian tissues, including the proximal tubule of the kidney. Our results show that cRNA from the human 4F2 heavy chain stimulates the uptake of dibasic and neutral amino acids (but not cystine) into oocytes. Unlike D2, the uptake of neutral but not dibasic amino acids is  $\text{Na}^+$  dependent. The D2 and 4F2 heavy chain amino acid sequences predict proteins with a single transmembrane domain, a structure not typical of known membrane transport proteins. We suggest that D2 and 4F2 represent a new family of proteins involved in amino acid transport, possibly functioning as transport activators or regulators. [Supported by NIH grant DK-43171 to M. A. Hediger.]

16. The Giant Membrane Patch Model for Macroscopic and Microscopic Studies of Carrier Proteins DONALD W. HILGEMANN and SATOSHI MATSUOKA, *Department of Physiology, The University of Texas Southwestern Medical Center at Dallas, Dallas, Texas*

A "giant" excised membrane patch preparation (15–25  $\mu\text{m}$  diameter, 2–10 G $\Omega$  seals) allows new types of studies of electrogenic carrier proteins (Hilgemann, 1989, *Pflügers Arch.* 415:247). With minor modifications, primarily of the hydrocarbon electrode coat used, the method can be used with many cell types. Relevant to carrier expression studies, *Xenopus* oocytes (30–40  $\mu\text{m}$  diameter, 2–5 G $\Omega$ ) and SF9 cells (15–20  $\mu\text{m}$  diameter, 2–5 G $\Omega$  seals) are readily used. Giant excised patches are stable (lifetimes of 20–45 min), pipette perfusion and rapid cytoplasmic solution switching (<100 ms) allow rigorous ion concentration control, and 150-kHz voltage clamp is achieved with a modified Axopatch 200 (Axon Instruments, Inc., Foster City, CA) patch clamp. Rim current can be minimized, if not eliminated, by appropriate electrode shaping. In recent work exploiting these capabilities, a likely functional homology between the cardiac Na/K pump and Na/Ca exchange has been identified. Half-cycle charge movements of sodium translocation can be monitored in concentration jump experiments for both systems. Fast charge movements (>10 kHz) are found in voltage pulse experiments when the transporters are forced into E2 configuration in the presence of extracellular sodium. These charge movements appear to be associated with the binding/unbinding of extracellular sodium, as predicted for an extracellular ion well. [Supported by a Grant-in-Aid and an Established Investigatorship of the American Heart Association and the NIH (HL-45240-04).]

17. Functional Studies of the Cloned Na<sup>+</sup>/Glucose Cotransporter LUCIE PARENT\* and ERNEST M. WRIGHT, *Department of Physiology, University of California Los Angeles School of Medicine, Los Angeles, California; and Department of Molecular Physiology and Biophysics, Baylor College of Medicine, Houston, Texas*

The cloned rabbit intestinal Na<sup>+</sup>/glucose cotransporter (SGLT 1) was expressed in *Xenopus laevis* oocytes and cotransporter currents were measured as a function of temperature with the two-electrode voltage-clamp method as described previously (Parent et al. 1992, *J. Membr. Biol.* 125:49). Increasing the bath temperature from 10 to 30°C increased steady-state cotransporter currents at saturating external [Na]<sub>o</sub> and [sugar]<sub>o</sub>. At  $V_m = -190$  mV,  $Q_{10}$  (~3) was constant over this temperature range, suggesting only one rate-limiting step in the cotransport cycle ( $E_a \approx 90$  kJ/mol). However, as the membrane potential was reduced from -190 to -30 mV,  $Q_{10}$  measured between 10 and 20°C differed from the one measured between 20 and 30°C. Between 20 and 30°C, the  $Q_{10}$  was always independent of the membrane potential, whereas the  $Q_{10}$  measured between 10 and 20°C increased from ~3 at  $V_m = -190$  mV to ~7 at  $V_m = -30$  mV. The voltage dependence of  $Q_{10}$  suggests that there are two rate-limiting steps in the transport cycle, one voltage dependent between 10 and 20°C and the other voltage independent between 20 and 30°C. The increase in cotransporter current as a function of temperature was correlated with increases in  $i_{\text{max}}^{\text{Na}}$  (as measured with 1 mM [D-glucose]<sub>o</sub>) and in  $i_{\text{max}}^{\text{glucose}}$  (as measured with 100 mM [Na]<sub>o</sub>). The absolute values of  $K_{0.5}^{\text{Na}}$  and  $K_{0.5}^{\text{glucose}}$ , as well as their voltage dependence, were found to be independent of the temperature between 20 and 30°C. Finally, the effect of temperature on the cotransporter pre-steady-state currents was studied between 10 and 20°C. The time constant of the cotransporter relaxation ( $\tau_2$ ) was found to decrease with the temperature with a  $Q_{10}$  factor of 3.4. The pre-steady-state current amplitude ( $i_2$ ) was left unchanged. This supports our interpretation that the pre-steady-state currents represent an intrinsic charge translocation of the Na<sup>+</sup>/glucose cotransporter. [Supported by NIH grant DK-19567.]

18. Exchange Diffusion, Single Filing, and Gating in Macroscopic Channels of One Conformation DUANPIN CHEN\* and ROBERT EISENBERG, *Department of Physiology, Rush Medical College, Chicago, Illinois*

Open channels are described by Nernst-Planck equations relating flux to the concentration of ions and their common electrical potential, usually assumed to be independent of concentration and flux.

But potential is a variable arising from permanent and induced charge on the channel's wall and ions in the channel's pore. The fluxes in Nernst-Planck equations are coupled by the potential of Poisson's equation when boundary conditions ensure zero current with zero driving force. Similar models describe current flow in semiconductors and transistors (e.g., thyristors). We describe a channel as a macroscopic cylinder of fixed structure, of just one conformation; yet, four rings of permanent charge (à la Numa) produce phenomena reminiscent of exchange diffusion. Unidirectional efflux increases with increasing external concentration, although the channel remains in its one conformation. Modest modifications in the charge produce phenomena reminiscent of single filing; unidirectional efflux declines with increasing external concentration, although these macroscopic Nernst-Planck equations allow ions to pass through each other. The coupled nonlinear equations of this theory have multiple solutions. Open, closed, and threshold current-voltage relations occur in open cylindrical pores without steric occlusions, with channel protein and permanent charge in their one conformation. We wonder if transitions between different current-voltage relations account for gating of single channels between zero, sub-, or full conductance states: either spontaneous opening-closing, flickering, or opening/closing mediated by agonists and voltage. Transistors are complex distributions of permanent charge connected to power supplies. It will be interesting to see what happens in branched channels—with shapes like Y,  $\Psi$ , or  $\times$ —if energy sources like multiple ionic gradients or ATP/ATPase are present. [Supported by NSF grant DIR-9012294.]

19. Bacterial Periplasmic Permeases as Model Systems for MDR and CFTR GIOVANNA FERRO-LUZZI AMES, *University of California, Berkeley, California*

The superfamily of membrane transporters called "traffic ATPases," which contains proteins that have in common extensive sequence homology, includes prokaryotic periplasmic permeases and the eukaryotic MDR, CFTR, and STE-6 proteins. The sequence homology extends to an ATP-binding motif and to the use of ATP as an energy source. The prokaryotic histidine permease is a well-characterized permease which can be used as a convenient model system. In this permease, a soluble receptor protein binds the transported substrate firmly and signals the membrane-bound complex to hydrolyze ATP and translocate the substrate. The topology of the membrane-bound complex resembles that of CFTR or MDR, and like them it contains two ATP-binding domains and two membrane-spanning domains. A structural model of the ATP-binding domain of periplasmic permeases was obtained by computer modeling and will be discussed. The relationship between prokaryotic and eukaryotic traffic ATPases will be presented. In particular, a structure-function analysis of numerous mutations in the histidine permease will be put in perspective relative to the known CFTR mutations. Since CFTR has been shown to be a channel, a number of analogies between channels and transporters and the reasons for placing these two categories of transporters within the same superfamily will be discussed. [Supported by NIH grant DK-12121.]

20. Functional and Structural Characterization of the Mouse Multidrug Resistance (*mdr*) Gene Family P. GROS,\* *Department of Biochemistry, McGill University, Montreal, Quebec, Canada*

Multidrug resistance (MDR) is caused by the overexpression of P-glycoprotein (P-gp) which is encoded by the *mdr* gene family. The mouse *mdr* gene family is composed of three closely related members, designated *mdr1*, *mdr2*, and *mdr3*, that share a high degree of sequence homology and identical predicted secondary structures. The *mdr* gene family is part of a larger super-gene family which includes, among others, human CFTR and HAM genes, the yeast STE-6, and the protozoan gene *pfmdr1*. Despite high similarities of their predicted amino acid sequences, the three mouse P-gp's are functionally distinct. While overexpression of either *mdr1* or *mdr3* directly confers multidrug resistance to stably transfected cells, *mdr2* does not. In addition, *mdr1* and *mdr3* show distinct substrate specificities. Exchange of homologous domains in chimeric cDNAs constructed between *mdr1* and *mdr2* reveals that both predicted NB binding sites of *mdr2* are functional and complement the drug resistance function of *mdr1*, while membrane-associated (transmembrane [TM]) domains of *mdr2* are incompatible with this function. A similar analysis in chimeric molecules

constructed between *mdr1* and *mdr3* indicates that all 12 predicted TM domains are absolutely required to fully reproduce the specific substrate specificities of each parental protein. Mutational analysis indicates that substitutions in either NB site of *mdr1* completely abrogate the capacity of this protein to confer MDR. Single amino acid substitutions within the predicted TM 11 of *mdr1* and *mdr3* modulate the overall activity and substrate specificity of the two drug efflux pumps; In the case of *mdr1*, a single Ser to Phe substitution at position 941 in this amphiphilic TM11 domain creates an unusual P-gp that retains the capacity to confer resistance to vinblastine but cannot confer resistance to colchicine or anthracyclines. Interestingly, mutations in the homologous domain of the *pfmdr1* gene of *Plasmodium falciparum* are associated with chloroquine resistance in this parasite, suggesting a common mechanism of action of these two distantly related proteins. Introduction and overexpression of the mouse *mdr3* gene in a *Saccharomyces cerevisiae* strain lacking a chromosomal *STE-6* gene is shown to restore the capacity of a cells to mate with alpha cells, suggesting that mouse *mdr3* can export the *a* mating pheromone in yeast cells. Mutations shown to modulate drug transport by *mdr3* in transfected mammalian cells also modulate the ability of *mdr3* to complement *STE-6* in yeast cells, suggesting a common mechanistic basis of action.

21. Studies of Disease-causing Mutations of CFTR in a Baculovirus-Insect Cell Expression System J. R. RIORDAN, T. J. JENSEN, C. E. BEAR, M. RAMJEESEINGH, and N. KARTNER, *Research Institute, The Hospital for Sick Children, Toronto, Ontario, Canada*

The CFTR is a novel member of the TM6-NBF superfamily of membrane transport proteins because it exhibits chloride ion channel activity. Hence, the elucidation of the structure-function relationships of the molecule should help gain greater understanding of the disease and also of this class of membrane proteins. The pursuit of this goal by in vitro mutagenesis and heterologous mammalian cell expression has been complicated by the fact that many mutations, including the most frequent disease-causing change ( $\Delta F508$ ), result in the biosynthetic arrest of CFTR. Therefore, most of the mutant protein doesn't reach its normal plasma membrane location but instead is trapped intracellularly. This makes it difficult to assay the functional capacity of the molecule. Fortunately, this arrest of biosynthesis does not seem to occur in the army worm Sf9 cells infected with CFTR-containing recombinant baculoviruses. In the case of  $\Delta F508$ , it accumulates to the same high level as the wild-type protein and is active at the cell surface. To a first approximation its activity is not different from that of normal CFTR. This allows the conclusion that the principal consequence of the major CF-causing mutation is at the level of protein assembly rather than its activity per se. A mutant that apparently does not undergo biosynthetic arrest, G551D can also be synthesized in large amounts in Sf9 cells, but it is inactive. These results demonstrate that in this system one can clearly distinguish between the influence of a given mutation on synthesis and intracellular trafficking as opposed to effects on regulated chloride channel activity. It is as yet unclear whether the insect cells lack the specific aspect of the quality control system that detects malformed CFTR molecules in mammalian cells, or if the reduced growth temperature (27°C) may have a permissive influence. [Supported by the Canadian and U.S. Cystic Fibrosis Foundations and the NIH-NIDDK.]

22. Structure-Function Studies of CFTR MICHAEL J. WELSH, *Howard Hughes Medical Institute, University of Iowa College of Medicine, Iowa City, Iowa*

Mutations in the gene encoding the cystic fibrosis transmembrane conductance regulator (CFTR) cause cystic fibrosis. Evidence from several studies indicates that CFTR is a  $\text{Cl}^-$  channel: (a) expression of CFTR in a wide variety of cells generates  $\text{Cl}^-$  channels; (b) CFTR is located in the apical membrane where the CF defect is observed; (c) cAMP-regulated  $\text{Cl}^-$  channels generated by recombinant CFTR have the same properties as those endogenous to epithelia; (d) alteration of specific residues in CFTR alters anion selectivity of  $\text{Cl}^-$  channels; and (e) incorporation of purified CFTR into planar lipid bilayers produces  $\text{Cl}^-$  channels. The channel is regulated by phosphorylation of the R domain. The evidence that supports this conclusion is the observation that cAMP-dependent protein kinase activates CFTR  $\text{Cl}^-$  channels in excised cell-free patches and in  $\text{Cl}^-$  channels incorporated into planar lipid bilayers. Phosphorylation of four specific residues in the R domain

activates the channel, and deletion of part of the R domain generates a constitutively active channel. In addition, the CFTR  $\text{Cl}^-$  channel has a novel regulation by ATP. Studies using excised cell-free patches indicate that ATP regulates the channel and suggest that ATP hydrolysis may be required for channel opening. Mutations in CFTR cause cystic fibrosis, and recent studies suggest that this results from defective cellular processing of several CF variants such that the mutant channel is not delivered to the apical membrane of airway epithelia.

23. Evolution of Coupled Transport PETER C. MALONEY and T. HASTINGS WILSON, *Department of Physiology, Johns Hopkins University School of Medicine, Baltimore, Maryland; and Department of Cellular and Molecular Physiology, Harvard Medical School, Boston, Massachusetts*

We postulate that early cells developed a proton economy in which a proton-motive force was used to support the operation of secondary carriers. Recent work shows how this might have been accomplished by a link between metabolism and a secondary carrier. Thus, in the anaerobic bacterium, *Oxalobacter formigenes*, a proton-motive force arises following the antiport of external oxalate, a divalent anion, and internal formate, the monovalent product of oxalate decarboxylation. The electrogenic anion exchange sustains the required membrane potential (negative inside), while oxalate decarboxylation, which consumes a single proton, ensures an internal alkalinity; together these events constitute an "indirect" or "metabolic" proton pump whose stoichiometry is  $1\text{H}^+/\text{turnover}$ . The proton economy established early in evolution is today retained at the plasma membranes of most living cells, including bacteria, the lower eukaryotes, and the plant kingdom. Because they arose by endosymbiosis of bacterial progenitors, mitochondria and chloroplasts display proton-linked reactions. And possibly because they derived from an internalization of the early (proton-linked) elements of the proto-eukaryote, the endomembrane system also has a proton economy. Only in the lineage yielding animal cells did further evolution establish a sodium economy at the plasma membrane, perhaps as a way to simplify the control of internal pH. Clearly, the switch from H to Na as the primary coupling ion was made easier by prior evolution of bifunctional exchange carriers such as the H/Na antiporter; as demonstrated by present day examples, such bifunctional systems function equally well in either setting. The idea that secondary carriers arrived early in evolution is supported by current views as to carrier structure, since sequence analysis predicts that membrane carriers all belong to a single superfamily. Thus, whether they come from bacterial or animal cell systems, carriers usually have 10–12 transmembrane  $\alpha$ -helices, often with a central cytoplasmic loop dividing the molecule in half. The Na/H antiporter, whether from *Escherichia coli* or animal cells, appears to have 10 such transmembrane segments, while band 3, the anion exchange carrier of the red cell, and the Pi-linked anion exchanger of *Escherichia coli* each have 12. As more and more examples continue to be described, this commonality of structure is strengthened.

24. Molecular Characterization of the Erythrocyte Chloride-Bicarbonate Exchanger REINHART A. F. REITHMEIER,\* *Medical Research Council Group in Membrane Biology, Departments of Medicine and Biochemistry, University of Toronto, Toronto, Ontario, Canada*

Human band 3 is a 911 amino acid glycoprotein that catalyzes the one-for-one exchange of anions across the erythrocyte membrane. The high content of the band 3 protein in the erythrocyte membrane has enabled extensive structural studies of this transport protein. Circular dichroism spectroscopy has shown that the transmembrane segments of band 3 are  $\alpha$ -helical in conformation. We have used energy minimization and computer modeling to study transmembrane helix-helix interactions in glycophorin and band 3. Enzymatic removal of the single oligosaccharide chain in band 3 had little effect on the structure of the protein or on its anion transport activity. The various oligomeric states of band 3 play different roles involving transport, cytoskeletal interactions, and red cell aging. Mutant band 3 isolated from patients with Southeast Asia ovalocytosis (SAO) exhibited a

variety of altered structural and functional properties. [Supported a group grant from the Medical Research Council of Canada.]

25. Molecular Biology and Hormonal Regulation of Vertebrate  $\text{Na}^+/\text{H}^+$  Exchanger Isoforms JACQUES POUYSSÉGUR, PIERRE FAFOURNOUX, CLAUDE SARDET, SHIGEO WAKABAYASHI, MING TSE, MARK DONOWITZ, FRANCK BORGESE, and RENÉE MOTAIS, *Centre de Biochimie-Centre National de la Recherche Scientifique, Université de Nice, Nice, France; Division of Gastroenterology, The Johns Hopkins University, Baltimore, Maryland; and Laboratoire J. Maetz, Commissariat à l'Energie Atomique, Villefranche/mer, France*

The first vertebrate  $\text{Na}^+/\text{H}^+$  exchanger to be cloned, referred to as NHE-1, is an amiloride-sensitive, ubiquitous plasma membrane transporter that regulates intracellular pH and is activated by diverse hormonal, mitogenic, and oncogenic signals through an increased affinity for  $\text{H}^+$  at the intracellular "modifier" site. The human NHE-1 isoform is a phosphoglycoprotein of 815 amino acids with an  $\text{NH}_2$ -terminal domain that contains 12 putative transmembrane-spanning segments followed by a carboxy-terminal cytoplasmic stretch of 315 residues. This NHE-1 cDNA facilitated the isolation, at lower stringency, of different Na-H exchanger isoforms referred to as NHE-2, NHE-3, NHE-4, and  $\beta$ -NHE. All these forms, which exhibit 45–70% identity with NHE-1, possess a similar hydropathy profile with two highly conserved transmembrane segments presumably involved in ion transport. All isoforms, when expressed into exchanger-deficient fibroblasts, are activated by intracellular  $\text{H}^+$ , regulate intracellular pH in a  $\text{Na}^+$ -dependent manner, and are inhibited by amiloride and 5-amino derivatives with distinct  $K_i$  values. NHE2 and NHE3, which are highly and differentially expressed in kidney, colon, small intestine, and stomach, represent putative, apically expressed, amiloride-resistant forms previously described in epithelial cells. Experiments with NHE-1, which is activatable by all growth factors, and with  $\beta$ -NHE, a trout red cell isoform that is activatable by  $\beta$ -adrenergic agonists, lead us to the following conclusions: NHE1 and presumably all other isoforms can be separated into two functional domains. One is the  $\text{NH}_2$ -terminal transporter domain which has the capacity to catalyze amiloride-sensitive Na-H exchange with a built-in  $\text{H}^+$ -modifier site. The other is a COOH-terminal cytoplasmic regulatory domain that determines the set point value of the exchanger and mediates hormonal signals in a phosphorylation-dependent manner. Evidence supporting these conclusions will be presented.

26. Molecular Aspects of Cardiac  $\text{Na}^+-\text{Ca}^{2+}$  Exchange KENNETH D. PHILIPSON, DEBORA A. NICOLL,\* ZHAOPING LI,\* JOY S. FRANK\* and DONALD HILGEMANN, *Cardiovascular Research Laboratory, University of California Los Angeles School of Medicine, Los Angeles, California; and Department of Physiology, University of Texas Southwest Medical Center, Dallas, Texas*

We have cloned and expressed the cardiac sarcolemmal  $\text{Na}^+-\text{Ca}^{2+}$  exchanger (Nicoll et al. 1990. *Science (Wash. DC)*. 250:562). The protein is modeled to have 12 transmembrane segments, a large intracellular loop, a cleaved signal peptide, and one glycosylation site. Short regions of the cardiac exchanger sequence have homology to regions of the  $\text{Na}^+, \text{K}^+$ -ATPase and the rod outer segment  $\text{Na}^+-\text{Ca}^{2+}, \text{K}^+$  exchanger. We are attempting to identify functionally important regions of the exchanger by deletion and site-directed mutations. An inhibitory peptide has been synthesized based on a region of the exchanger sequence that resembles a calmodulin-binding site (Li et al. 1991. *J. Biol. Chem.* 266:1014). The inhibitory peptide acts at the intracellular surface of the exchanger protein with a  $K_i$  between 0.15 and 1.5  $\mu\text{M}$ . The kinetics of the native and cloned exchanger have been analyzed electrophysiologically using the giant excised patch technique. The exchanger operates with a consecutive reaction mechanism. Charge movement is primarily associated with  $\text{Na}^+$  translocation (Hilgemann et al. 1991. *Nature (Lond.)*. 352:715). Immunolocalization studies indicate high levels of the  $\text{Na}^+-\text{Ca}^{2+}$  exchange protein in sarcolemma of the transverse tubules. This localization is possibly due to interactions of the exchanger with the cytoskeletal protein ankyrin (Frank et al. 1992. *J. Cell Biol.* In press). [Supported by NIH grant HL-27821.]

27. Characterization of the Na-K-Cl Cotransporter of Shark Rectal Gland BLISS FORBUSH III, CHRISTIAN LYTLE, JIAN-CHAO XU,\* JOHN PAYNE,\* MARK HAAS, EDWARD BENZ, JR.,\* and DAN BIEMESDERFER,\* *Departments of Cellular and Molecular Physiology and Internal Medicine, Yale University School of Medicine, New Haven, Connecticut; and Mount Desert Island Biological Laboratory, Salsbury Cove, Maine*

The Na-K-Cl cotransport system mediates the coupled movement of one Na<sup>+</sup>, one K<sup>+</sup>, and two Cl<sup>-</sup> ions across the plasma membrane of most animal cells. The salt-secreting rectal gland of the dogfish shark affords an excellent preparation for combined physiological and biochemical study of cotransport regulation, and membranes from this tissue are the richest known source of the cotransport protein. This report summarizes our progress over the last three years in characterizing the cotransporter. We achieved partial purification of the CHAPS-solubilized protein using DEAE Sepharose chromatography, and raised a battery of monoclonal antibodies using this material as antigen. The antibodies react with four different epitopes, based on differential reactivity with proteolytic fragments of the parent protein. All of the antibodies are suitable for Western blot analysis, ELISA, immunoprecipitation (monitored by bound [<sup>3</sup>H]benzmetanide), and immunofluorescence localization. Immunoaffinity columns using the antibodies permit a one-step purification of the 195-kD protein, the mass of which is reduced to ~135 kD by treatment with N-glycanase. Two of the antibodies were used to identify clones in a rectal gland cDNA library. A full-length clone encoding the 1,191-amino acid cotransport protein has been isolated, sequenced, and expressed in a mammalian cell line (Xu et al., this Symposium). The predicted sequence for a 129.8-kD protein includes five regions obtained by sequencing the trypsin-cleaved 195-kD protein; it includes a large central hydrophobic stretch of 460 amino acids presumed to form ~12 membrane-spanning domains. To investigate regulation of cotransport in the intact rectal gland cell we examined [<sup>3</sup>H]benzmetanide binding to collagenase-isolated tubules, finding that the amount of specific binding reflects the prevailing number of active transporters; we found a 10–30-fold increase in the level of [<sup>3</sup>H]benzmetanide binding ( $t_{1/2}$  ~3 min) upon stimulation with secretagogues that raise [cAMP], or with osmotic cell shrinkage, which does not. By manipulations of the ionic composition of the medium we have concluded that reduced [Cl<sup>-</sup>] appears to be both necessary and sufficient for activation of the Na-K-Cl cotransporter. Our data support a model in which [Cl<sup>-</sup>] is the essential regulating element in a pathway common to hormonal stimulation and shrinkage-induced activation. Protein kinase inhibitors were found to block activation of the cotransporter by both cAMP and cell shrinkage. To further investigate the role of phosphorylation, we labeled the cellular ATP pool with <sup>32</sup>P, and isolated the cotransporter by CHAPS solubilization and immunoprecipitation. <sup>32</sup>P was incorporated into the 195-kD protein on Thr<sub>189</sub> and several other residues. The level of incorporation increased dramatically upon stimulation, and under a wide variety of conditions the level of phosphorylation paralleled the level of cotransport activation. Our results strongly suggest that the cotransporter is activated by phosphorylation. [Supported by NIH grant AM-17433.]

28. The Melibiose Permease of *Escherichia coli*: Importance of the NH<sub>2</sub>-terminal Hydrophobic Domains for Na/Sugar Cotransport G. LEBLANC, T. POURCHER, and M. L. ZANI, *Laboratoire J. Maetz, Département de Biologie Cellulaire et Moléculaire, Commissariat à l'Energie Atomique, Villefranche-sur-mer, France*

The melibiose (mel) permease of *Escherichia coli* is a hydrophobic membrane protein that cotransports α-D-galactoside with either H<sup>+</sup>, Na<sup>+</sup>, or Li<sup>+</sup>, the monovalent cations increasing the affinity of the permease for the ligand. Secondary structure predictions suggest that mel permease contains 12 hydrophobic membrane segments in α-helical conformation. Domains and/or residues of the permease involved in catalysis are not yet identified. Site-directed mutagenesis was used to investigate the role of several acidic and polar amino acids, putatively located in the first four helices of the NH<sub>2</sub> terminus of the protein (Asp31, Tyr 24, 27, and 28 in helix I; Asp51 and 55 in helix II; Asn 83 in helix II; Asp 120, Tyr109, and 116 in helix IV). Individual replacement of D51, 55, and 120 with Cys or Asn, and Tyr116 with Phe completely abolishes Na<sup>+</sup>-dependent sugar transport. Importantly, however, the mutant permeases retain low affinity sugar binding (typical of H<sup>+</sup>-coupled reactions) and counter-transport activities, but the activities are independent of Na<sup>+</sup>. In addition,

(Asp31 → Asn)-permease, but not (Asp31 → Cys)-permease catalyzes Na<sup>+</sup>-coupled transport, but requires higher concentration of Na<sup>+</sup> for complete activation. Finally, mutations in the remaining Tyr residues or Asn83 have no effect. These observations suggest that: (a) the NH<sub>2</sub>-terminal domain of the mel permease is important for recognition of the coupling cation; and (b) Asp51, 55, 120, and Y116 (and probably D31) are at or near the Na<sup>+</sup>-binding site. The topological distribution of the acidic and polar residues proposed to be in the cationic binding site of mel permease was analyzed by constructing mel permease-alkaline phosphatase fusion proteins (Manoil and Beckwith, 1986, *Science* (Wash. DC), 233:1403). The results provide experimental support for their localization in membrane-spanning segments.

29. The Sodium/Glucose Cotransporter (SGLT1) ERNEST M. WRIGHT, *Department of Physiology, University of California, School of Medicine, Los Angeles, California*

SGLT1 belongs to an extended gene family of Na<sup>+</sup> cotransporters expressed in organisms from bacteria to man. Members include the mammalian nucleoside and myoinositol transporters and the bacterial proline and pantothenate transporters. Accumulation of these solutes in cells is driven by Na<sup>+</sup> electrochemical potential gradients, and phlorizin blocks sugar (glucose, myoinositol, and adenosine) transport. Identity of the primary amino acid sequences ranges from 22 to 100%, and similarity from 53 to 100%. The sequences differ most near the carboxy termini. Secondary structure analysis predicts that these proteins span the membrane ~12 times. Experimental challenges to the secondary structure are just emerging, and for SGLT1 two extracellular hydrophilic loops have been identified by N-linked glycosylation and proteolytic cleavage sites. We have begun to examine the functional significance of conserved residues. For example, an aspartic acid is conserved at the interface between the NH<sub>2</sub>-terminal and the first transmembrane segment (Asp<sub>28</sub>), and mutation of this residue severely impairs glucose transport. An Asp<sub>28</sub> to Asn<sub>28</sub> mutation accounts for glucose-galactose malabsorption syndrome in two sisters. Electrophysiological techniques are now being exploited to examine the pre-steady-state and steady-state kinetics of SGLT1 mutants. Transient charge transfer is used to monitor conformational changes in the empty carrier, and steady-state currents are used to measure the binding and translocation of Na<sup>+</sup> and sugar.

30. Structure and Function of the GABA Transporter BARUCH I. KANNER, SHOSMI KEYNAN, NICOLA MABJEESH, YOUNG-JIN SUH, and GARY RUDNICK, *Department of Biochemistry, Hadassah Medical School, The Hebrew University, Jerusalem, Israel; and Department of Pharmacology, Yale University School of Medicine, New Haven, Connecticut*

Synaptic transmission at most vertebrate synapses is thought to be terminated by a rapid uptake of the neurotransmitter into presynaptic nerve terminals or glial cell processes. Such uptake is catalyzed by sodium-coupled neurotransmitter transporter systems. The GABA transporter catalyzes cotransport of sodium, chloride, and GABA. The protein was purified from rat brain and reconstituted into liposomes in an active form. This glycoprotein migrates as an 80-kD polypeptide on SDS-PAGE. Using antibodies, the distribution of the transporter in rat brain has been studied by immunocytochemistry. It was found to be associated with neuronal GABA-ergic terminals. The transporter is inhibited by ACHC but not by β-alanine. We have, in collaboration with the laboratories of H. Lester (California Institute of Technology, Pasadena, CA) and N. Nelson (Roche Institute of Molecular Biology, Nutley, NJ), isolated and expressed a cDNA clone encoding for the GABA transporter. Subsequently, we studied the transient and stable expression of the cloned transporter in mammalian cells. Antibodies were raised against synthetic peptides corresponding to several regions of the GABA transporter. Upon papain or pronase treatment a reconstitutively active transporter can be isolated with lectin chromatography. On SDS-PAGE these fragments exhibit increased mobility, indicating an apparent reduction of 20 kD in molecular mass. The fragment obtained after pronase digestion reacts with the antibodies against the internal loops but not with those raised against amino and carboxy termini. We conclude that the amino- and carboxy-terminal parts of the transporter are not required for the transport function. This is confirmed by preliminary experiments using truncated clones lacking distinct parts of amino and carboxy termini. Conformational changes of the transporter have

been monitored using accessibility to pronase and monitoring the cleavage products with sequence-directed antibodies. The results indicate that in the presence of all three substrates, it goes from a "relaxed" to a "tight" conformation.

31. The Sodium/Iodide Symporter of the Thyroid Gland STEPHEN KAMINSKY,\* ORLIE LEVY,\* CAROLINA SALVADOR,\* and NANCY CARRASCO,\* *Department of Molecular Pharmacology, Albert Einstein College of Medicine, Bronx, New York*

The sodium/iodide symporter of the thyroid gland is a membrane protein responsible for the sodium-dependent active transport of iodide by the thyroid follicular cells, a process induced by thyroid-stimulating hormone (TSH) via cAMP. Iodide uptake is the first step in the biosynthesis of the thyroid hormones tri-iodothyronine (T3) and thyroxine (T4). Rat thyroid-derived FRTL-5 cells have been used extensively as a thyroid model system in culture. These cells display active accumulation of iodide to a ~40-fold concentration gradient in the presence of TSH. Withdrawal of the hormone from the medium (TSH [-] FRTL-5 cells) leads to a decline of intracellular cAMP and complete loss of iodide transport within 5–6 d. However, we report that mixed membrane vesicles prepared from TSH (-) FRTL-5 cells unexpectedly accumulate iodide, although to a lesser extent than mixed membrane vesicles from TSH (+) cells. Hence, TSH-(+) and (-) cells have been subjected to subcellular fractionation, and the resulting membrane fractions have been characterized by enzyme markers and assayed for iodide transport activity. Transport was observed to a significant degree only in the plasma membrane fraction from both TSH (+) and (-) cells. These results suggest that, in the absence of TSH, inactive sodium/iodide symporter molecules are present in FRTL-5 cells. The vesicle preparation process seems to mimic the effect of TSH. The absence of protease inhibitors during the vesicle preparation process enhances activation of the symporter in membrane vesicles from both TSH (+) and (-) cells. Thus, a proteolytic event may participate in the mechanism by which TSH stimulates iodide accumulation in the thyroid gland. [Supported by NIH grant DK-41544 and by the Pew Scholars Program in Biomedical Sciences.]

#### CONTRIBUTED PAPERS

32. Measurement of Okadaic Acid-sensitive Serine/Threonine Phosphatases in Rabbit Red Cells LAWRENCE C. STARKE,\* ANIL N. NAMBOODIRIPAD,\* and MICHAEL L. JENNINGS, *Department of Physiology and Biophysics, University of Texas Medical Branch, Galveston, Texas*

When rabbit red cells are swollen, they lose potassium via [K-Cl] cotransport. Activation of this cotransport pathway is blocked by doses of okadaic acid known to inhibit two serine/threonine phosphatases, type 1 (PP-1) and type 2A (PP-2A) (Cohen et al. 1990. *Trends Biochem. Sci.* 15:98). Okadaic acid has little effect on cotransport at doses that completely block PP-2A (0.5–1 nM; Cohen et al. 1990. *Trends Biochem. Sci.* 15:98), but half-maximally inhibits K (Rb) influx (40 nM; Jennings and Schulz. 1991. *J. Gen. Physiol.* 79:799) in the same concentration range where PP-1 is also half-maximally inhibited (10–20 nM; Cohen et al. 1990. *Trends Biochem. Sci.* 15:98). Therefore, cell swelling appears to activate [K-Cl] cotransport via a net dephosphorylation involving PP-1. The relative activities of PP-1 and PP-2A in lysates from rabbit red cells were measured directly as the rate of dephosphorylation of <sup>32</sup>P-labeled phosphorylase a. Nearly identical results were obtained from lysates of isotonic and swollen cells: 3 nM okadaic acid—a dose sufficient to inhibit only PP-2A—had no effect on the rate of dephosphorylation, whereas 100 nM—a dose sufficient to inhibit both PP-1 and PP-2A—inhibited by 60–70%. Thus, cell swelling appears to activate [K-Cl] cotransport via a net dephosphorylation that results from inhibition of a kinase rather than stimulation of a phosphatase. Autoradiographs of sodium dodecyl sulfate polyacrylamide gels revealed a number of endogenous

substrates whose rate of dephosphorylation is inhibited by enough okadaic acid (400 nM) to inhibit both PP-1 and PP-2A. In none of these bands, however, was the rate of dephosphorylation found to be markedly inhibited by concentrations of okadaic acid (3 nM) sufficient to inhibit only PP-2A. Furthermore, 400 nM okadaic acid inhibited dephosphorylation of some membrane proteins only when cytoplasm was present, but this drug had no effect on dephosphorylation of either membrane or cytoplasmic proteins alone. We conclude that PP-1 is more active than PP-2A in rabbit red cells, and most of the endogenous substrates for PP-1 appear to be found in the plasma membrane. [Supported by NIH grants R01 HL-37479 and F32 HL-08394.]

33. Expression of SGLT1 in Fetal Lamb Intestine JANE DYER,\* MOHSEN ANI,\* R. BRIAN BEECHEY,\* and SORAYA SHIRAZI-BEECHEY,\* *Epithelial Function and Development Group, Department of Biochemistry, University of Wales, Aberystwyth, Dyfed, Wales, United Kingdom*

We have shown that Na<sup>+</sup>-dependent D-glucose transport is regulated by diet during the normal postnatal development of lambs as well as by exposure to luminal sugar substrates in the adult ruminant sheep (Shirazi-Beechey et al. 1991, *J. Physiol. (Lond.)* 437:699). We have also demonstrated that infusion of the sugars D-glucose, methyl- $\alpha$ -D-glucose, 3, O-methyl-glucose and D-fructose directly into the intestine of the adult sheep induces the re-expression of the transport protein (SGLT1). However, 2-deoxy-D-glucose and D-mannitol do not induce expression (Lescale-Matys et al. *Biochem. J.*, submitted). In this study we have investigated the expression of SGLT1 in the intestine of 80–149 (term) d post-conception fetal lambs. Both the activity and the abundance of the SGLT1 protein is high in all these tissues. During transition from prenatal to postnatal development there are dramatic changes in the intestinal luminal contents. It is known that sheep amniotic fluid contains 9–11 mM D-fructose (Mellor and Slator. 1974. *Br. Vet. J.* 130:238). Fructose is the major sugar in the amniotic fluid. The possible role of fructose in regulating the activity and the abundance of SGLT1 is being investigated.

34. Intestinal Na<sup>+</sup>/Bile Salt Cotransport Is Regulated Posttranslationally JONATHAN G. L. MULLINS,\* R. BRIAN BEECHEY,\* and SORAYA SHIRAZI-BEECHEY,\* *Epithelial Function and Development Group, Department of Biochemistry, University of Wales, Aberystwyth, Dyfed, Wales, United Kingdom*

The Na<sup>+</sup>/bile salt cotransporter of the pig small intestine has been investigated in brush border membrane vesicles (BBMV) and expressed in *Xenopus laevis* oocytes. Na<sup>+</sup>-dependent taurocholate transport was found to be absent in BBMV prepared from the intestines of suckling piglets (14 d old), and restricted to the distal ileum in adult pigs. Na<sup>+</sup>/taurocholate transport in adult pig ileal BBMV was saturable ( $K_m$  40  $\mu$ M) and competitively inhibited by taurodeoxycholate and other bile salts. Injection of poly (A)<sup>+</sup> RNA isolated from all regions of adult pig small intestine resulted in the functional expression of Na<sup>+</sup> gradient stimulated taurocholate uptake within 2–5 d (Mullins et al. 1992. *Biochem. J.* in press). The expressed Na<sup>+</sup>-dependent taurocholate transport exhibited saturation kinetics ( $K_m$  48  $\mu$ M) and displayed similar competitive substrate inhibition by taurodeoxycholate as the native brush border protein. The finding that the mRNA coding for the cotransporter is present in enterocytes lining the whole length of the small intestine, but that the protein is only expressed in the brush border of the distal small intestine, suggests that the cellular synthesis of the cotransporter is regulated translationally or posttranslationally.

35. Effects of Charged Amino Acids on Membrane Insertion and Orientation of Truncated P-Glycoproteins as Studied by In Vitro Translation JIAN-TING ZHANG\* and VICTOR LING,\* *Division of Molecular and Structural Biology, Ontario Cancer Institute, Toronto, Ontario, Canada*

P-glycoprotein (Pgp) is a polytopic plasma membrane protein thought to function as a drug efflux pump. It is a member of a superfamily of structurally similar eukaryotic and prokaryotic ABC proteins

that transport a wide variety of substrates including ions, drugs, peptides, and proteins. Two functional groups of Pgp have been identified in mammalian cells. One group (classes I and II) is associated with MDR and the other (class III) is not. Transmembrane (TM) sequences in Pgp have been postulated to be important for determining drug specificity. Whether or not the membrane insertion and orientation of TM segments differ among the different classes of Pgp has not been examined directly. In this study we examined whether charged amino acids surrounding the TM11 and TM12 of Pgp play a role in determining the topology of Pgp using an in vitro transcription and translation system. Charged amino acids surrounding TM domains are thought to be important in determining the topology of membrane proteins. We observed that membrane insertion and orientation of MDR-associated Pgp (classes I and II) differ from the non-MDR-associated Pgp (class III). The positively charged amino acids surrounding TM11 and TM12 of these two forms of Pgp are different. By site-directed mutagenesis we showed that these amino acids affect the membrane insertion and orientation of these TMs. We speculate that a difference in membrane anchorage may be the underlying cause for the functional difference between the two groups of Pgp. [Supported by the National Cancer Institute of Canada and by NIH grant CA-37130.]

**36. Role of the Cystic Fibrosis Conductance Transmembrane Regulator (CFTR) in the pH Homeostasis of Endomembranes** GERGELY L. LUKACS, XIU-BAO CHANG,\* NORBERT KARTNER,\* KEVIN FOSKETT, JOHN R. RIORDAN,\* and SERGIO GRINSTEIN, *Research Institute, Hospital for Sick Children, Toronto, Ontario, Canada*

Acidification of several intracellular organelles (e.g., endosomes, lysosomes, coated vesicles) is mediated by the electrogenic vacuolar H<sup>+</sup>-ATPase. It has been proposed that, by electrically limiting H<sup>+</sup> pumping, Cl<sup>-</sup> conductance is the primary determinant of intraorganellar pH. Accordingly, if the purported Cl<sup>-</sup> channel CFTR were present in endomembranes, its activation would promote acidification. When using conductive protonophores, the net H<sup>+</sup> flux across membranes is limited by the movement of counterions. Thus, counterion (e.g., Cl<sup>-</sup>) permeability of endomembranes could be estimated indirectly from the changes in luminal pH. To determine endomembrane pH in Chinese hamster ovary (CHO) cells stably expressing CFTR, endosomes and lysosomes were labeled selectively in situ with pH-sensitive fluorescein dextran derivatives. Localization of the dye in the appropriate compartment was verified by subcellular fractionation and marker enzyme assays. Fluorescence was determined in suspensions of cells or isolated organelles or by single cell imaging. Measurements in situ and in cell-free microsomal preparations indicate the presence of a protein kinase A (PKA)-activated anion conductance in endosomes from CHO cells transfected with CFTR, but not in wild type or mock-transfected cells. In endosomes isolated from CFTR-expressing cells, the stimulatory effect of PKA was diminished by a specific peptide inhibitor of PKA, by alkaline phosphatase treatment, or by a monoclonal antibody against the second nucleotide binding fold of CFTR. Increasing counterion permeability by phosphorylation of CFTR or by addition of valinomycin failed to alter the rate or extent of endosomal acidification in situ. These observations indicate that functional CFTR, susceptible to activation by PKA, is present in endosomes. More importantly, the data suggest that factors other than counterion permeability are the major determinants of endosomal pH. In contrast to endosomes, the PKA-activated anion conductance was not detectable in the lysosomal compartment. Endosomal CFTR may cycle back to the plasma membrane or may be degraded and inactivated in the lysosomes.

**37. Cellular Regulation of ATP- and Calcium-sensitive K Channels in Frog Skin and Distal Renal Cell Culture (A6) Epithelia** BRIAN J. HARVEY and VALÉRIE URBACH,\* *Département de Biologie Cellulaire et Moléculaire, Commissariat à l'Energie Atomique, Laboratoire Jean Maetz, Villefranche-sur-mer, France*

Principal (P) cells of isolated frog skin epithelium and A6 monolayers mounted in Ussing chambers and bathed in standard amphibian Ringer solution recycle K<sup>+</sup> across the basolateral membranes (BLM) via an ATP-sensitive, 25-pS inward-rectifier K<sup>+</sup> channel (K<sub>ATP</sub>) (Harvey et al. 1991. *J. Physiol.*

(Lond.). 438:264p). The maintenance of equilibrium (cross-talk) between transepithelial Na transport (J<sub>Na</sub>) and K recycling involves a concerted action of cellular signals which were investigated using the patch-clamp technique. The open probability ( $P_o$ ) of single  $K_{ATP}$  channels in excised inside-out patches was reduced by cytosolic  $H^+$  ( $pK = 7.2$ ),  $Ca^{2+}$  ( $K_i \approx 180 \mu M$ ), and reactivated after run-down by GTPyS ( $10 \mu M$ ). The  $K_{ATP}$  channel activity is inhibited by  $Ba^{2+}$  but is insensitive to tetraethylammonium (TEA) and quinidine. Aldosterone ( $10 nM$ ) produces rapid ( $< 20 min$ ) activation of  $K_{ATP}$  channels in previously quiescent principal cell-attached patches, which is accompanied by an intracellular alkalinization from  $pH_i$   $7.23 \pm 0.09$  to  $7.45 \pm 0.05$  ( $n = 11$ ) measured with double-barreled  $H^+$ -sensitive microelectrodes. The hormone-induced increases in  $P_o$  and  $pH_i$  are inhibited by amiloride ( $10^{-5} M$  added to basolateral side) and may be mediated by activation of the BLM  $Na^+/H^+$  exchanger.  $K_{ATP}$  channels are under metabolic control and  $P_o$  is reduced by cytosolic ATP with a  $K_i$  in the range of  $30-80 \mu M$ , which shifts into the millimolar range when physiological levels of ADP ( $100 \mu M$ ) are also present. The Na/K pump accounts for  $> 60\%$  of  $O_2$  consumption in tight epithelia and has an important role in determining the intracellular ATP/ADP ratio which may be of most relevance in coupling the activity of pump and channel. Exposure of P cells and A6 cells to hypo-osmotic (200 mosM) Ringer solution activates a stretch-sensitive, 26 pS inward-rectifier  $Ca^{2+}$  channel (SACa) in the BLM. The SACa channel is blocked by gadolinium ions ( $10 \mu M$ ) and becomes permeable to  $K^+$ ,  $Na^+$ , or  $Ba^{2+}$  in low ( $< 100 \mu M$ ) external  $Ca^{2+}$ . Hypotonic shock, oxytocin ( $50 mU/ml$ ), or dibutyl-cAMP ( $100 \mu M$ ) activate a TEA-sensitive, 35-pS outward-rectifier  $K^+$  channel ( $K_{Ca}$ ), with  $P_o$  increased by raised cytosolic  $Ca^{2+}$  ( $K_i \approx 380 \mu M$ ). Measurements of membrane capacitance and TEA-sensitive noise in the "slow" whole-cell patch-clamp mode indicate that  $K_{Ca}$  channels are inserted into the BLM by  $Ca^{2+}$ -dependent exocytosis.

38. Charge Translocation Associated with Conformational Transitions of the  $Na^+$ /Glucose Cotransporter DONALD D. F. LOO,\* AKIHIRO HAZAMA,\* STEPHANE SUPPLISSON,\* ERIC TURK,\* and ERNEST M. WRIGHT, *Department of Physiology, School of Medicine, University of California, Los Angeles, Los Angeles, California*

The cloned human  $Na^+$ /glucose cotransporter expressed in *Xenopus* oocytes exhibits a slow transient outward current when the membrane potential is rapidly depolarized in the absence of sugar. We have isolated these currents from the capacitive and leakage currents and determined their dependence on holding ( $V_h$ ) and test ( $V_t$ ) potentials. For both positive and negative voltage steps from  $V_h$ , pre-steady-state currents rapidly rose to a peak ( $\sim 1 ms$ ) before decaying to the steady state (1–10 ms).  $Q$ , the total charge obtained as the integral of the current transients, was equal for the on and off responses. For each  $V_h$ ,  $Q$  showed a sigmoidal dependence on  $V_t$  and the maximal charge transfer,  $Q_{max}$ , was independent of  $V_h$ .  $Q_{max}$  gives an index of the carrier density  $C_T$  since  $Q_{max} = C_T z_c e$  ( $z_c$  is the carrier valence and  $e$  is elementary charge). Moreover, since the maximal steady-state, sugar-induced current  $I_{max} = k C_T z_c e$ , the apparent rate constant  $k$  for the translocation of the sugar-loaded carrier from the external to the internal membrane surface can be estimated from the ratio  $I_{max}/Q_{max}$ . For example, for an oocyte with an apparent  $I_{max} = 750 nA$ , where  $Q_{max}$  was  $17 \times 10^{-9} C$ ,  $k$  was  $\sim 45 s^{-1}$ . This agrees with previous estimates from analysis of steady-state kinetics. We conclude that pre-steady-state currents are due to the conformational transitions of a negatively charged carrier between the external and internal membrane surfaces. Studies of the charge translocation together with steady-state currents can provide unique information on individual steps of the transport process.

39. Secondary Structure of the  $Na^+$ /Glucose Cotransporter BRUCE A. HIRAYAMA,\* CHARI D. SMITH,\* and ERNEST M. WRIGHT, *Department of Physiology, School of Medicine, University of California, Los Angeles, Los Angeles, California*

The major  $Na^+$ -dependent glucose transporter of the rabbit and human intestine (SGLT1) has been cloned, sequenced, and expressed in several types of cells. Analysis of the primary amino acid sequence suggests that the 662-residue protein spans the plasma membrane 11–12 times. So far,

limited experimental information is available about the validity of the proposed secondary structures: Asn248 is glycosylated, which indicates that the hydrophilic region Glu229-Thr271, between proposed helices 5 and 6, is on the external face of the membrane. This restriction places the NH<sub>2</sub> terminus on the cytoplasmic face. To further test the secondary structure predictions, we have begun to map externally exposed segments of SGLT1. Our strategy is to treat sealed, right-side-out brush border vesicles with proteases (thus restricting cleavage to external sites), identify specific proteolytic fragments of SGLT1 using anti-peptide antibodies on Western blots, and purify the fragments for amino acid analysis and NH<sub>2</sub> terminal sequencing. Chymotrypsin produced a major 14-kD fragment recognized by one anti-peptide antibody (Arg602-Asp613) but not another (Ser402-Lys420). This fragment was purified by immunoprecipitation and SDS-PAGE. NH<sub>2</sub>-terminal sequencing revealed that the cleavage was at Trp561, and amino acid analysis suggested that the peptide extends through the COOH terminus. These results indicate that the large hydrophilic region Thr548-Arg640 is on the external face of the protein, and provides support for a structure composed of 12 membrane-spanning domains. We are pursuing these studies with endoproteases and peptide antibodies with different specificities to further elucidate SGLT1's topology and intramolecular associations.

40. Insulin Activates Red Blood Cell Na/Li and Na/H Exchanges by Increasing the  $K_m$  for External Na GIANPAOLO ZERBINI, ROBERTO PONTREMOLI, ALICIA RIVERA, and MITZY CANESSA, *Endocrine-Hypertension Division, Brigham and Women's Hospital, and Harvard Medical School, Boston, Massachusetts*

Early studies on the regulation of Na/H exchange (EXC) by insulin in skeletal muscle led us to examine its action on this antiporter in human red blood cells (RBC) that possess well-characterized insulin receptors. Na/H EXC activity was studied in RBCs of fasted subjects varying intracellular (i) pH between 6 and 7 and external (e) Na between 0 and 150 mM. Upon incubation with 50  $\mu$ U/ml insulin for 1 h, the  $V_{max}$  of Na<sub>e</sub>/H<sub>i</sub> EXC increased from  $28 \pm 6$  to  $49 \pm 8$  U (U = mmol/liter cells per h;  $M \pm SE$ ,  $n = 10$ ,  $P < 0.0005$ ), the  $K_m$  for Na<sub>e</sub> increased from  $72 \pm 10$  to  $142 \pm 19$  mM ( $n = 4$ ,  $P < 0.05$ ), and the  $K_m$  for H<sub>i</sub> did not change. Insulin stimulation of Na<sub>e</sub>/H<sub>i</sub> EXC was dose dependent, occurring at physiologic concentrations (30–100  $\mu$ U/ml). Insulin did not affect Na<sub>e</sub>/Li<sub>i</sub> EXC activity at pH<sub>i</sub> = pH<sub>e</sub> = 7.4, 150 mM Na<sub>e</sub>, but induced a significant increase of the calculated  $V_{max}$  from  $0.34 \pm 0.03$  to  $0.45 \pm 0.04$  U ( $n = 10$ ,  $P < 0.005$ ) and a twofold increase in the  $K_m$  for Na<sub>e</sub> from  $31 \pm 3$  to  $76 \pm 10$  mM. Insulin modulation of Na<sub>e</sub>/H<sub>i</sub> and Na<sub>e</sub>/Li<sub>i</sub> EXC did not require Ca<sub>e</sub>, but its kinetic effects were mimicked by okadaic acid, a phosphatase inhibitor that also increased the  $K_m$  for Na<sub>e</sub>. The marked effects of insulin action on the Na<sub>e</sub> affinity of both Na EXC modes provides further evidence that Na<sub>e</sub>/Li<sub>i</sub> EXC is a mode of operation of Na<sub>e</sub>/H<sub>i</sub> EXC. We hypothesize that insulin activates Na<sub>e</sub>/H<sub>i</sub> EXC by inhibiting the dephosphorylation of the antiporter by a Na-dependent phosphatase. In our proposed model of Na<sub>e</sub>/H<sub>i</sub> EXC, different Na sites (Na<sub>i</sub> and Na<sub>e</sub> sites) control its turnover rate. Agonist-induced activation of the antiporter by PKC phosphorylation produces a high-affinity Na<sub>e</sub> site, while insulin-induced inhibition of antiporter dephosphorylation generates low-affinity Na<sub>i</sub> sites which facilitate Na release into the cytosol and sequential occupancy by H<sub>i</sub>.

41. Identification of Amino Acids Involved in the Amiloride Binding Site of the Na<sup>+</sup>/H<sup>+</sup> Exchanger LAURENT COUNILLON,\* ARLETTE FRANCHI,\* and JACQUES POUYS-SEGUR, *Centre de Biochimie, Université de Nice, Nice, France*

Using proton-killing procedures, we have selected a cell line expressing a mutated Na<sup>+</sup>/H<sup>+</sup> exchanger possessing a lower affinity for its inhibitors, amiloride and 5-amino substituted derivatives. To investigate amino acids involved in amiloride binding, we cloned the cDNA coding for this mutated antiporter and compared its sequence to the wild-type one. This approach allowed us to identify one point mutation changing a leucine into a phenylalanine at position 167 in the fourth transmembrane domain of the antiporter. When introduced by site-directed mutagenesis into the wild-type cDNA, this single change was able to confer the mutant phenotype to the encoded protein.

indicating that this amino acid is involved in the binding of amiloride. The four cloned  $\text{Na}^+/\text{H}^+$  exchanger isoforms (NHE1-4) which possess different pharmacological profiles exhibit primary sequence differences in the previously identified amiloride binding region. To determine which of these amino acids are contacting amiloride, we introduced these changes into the NHE1 isoform. The substitution of a phenylalanine by a tyrosine in position 165 was able to reduce the affinity for amiloride, therefore showing that amiloride also contacts this position.

42. Monoclonal Antibody against Red Blood Cell CHIP 28 Protein MICHAEL L. JENNINGS,\* *Department of Physiology and Biophysics, University of Texas Medical Branch, Galveston, Texas* (Sponsor: Luis Reuss)

Agre and co-workers have recently characterized a human red cell membrane protein known as CHIP 28 (Preston and Agre, 1991, *Proc. Natl. Acad. Sci. USA*, 88:11110). Expression of CHIP 28 in oocytes causes an increase in water permeability (Preston et al. 1992, *Science (Wash. DC)*, 256:385). CHIP 28 is a member of a superfamily that includes proteins from mammals, insects, higher plants, and bacteria. Of these proteins, the one for which a function is most clearly defined is the glycerol carrier of *E. coli* (Sweet et al. 1990, *J. Bacteriol.* 172:424). Human red cells exhibit a high rate of carrier-mediated glycerol permeability. It is therefore possible that the function of red cell CHIP 28 is as a glycerol transporter. We have raised a monoclonal antibody against rabbit CHIP 28. The antibody recognizes both the glycosylated and nonglycosylated forms of the protein. The antibody was immobilized on Sepharose and was used to purify CHIP 28 from dog red cell membranes. The  $\text{NH}_2$ -terminal sequence of the purified protein is A S E F K K K L F, which is identical to that determined by Agre and co-workers for human CHIP 28. This confirms that the antibody is in fact directed against CHIP 28 and that dog CHIP 28 has been processed similarly to that of human; i.e., the initiator methionine has been removed. The presence of CHIP 28 in dog red cells is of interest because, unlike those of human and rabbit, dog red cells have no detectable carrier-mediated glycerol transport. Since dog red cells have large amounts of CHIP 28 but do not have a functioning glycerol transporter, it is unlikely that the function of CHIP 28 is glycerol transport. The most probable function is as a water channel. [Supported by NIH grant R01 GM-26861.]

43. Changes in Intracellular  $\text{Ca}^{2+}$  Concentration Induced by Inositol 1,4,5 Trisphosphate in Human Malignant Hyperthermia Skeletal Muscle CARMEN PEREZ,\* JOSE LOPEZ,\* MIGUEL ALFONZO,\* NANCY LINARES,\* and PAUL ALLEN, *Laboratorio de Fisiopatología Muscular, Instituto Venezolano de Investigaciones Científicas, Caracas, Venezuela*

Malignant hyperthermia (MH) is a pharmacogenetic disorder of skeletal muscle triggered when susceptible subjects are exposed to volatile anesthetic agents and/or depolarizing muscle relaxants. We have used  $\text{Ca}^{2+}$ -selective microelectrodes to measure in vitro the effects of  $\text{InsP}_3$  on intracellular  $[\text{Ca}^{2+}]_i$  in intact human skeletal muscle fibers obtained from nine MH susceptible subjects (six females and three males) and from six nonsusceptible subjects (four males and two females). In quiescent nonsusceptible muscle fibers the microinjection of 0.5 or 1  $\mu\text{M}$  of  $\text{InsP}_3$  induced a transient increment in resting calcium, from  $0.12 \pm 0.01$  to  $0.37 \pm 0.03 \mu\text{M}$  and from  $0.11 \pm 0.01$  to  $0.81 \pm 0.04 \mu\text{M}$ , respectively. In MH susceptible muscle fibers microinjection of  $\text{InsP}_3$  produced a qualitatively similar, but much greater and sustained, effect on  $[\text{Ca}^{2+}]_i$  (from  $0.32 \pm 0.02$  to  $1.32 \pm 0.08 \mu\text{M}$  with 0.5  $\mu\text{M}$   $\text{InsP}_3$ , and from  $0.36 \pm 0.02$  to  $1.48 \pm 0.10 \mu\text{M}$  with 1  $\mu\text{M}$  of  $\text{InsP}_3$ ). We observed a local contraction around the microinjection sites. The  $\text{InsP}_3$  effect was not associated with changes in resting membrane potential. Incubation of muscle fibers in 50  $\mu\text{M}$  Dantrolene for 20 min before the microinjection of  $\text{InsP}_3$  blocked the observed effects of  $\text{InsP}_3$  on  $[\text{Ca}^{2+}]_i$ . This study shows that microinjection of  $\text{InsP}_3$  into intact human skeletal muscle induced calcium release from intracellular stores that were greater in MH susceptible fibers than in control. In addition, Dantrolene inhibits the effects of  $\text{InsP}_3$ . These results allow us to suggest that  $\text{InsP}_3$  plays an important role in the pathophysiology of this syndrome and suggest its possible role as chemical messenger in excitation-

contraction coupling in normal skeletal muscle. [Partially supported by a grant from Angelini Pharmaceuticals.]

44. Changes in Skeletal Muscle  $[Na^+]_i$  and  $[Ca^{2+}]_i$  Related to the Insulin-sensitive Cation Channel J. E. M. McGECH,\* A. MORIELLI,\* and G. GUIDOTTI, *Department of Biochemistry and Molecular Biology, Harvard University, Cambridge, Massachusetts*

Changes in  $[Ca^{2+}]_i$  and  $[Na^+]_i$ , associated with the function of an insulin-sensitive cation channel (McGeoch and Guidotti. 1992. *J. Biol. Chem.* 267:832) were monitored by quantitative fluorescence imaging of isolated neonatal soleus muscle loaded with Fura-2 (to detect  $[Ca^{2+}]_i$ ) and SBFI (to detect  $[Na^+]_i$ ). External application of 1–10 nM insulin to the muscle caused a transient  $38 \pm 14$  nM rise in  $[Ca^{2+}]_i$ , which was inhibited by external application of  $\mu$ -conotoxin (inhibitor of the cation channel) and not by tetrodotoxin. The insulin-dependent  $[Ca^{2+}]_i$  rise was dependent on mM  $[Ca^{2+}]_o$ , as reducing  $[Ca^{2+}]_o$  to  $< 100$  nM with BAPTA eliminated the rise. The return of  $[Ca^{2+}]_i$  after insulin, to the baseline level (80–100 nM) was dependent on  $[Na^+]_o$ , suggesting  $Na^+/Ca^{2+}$  exchanger involvement. (Replacing  $[Na^+]_o$  with *N*-methyl-D-glucamine increased the decay constant of the  $[Ca^{2+}]_i$  rise from  $17.2 \pm 1.4$  to  $32.4 \pm 5$  s). The  $[Na^+]_i$  response to insulin involved a transient decrease in the ion with a similar time constant to the transient  $[Ca^{2+}]_i$  rise. This transient  $[Na^+]_i$  decrease, like the  $[Ca^{2+}]_i$  rise, was inhibited by  $\mu$ -conotoxin and not by TTX. The insulin-sensitive cation channel is known to be strongly inhibited by a rise in  $[Ca^{2+}]_i$ . It appears that the transient decrease in  $[Na^+]_i$  is due to the interruption of a steady background  $Na^+$  entry (via the cation channel) by the transient  $[Ca^{2+}]_i$  rise. This demonstrates that the control of  $[Na^+]_i$  is mediated by  $Ca^{2+}$ . Insulin also affects the  $[Ca^{2+}]_i$  rise of excitation-contraction (EC) coupling. A  $495 \pm 127$  nM  $[Ca^{2+}]_i$  rise is decreased to  $139 \pm 101$  nM when the muscle is pretreated with insulin before a depolarizing dose of KCl. However, if the protein kinase inhibitor HA1004 is given before insulin, then there is no reduction in the EC coupling  $[Ca^{2+}]_i$  rise ( $475 \pm 176$  nM). [Supported by NIH grant DK-27626 to G. Guidotti.]

45. Na-K-2Cl Cotransport in Vascular Endothelial Cells Is Regulated by Protein Phosphorylation PAMELA B. PERRY,\* JANET D. KLEIN,\* and W. CHARLES O'NEILL, *Renal Division, Department of Medicine, and Department of Physiology, Emory University School of Medicine, Atlanta, Georgia*

Na-K-2Cl cotransport in bovine aortic endothelial cells is activated by cell shrinkage and mediates regulatory volume increase (O'Neill and Klein. *Am. J. Physiol.* 262:C436). The role of protein phosphorylation was examined using inhibitors of protein phosphatases and protein kinases. Okadaic acid (OKA) and calyculin (CAL) stimulated cotransport (bumetanide-sensitive K flux) in isotonic medium; CAL (a more potent inhibitor of type 1 protein phosphatase) was 25-fold more potent than OKA. Activation by CAL was immediate, complete by 5 min, and not associated with any change in cell ion content. OKA and CAL had no effect in shrunken cells, indicating that the effects of shrinkage and phosphatase inhibition on cotransport are not additive. Activation of cotransport by CAL was delayed in swollen cells ( $8.0 \pm 0.3$  vs.  $4.4 \pm 0.4$  min), suggesting that phosphorylation is volume sensitive. Activation of cotransport by shrinkage (isotonic  $\rightarrow$  hypertonic medium) was more rapid ( $6.4 \pm 0.5$  vs.  $8.3 \pm 0.5$  min) than inactivation (hypertonic  $\rightarrow$  isotonic medium), consistent with phosphorylation rather than dephosphorylation as the volume-sensitive step. ML-7, an inhibitor of myosin light chain kinase, blocked activation of cotransport by shrinkage without inhibiting basal cotransport activity. Calphostin and staurosporine, inhibitors of protein kinase C, reduced basal cotransport activity but not the stimulation by shrinkage. K252a, a nonspecific protein kinase inhibitor, reduced basal cotransport activity and the activation by shrinkage. We conclude that, in vascular endothelial cells, Na-K-2Cl cotransport is activated by protein phosphorylation and that the phosphorylation is regulated by cell volume. Both the phosphorylation and dephosphorylation reactions are constitutively active. The differing kinase inhibitor profiles suggest that separate kinases are responsible for basal and shrinkage-activated cotransport activity. [Supported by NIH grant DK-01643 and the American Heart Association of Georgia.]

46. Identification of a mRNA and Screening of a Library from Human Skeletal Muscle Tissue for a Gene Homologous to the Novel  $\text{Ca}^{2+}$ -mobilizing Enzyme from *Aplysia* Eggs HOLLY GROELLE\* and FELIX STRUMWASSER, Laboratory of Neuroendocrinology, Marine Biological Laboratory, Woods Hole, Massachusetts

An ADP ribosyl cyclase that generates cyclic ADP-ribose (cADPR) and nicotinamide from NAD has been isolated from *Aplysia californica* ovotestis. The cDNA was cloned and the primary structure determined (Hellmich and Strumwasser. 1991. *Cell Regul.* 2:193; Glick et al. 1991. *Cell Regul.* 2:211). This enzyme is unique in that it produces cADPR, rather than ADPR, from NAD. Cyclic ADPR is a potent  $\text{Ca}^{2+}$ -mobilizing agent, as or more effective than  $\text{IP}_3$  in releasing  $\text{Ca}^{2+}$  from internal stores in a sea urchin egg extract (Dargie et al. 1990. *Cell Regul.* 1:279). We are interested in determining if there is a homologous human gene for this novel second messenger enzyme. We probed Northern blots of human poly (A)<sup>+</sup> mRNA isolated from various tissues (heart, brain, placenta, lung, liver, skeletal muscle, kidney, pancreas) (Clontech Laboratories, Inc., Palo Alto, CA) with a hexanucleotide primer-labeled 1.2-kb cDNA clone from *Aplysia*. The probe contained the complete coding sequence plus 333-bp 3' to the coding region. Under conditions of moderately high stringency a transcript of ~4 kb was identified in human skeletal muscle on the Northern blots. The *Aplysia* mRNA transcript is 1.85 kb. A human skeletal muscle library (Clontech) is presently being screened and positive clones have been identified using a 1-kb Nru I/Xho I fragment of the *Aplysia* clone which includes 258 bp 3' to the coding region. [Supported by a grant from The Rockefeller Foundation.]

47. Expression of  $\text{Na}^+$ -dependent AIB Transporter in *Xenopus* Oocytes GUORONG LIN, JOHN I. McCORMICK, and ROSE M. JOHNSTONE, Department of Biochemistry, McGill University, Montreal, Quebec, Canada

We have been studying the purification and reconstitution of the  $\text{Na}^+$ -dependent A transport system. The system is characterized by its unique capacity to tolerate methylation of the amino group in its transported substrates. Using this characteristic as a guide, we have initiated attempts to express this system in *Xenopus* oocytes. For these studies, GF-14 lymphocytes (obtained from Dr. E. Adeberg, Yale University) have been used as a source of mRNA. Injection of mRNA from GF-14 cells into oocytes resulted in the expression of MeAIB-inhibitable,  $\text{Na}^+$ -dependent AIB transport. Attempts to obtain expression of AIB transport with mRNA from Ehrlich cells, the cell line used for purification and reconstitution studies, were not successful. In GF-14 cells pretreated with 10  $\mu\text{g}/\text{ml}$  of insulin, expression of  $\text{Na}^+$ -dependent, MeAIB-inhibitable transport of AIB was increased 2.5-fold over controls. mRNA extracted from the insulin-treated cells and injected into oocytes induced a similar increase in transport when compared with mRNA from untreated GF-14 cells. Poly A RNA, isolated from GF-14 cells treated with insulin, was fractionated on a 5–33% sucrose gradient to obtain the approximate size of the active mRNA fraction. The peak of transport activity was obtained with a 2–2.2-kb fraction of mRNA. The expressed transport system has characteristics of the system A transport, including  $\text{Na}^+$  dependence and complete inhibition by MeAIB, methionine, and serine. A cDNA library was constructed with the Superscript system from the active mRNA fraction. About  $1.5 \times 10^4$  colonies were obtained (22 pools). Primary screening showed capped cRNA only from one pool of DNA capable of inducing  $\text{Na}^+$ -dependent AIB transport with MeAIB sensitivity. Attempts are underway to identify the cDNA for the A system transporter.

48. Structure-Function Analysis of the Catalytic Loop of Gastric ( $\text{H}^+$ ,  $\text{K}^+$ )-ATPase JEAN CLAUDE ROBERT,\* DENIS BAYLE,\* MIGUEL LEWIN,\* and ANNICK SOUMAR-MON,\* Institut National de la Recherche Scientifique U10, Hôpital Bichat, Paris, France

We raised a monoclonal antibody (mAb 95–111) against the catalytic subunit  $\alpha$  of ( $\text{H}^+$ ,  $\text{K}^+$ )-ATPase. The epitope is cytoplasmic (Bayle et al. 1992. *Comp. Biochem. Biophys.* 101B:519) and its titration by  $^{125}\text{I}$  mAb 95–111 indicated a  $K_D$  of  $2 \times 10^{-9}$  M. By restricting the cDNA of  $\alpha$  and expressing the fragments in *Escherichia coli* we were able to map the epitope between amino acids 529 and 561 (Bayle et al. 1992. Submitted), i.e., in the catalytic loop between M4 and M5 (Shull et al. 1986. *J. Biol. Chem.*

261:16788) close to the putative ATP and FITC binding site (Lys<sub>518</sub>). mAb 95-111 inhibits (H<sup>+</sup>,K<sup>+</sup>)-ATPase activity in a noncompetitive manner with respect to ATP, suggesting no overlapping of the epitope and ATP sites. Inhibition was, however, competitive with respect to luminal binding of K<sup>+</sup>, suggesting involvement of the epitope in the transmission of K<sup>+</sup> activation from lumen to catalytic loop. The binding of FITC inhibited 75% of ATPase activity and increased mAb 95-111 binding capacity by 50%, indicating the existence of hidden epitopes in the native ATPase. Since hidden epitopes are inaccessible to small hydrophilic denaturing agents, they are likely to be embedded in a hydrophobic pouch. These results show that the cytoplasmic sequence between amino acids 529 and 561 plays a role in the stimulation of Asp<sub>385</sub> dephosphorylation by luminal K<sup>+</sup> probably by changing conformation in the course of the E1-E2 cycle. Since FITC unmasks epitopes on the one hand and induces E1 on the other, we suggest that the 529-561 sequence is externalized in E1 and molecule-embedded in E2-P.

49. Functional Expression of a Rat Anion Exchanger (AE2) in Insect Cells by a Recombinant Baculovirus XINJUN HE,\* XIAOZAI WU,\* LAWRENCE A. TABAK,\* and JAMES E. MELVIN,\* *Departments of Biochemistry and Dental Research, University of Rochester, Rochester, New York* (Sponsor: Dr. Philip Knauf)

Detailed structural and functional characterization of anion exchangers in mammalian cells would be greatly facilitated by expression of the cloned anion exchanger (AE) cDNAs in heterologous systems. Unfortunately, the widespread endogenous expression of Cl<sup>-</sup>/HCO<sub>3</sub><sup>-</sup> exchange and the low turnover number of electroneutral transport have hindered such studies. We have used the baculovirus-insect cell-based transient expression system to overcome these problems. A recombinant baculovirus, *Autographa californica* nuclear polyhedrosis virus, containing the full-length rat AE2 coding sequence under control of the polyhedrin promoter, was constructed. The recombinant virus was used to infect the insect cell line Sf9, derived from the army worm caterpillar *Spodoptera frugiperda*. The expression of Cl<sup>-</sup>/HCO<sub>3</sub><sup>-</sup> exchange activity was determined by intracellular pH measurements in individual infected cells loaded with the pH-sensitive fluorescent dye, 2',7'-bis(carboxyethyl)-5,6-carboxyfluorescein. The Sf9 insect cells or the wild-type baculovirus-infected cells had little detectable Cl<sup>-</sup>/HCO<sub>3</sub><sup>-</sup> exchange activity. Anion exchange activity in the recombinant virus-infected cells appeared as early as 24 h after infection and continued over the next 3 d. The expressed AE2 anion exchange activity was inhibited by >80% when 250 μM 4,4'-diisothiocyanostilbene-2,2'-disulfonate (DIDS) was added to the incubation medium. After exposure to DIDS for 3 min in pH 7.4 physiological saline at room temperature, the inhibition was reversed by simply washing away DIDS for 5 min. These results indicate that the rat AE2 protein produced in the recombinant virus-infected insect cells is inserted into the membrane in a biologically active form and appears suitable for structural and functional studies. The baculovirus system, which has been used successfully for high-level expression of soluble proteins from higher eukaryotes, may be appropriate for producing large amounts of cloned anion exchanger proteins as well. [Supported by NIH grant R01 DE-09692.]

50. The Formation of the Translocation Complex on the (Na<sup>+</sup> + Cl<sup>-</sup>)-coupled GABA<sub>A</sub> Transporter Renders It in a Form Resistant to Cleavage by Pronase NICOLA J. MABJEESH and BARUCH I. KANNER, *Department of Biochemistry, Hadassah Medical School, The Hebrew University, Jerusalem, Israel*

Membrane vesicles from rat brain were digested with pronase. The proteolytic fragments of the sodium- and chloride-coupled GABA<sub>A</sub> transporter were analyzed with a variety of sequence-directed antibodies generated against the GABA<sub>A</sub> transporter. The major fragments detected by the various antibodies had an apparent size of ~10 kD. When protease treatment was carried out in the presence of GABA, the generation of these fragments was almost completely blocked. This was paralleled by an increase in reconstitutable GABA transport activity. The effect was specific for GABA and was not observed with a variety of other neurotransmitters and analogues. Furthermore, this protection was

seen only in the presence of both sodium and chloride, the cosubstrates of the transporter. It was not observed when GABA was present only from the inside. The results indicate that the transporter can exist in at least two conformations. In the absence of one or more of the substrates, many epitopes located throughout the transporter are accessible to the protease. In the presence of all three substrates it goes from a "relaxed" to a "tight" conformation and these epitopes become inaccessible to protease action.

51. Intracellular pH Regulation in J774.1 Murine Macrophages LESLIE C. MCKINNEY and ARIE MORAN, *Department of Physiology, Armed Forces Radiobiology Research Institute, Bethesda, Maryland; and Department of Physiology, Ben Gurion University of the Negev, Beersheba, Israel*

This study examines whether, under nominally bicarbonate-free conditions, inhibitors of vacuolar type H-ATPases can affect intracellular pH ( $\text{pH}_i$ ) homeostasis in murine macrophage-like J774.1 cells. Previously (McKinney and Moran, 1989, *Ann. NY Acad. Sci.* 574:388), we showed that resting  $\text{pH}_i$  of J774 cells in HEPES-buffered Na Hanks was  $\sim 7.5$  and was not affected by amiloride (100  $\mu\text{M}$ ). An amiloride-sensitive ( $K_i = \sim 10 \mu\text{M}$ ) Na/H exchanger was primarily responsible for recovery from an imposed acid load. A slow, amiloride-insensitive component of recovery was observed but not fully characterized. The effect of the H-ATPase inhibitors *N*-ethylmaleimide (NEM), *p*-chloromercuribenzenesulfonic acid (pCMBS), and 7-chloro-4-nitrobenz-2-oxa-1,3-diazole (NBD) was tested on resting  $\text{pH}_i$ , steady-state  $\text{H}^+$  extrusion, and recovery from an acid load. Inhibitors of other ATPases or exchangers (amiloride, ouabain, vanadate, oligomycin, and Na azide) were also tested.  $\text{pH}_i$  was measured with the fluorescent dye BCECF. Cells were acidified with an ammonium prepulse and allowed to recover in either Na Hanks or Na-free Hanks with amiloride.  $\text{H}^+$  extrusion was assessed by measuring the change in  $\text{pH}_o$  of a suspension of J774 cells in weakly buffered (100  $\mu\text{M}$  HEPES) Na Hanks. 1 mM NEM, 50  $\mu\text{M}$  NBD, and 250  $\mu\text{M}$  pCMBS all caused intracellular acidification (up to  $\sim 0.4$  pH unit) of resting J774 cells. NBD produced  $\text{pH}_i$  changes within seconds, while NEM and pCMBS required minutes.  $\text{H}^+$  extrusion was also inhibited by these compounds. Neither resting  $\text{pH}_i$  nor  $\text{H}^+$  extrusion was significantly affected by amiloride (1 mM), ouabain (1 mM), oligomycin (1–3  $\mu\text{M}$ ), Na azide (1 mM), or vanadate (100  $\mu\text{M}$ ). pCMBS appeared to inhibit only the amiloride-insensitive component of recovery, while NEM and NBD inhibited both the amiloride-sensitive and -insensitive portions. These results are consistent with the idea that a H-ATPase is present in J774 macrophages, that it contributes to the resting  $\text{pH}_i$  of the cell, and that it is responsible for a small portion of recovery from an acid load.

52.  $\alpha$ -Adrenergic Receptor-mediated, Biphasic Diacylglycerol Metabolism in Human Airway Epithelial Cells CAROLE M. LIEDTKE and PATRICIA VANAH,\* *Departments of Pediatrics and Physiology & Biophysics, Case Western Reserve University, Cleveland, Ohio*

$\text{NaCl(K)}$  cotransport in human airway epithelial cells (AEC) is activated through an  $\alpha$ -adrenergic ( $\alpha$ -AR) mechanism that is dependent on intracellular  $\text{Ca}$  ( $\text{Ca}_i$ ). Because of the requirement for elevated  $\text{Ca}_i$ , we hypothesized that  $\alpha$ -AR agonists stimulate membrane-bound phospholipase C (PLC) with subsequent hydrolysis of phosphatidylinositol-4,5-bisphosphate to generate inositol-1,4,5-trisphosphate ( $\text{IP}_3$ ), a  $\text{Ca}$  mobilizing mediator. We recently reported that, in human AEC,  $\alpha$ -AR agonists transiently decreased phosphatidylinositol (polyPI) levels and increased  $\text{IP}_3$  in a pertussis toxin (PTX)-sensitive manner (Liedtke, 1992, *Am. J. Physiol.* 262 [Lung Cell. Mol. Physiol. 6]:L183). These findings support the hypothesis that  $\alpha$ -AR agonists activate a G protein-regulated PLC and suggest that diacylglycerol (DG) is also transiently metabolized by AEC. The present studies focus on the kinetics of DG metabolism. DG was measured in Li-pretreated AEC grown in cell culture for 6–9 d and prelabeled with 0.5  $\mu\text{Ci}$  [ $^3\text{H}$ ]arachidonic acid for 2 h. DG levels are expressed as a ratio of drug-treated cells (dpm/ $\mu\text{g}$  DNA) to untreated cells (dpm/ $\mu\text{g}$  DNA). In normal human AEC, addition of the endogenous AR agonist epinephrine (EPI) produced a biphasic elevation of DG with peaks of  $2.23 \pm 0.8$  ( $n = 3$ ) at 10 s and  $2.30 \pm 0.8$  ( $n = 4$ ) at 6 min. The  $\alpha$ -AR antagonist prazosine (PRZ)

reduced the biphasic response to EPI to  $0.94 \pm 0.3$  ( $n = 5$ ) at 10 s and  $1.12 \pm 0.1$  ( $n = 3$ ) at 6 min, but the  $\beta$ -AR antagonist propranolol had no effect. Indeed, the  $\beta$ -AR agonist isoproterenol did not increase DG levels. Methoxamine (MOX), an  $\alpha_1$ -AR agonist, also produced a PRZ-sensitive biphasic increase in DG levels with peak levels of  $1.79 \pm 0.5$  ( $n = 4$ ) at 10 s and  $1.41 \pm 0.1$  ( $n = 3$ ) at 6 min. PTX at a final concentration of 100 ng/ml blocked the biphasic response to EPI and the initial DG peak to MOX. These findings provide additional evidence for  $\alpha$ -AR activation of PTX-sensitive PLC in AEC and suggests the involvement of phospholipase D in the late phase DG peak. [Supported by grant HL-43907 from the NIH. CML is an Established Investigator of the American Heart Association.]

53. Determination of a Role for MAP Kinases in the Phosphorylation of the  $\text{Na}^+/\text{H}^+$  Exchanger REBECCA L. MCSWINE-KENNICK,\* MARK W. MUSCH,\* GYORGY BABNIGG,\* MATTHEW J. BRADY,\* EUGENE B. CHANG,\* and MITCHEL L. VILLEREAL, *Department of Pharmacological and Physiological Sciences, The University of Chicago, Chicago, Illinois*

Since activation of the  $\text{Na}^+/\text{H}^+$  exchanger by such diverse agents as phorbol myristate acetate (PMA), epidermal growth factor (EGF), thrombin, and serum produces a similar pattern of phosphorylated peptides upon tryptic digestion (Sardet et al. 1990. *Science (Wash. DC)*. 247:723; Sardet et al. 1991. *J. Biol. Chem.* 266:19166), it has been suggested that a "switch kinase" may mediate exchanger phosphorylation by these various agents. The MAP kinase family of serine/threonine kinases has been shown to be activated by such diverse stimuli (Rossomando et al. 1989. *Proc. Natl. Acad. Sci. USA*. 86:6940; Cobb et al. *Cell Regul.* 2:965-978). An examination of the cytoplasmic tail of the  $\text{Na}^+/\text{H}^+$  exchanger reveals a MAP kinase-like consensus sequence. If MAP kinase phosphorylates this site it would imply that MAP kinases are the pathway by which these diverse mitogens converge to phosphorylate and activate the exchanger. To examine the role for MAP kinases in the activation of the exchanger, cytosolic extracts from fibroblasts were used to phosphorylate a fusion protein ( $\text{XB}_{17}$ ) derived from the cytoplasmic tail of the exchanger. This fusion protein contains a typical MAP kinase consensus sequence Pro-Ala-Ser<sup>723</sup>-Pro-Gln-Ser<sup>726</sup>-Pro. After stimulation with serum, PMA and EGF cytosolic extracts from WI-38 (human lung embryonic fibroblasts) and HSWP (human foreskin fibroblasts) show equal ability to phosphorylate myelin basic protein (MBP) under conditions optimized for MAP kinases. The exchanger fusion protein was similarly phosphorylated by extracts from stimulated cells, although to a lesser degree than was MBP. Competition studies between substrates revealed that phosphorylation of MBP was inhibited by  $\text{XB}_{17}$ , yet phosphorylation of  $\text{XB}_{17}$  was not inhibited by MBP. These observations suggest substrate specificity by members of the MAP kinase family. Tryptic phosphopeptide maps of the fusion protein after phosphorylation by cytosolic extracts show a similar pattern of phosphorylation by PMA, EGF, and serum. Phosphorylation of  $\text{XB}_{17}$  by purified MAP kinase resulted in a similar phosphorylation pattern. These data suggest that  $\text{XB}_{17}$  is phosphorylated by MAP kinase in response to stimulation by PMA, EGF, and serum, and that the MAP kinase consensus sequence contained in the cytoplasmic tail of the exchanger may represent a unique substrate for MAP kinases. [Supported by NIH grant GM-28359.]

54. Sodium Current In Cardiac- and Neuron-like Cells Derived from an Embryonal Carcinoma Cell Line by In Vitro Differentiation JORGE ARREOLA, SHERRILL SPIRES, and TED BEGENISICH, *Departments of Physiology and Dental Research, University of Rochester, Rochester, New York*

Pluripotent murine embryonal carcinoma cells (P19) were differentiated into cardiac- and neuron-like cells with dimethyl sulfoxide (0.5%) and retinoic acid (0.5  $\mu\text{M}$ ), respectively. Cardiac-like cells (20-30  $\mu\text{m}$ ) have characteristic beats at  $\sim 1$  Hz at room temperature. In contrast, neuron-like cells are smaller (10-15  $\mu\text{m}$ ) and express extensive neurites. Voltage-gated sodium currents recorded with whole cell voltage clamp have a maximum amplitude of  $-3.07 \pm 0.55$  and  $-1.22 \pm 0.25$  nA in cardiac- and neuron-like cells, respectively. Control undifferentiated cells have a very small inward

current with a maximum amplitude of  $-0.15 \pm 0.02$  nA. The voltage dependence of the peak sodium current in both cell types was similar. Significant inward current was recorded at  $-40$  mV and was maximum around  $-10$ – $0$  mV of membrane potential. Cardiac-like sodium channels were 50% inactivated at  $-80.6 \pm 3.7$  mV with a slope factor of  $12.1 \pm 0.9$  mV. In contrast, these values for neuron-like sodium channels were  $-45.9 \pm 0.8$  and  $7.0 \pm 0.5$  mV. The time course and current-voltage relationship of sodium currents recorded from the cardiac-like cells were quite similar to those from guinea pig ventricular myocytes. Tetrodotoxin (TTX) blocks cardiac- and neuron-like sodium channels in a dose-dependent manner with  $K_d$ 's of 650 and 8.6 nM, respectively. Maximum current through cardiac-like sodium channels was inhibited 23 and 42% by 15  $\mu$ M dibutyryl cyclic AMP and 50 nM phorbol 12,13-dibutyrate, respectively. It is concluded that in vitro generated cardiac- and neuron-like cells express sodium channels with different TTX sensitivity. Cardiac-like sodium channels are targets of regulatory processes. Finally, P19 is a cell line that may be a suitable model to study in vitro the electrophysiological changes during the cellular differentiation process toward an excitable cell.

55. The Pore of the *Shaker* K<sup>+</sup> Channel Exhibits Multi-ion Characteristics G. PATRICIA PEREZ\* and TED BEGENISICH, *Department of Physiology, University of Rochester, Rochester, New York*

The cell line Sf9, derived from the army worm caterpillar *Stodoptera frugiperda*, was infected with a recombinant baculovirus, containing the *Shaker* H4 K<sup>+</sup> channel cDNA, to express functional transient K<sup>+</sup> currents. Voltage-activated K<sup>+</sup> currents were recorded with whole cell voltage clamp. Selectivity of the channel was studied by determining the permeability ratio of Rb<sup>+</sup> to K<sup>+</sup> ( $P_{Rb}/P_K$ ). Measurements of reversal potentials under bi-ionic conditions were used to compute the permeability ratio from the Goldman-Hodgkin-Katz equation:

$$P_{Rb}/P_K = ([K^+]/[Rb^+]) \exp(E_{rev}F/RT)$$

K channel permeability ratios are not a direct function of ion concentration, but rather they differ for ion substitution on one side vs. the other side of the membrane. Our data show that  $P_{Rb}/P_K$  did not change much when: (a) the internal K<sup>+</sup> concentration was kept constant and the external Rb<sup>+</sup> concentration was increased fourfold, and (b) the internal Rb<sup>+</sup> concentration was kept constant and the external K<sup>+</sup> concentration was increased ninefold. However, the substitution of internal K<sup>+</sup> (134 mM) for Rb<sup>+</sup> (110 mM) decreases the permeability ratio from 0.75 to 0.55. Thus the *Shaker* K<sup>+</sup> channel shows an apparent selectivity change which is asymmetric with respect to the membrane surface. We have also done experiments to study the voltage-dependent block of the channel by external Cs<sup>+</sup>. The value determined for  $\delta$  (fraction of the electrical field traversed by the Cs<sup>+</sup> in moving from the solution into the blocking site) increased with the  $[K^+]_o$ . These experiments, together with the data from the selectivity ratios, suggest that the *Shaker* K<sup>+</sup> channel has a multi-ion nature.

56. Functional Expression of the Mouse Multiple Drug Resistance Protein in *Escherichia coli* EITAN BIBI, PHILLIPE GROS, and H. RONALD KABACK, *Howard Hughes Medical Institute, Department of Physiology, Department of Microbiology & Molecular Genetics, University of California Los Angeles, Los Angeles, California; and Department of Biochemistry, McGill University, Montreal, Quebec, Canada*

Expression of polytopic integral membrane proteins of eukaryotic origin in *Escherichia coli* could provide an invaluable system for detailed study of their function. We have chosen to use the mouse P-glycoprotein encoded by *mdr1* in our attempts to express eukaryotic integral membrane proteins in *E. coli*. The tendency of cultured cells and tumors in patients to exhibit simultaneous resistance to multiple chemically unrelated chemotherapeutic agents is mainly due to a family of multidrug transport proteins encoded by *mdr* genes in humans, mice, and other species. Highly resistant cells express large quantities of a ~170-kD membrane phosphoglycoprotein known as P170, P-glycopro-

tein, or *mdr* (for review, see Endicott and Ling, 1989. *Annu. Rev. Biochem.* 58:137). The *mdr1* cDNA from mouse (Gros et al. 1986. *Cell*. 47:371) was cloned under the control of the *lac* promoter/operator. The protein expressed in *E. coli* strain UT5600 was found in the membrane fraction, and displayed an apparent molecular weight similar to that of the unglycosylated *mdr1*. The heterologous protein was recognized by monoclonal antibodies against *mdr* (C219). Cells expressing the *mdr1* protein acquire resistance against the lipophilic cation tetraphenylphosphonium ( $\text{TPP}^+$ ), a known substrate of *mdr1* (Gros et al. 1992. *Biochemistry*. 31:1992) and a probe for membrane potential in many systems (Schuldiner and Kaback, 1975. *Biochemistry*. 14:5451). Transport experiments demonstrate that  $\text{TPP}^+$  resistance is due to the low level of accumulation in cells expressing *mdr1*. The membrane potential in cells expressing *mdr1* is normal, as demonstrated independently by lactose transport assay. These findings support the idea that  $\text{TPP}^+$  is actively extruded in cells expressing *mdr1*. Finally, the results demonstrate that mouse *mdr1* is expressed and assembled in *E. coli* membranes in a functional state. [Supported by a grant from the Cystic Fibrosis Foundation.]

57. The  $\beta$ -Subunit Is Involved in Functional Activity of the Gastric H,K-ATPase DAR CHOW\* and JOHN G. FORTE,\* *Department of Molecular and Cell Biology, University of California, Berkeley, California* (Sponsor: Terry Machen)

The H,K-ATPase, the gastric proton pump that exchanges  $\text{H}^+$  and  $\text{K}^+$  in the parietal cell, operates as a heterodimer consisting of a 114-kD peptide, called the catalytic  $\alpha$ -subunit, and a heavily glycosylated  $\beta$ -subunit with a 34-kD core peptide. We have developed new monoclonal antibodies against the H,K-ATPase  $\beta$ -subunit. One clone (2G11) recognizes the native  $\beta$ -subunit as well as its deglycosylated core peptide, but does not recognize Na,K-ATPase  $\beta$ -subunit. Previous studies showed that 2G11 recognizes the cytoplasmic domain of the  $\beta$ -subunit and inhibits H,K-ATPase activity upon binding to the enzyme, with maximum inhibition of  $\sim 50\%$  (Chow and Forte, 1992. *FASEB [Fed. Am. Soc. Exp. Biol.] J.* 6:A1187). Here we further investigate the functional interaction between the  $\beta$ -subunit and the antibody. Binding of 2G11 to the enzyme differentially changed the kinetics of  $\text{K}^+$  activation of the hydrolysis of ATP (full enzymatic cycle) vs. the hydrolysis of *p*-nitrophenylphosphate (*p*NPP, phosphatase part of full cycle). For ATP hydrolysis, there was no change in the  $K_m$  for  $\text{K}^+$ , but the  $V_{\max}$  was decreased by 50%, whereas for *p*NPP hydrolysis the  $K_m$  for  $\text{K}^+$  was doubled and  $V_{\max}$  was lowered by only  $\sim 20\%$ . Furthermore, phosphorylation studies showed that under certain conditions, when the steady-state E-P levels were severely reduced (i.e., 50  $\mu\text{M}$  ATP, 2 mM Pi), binding of 2G11 increased E-P back to control levels. These data can be interpreted in terms of a "2G11"-altered activity of the low affinity  $\text{K}^+$  site. Previous work has shown that the  $\beta$ -subunit of monovalent cation pump ATPases is necessary for functional maturation and conformational stability of the holoenzyme (for review see McDonough et al. 1990. *FASEB [Fed. Am. Soc. Exp. Biol.] J.* 4:1598). The present results provide the first evidence for direct involvement of the  $\beta$ -subunit in the enzymatic activity of an ion pump ATPase. Since the  $\beta$ -subunit of the H,K-ATPase can act as surrogate for the Na,K-ATPase (Horisberger et al. 1991. *J. Biol. Chem.* 266:19131), we propose by analogy that the  $\beta$ -subunit of the Na,K-ATPase may function directly in  $\text{K}^+$  translocation, as well as stabilizing the functional conformation. [Supported by NIH grants DK-38972 and DK-10141.]

58. Molecular Analysis of the Structure and Physiological Role of  $\text{Na}^+/\text{H}^+$  Antiporters in *Escherichia coli* SHIMON SCHULDINER and ETANA PADAN, *The Alexander Silberman Institute of Life Sciences, Hebrew University, Jerusalem, Israel*

All living cells maintain a sodium concentration gradient directed inward and a constant intracellular pH at around neutrality. The mechanisms involved in  $\text{Na}^+$  extrusion and regulation of pH differ from cell to cell, but in all cases  $\text{Na}^+/\text{H}^+$  antiporters have been suggested to play a major role. In most microorganisms the antiporters are the only mechanisms known to actively extrude  $\text{Na}^+$  ions from the cell. We have cloned two genes coding for two distinct antiporters in *Escherichia coli*: *nhaA* (Goldberg et al. 1987. *Proc. Natl. Acad. Sci. USA*. 84:2615; Karpel et al. 1988. *J. Biol. Chem.* 263:10408) and *nhaB* (Pinner et al. 1992. *J. Biol. Chem.* In press), purified one of the proteins (NhaA; Taglicht et

al. 1991. *J. Biol. Chem.* 263:11289) to homogeneity, and generated mutants in which these genes are inactivated (Padan et al. 1989. *J. Biol. Chem.* 264:20297). In addition, we have identified a regulatory gene (*nhaR*) which acts as a positive transcriptional activator of *nhaA* (Karpel et al. 1991. *J. Biol. Chem.* 266:21753; Rahav Manor et al. 1992. *J. Biol. Chem.* In press). From our results it is evident that in *E. coli* adaptation to pH and high salinity is mediated by a multicomponent system: NhaA, whose activity is highly regulated by pH and whose levels of expression are controlled by the  $\text{Na}^+$  concentration; NhaR, which senses, directly or indirectly, the  $\text{Na}^+$  concentration and regulates the levels of NhaA in which there seems to be a novel signal transduction pathway; and NhaB, which seems to be the system active mostly at low  $\text{Na}^+$  concentrations. It is becoming evident that the catalysis of  $\text{Na}^+/\text{H}^+$  exchange is performed by various different proteins which significantly differ in their amino acid sequence and in details of the exchange reaction. There seems to be little conservation of sequences between the eukaryotic and prokaryotic ones and also within the prokaryotic sequences themselves. In one 16-amino acid stretch, however, the homology between NhaA and NhaB is significant (35% identity and 52% similarity). Moreover, NheI (Sardet et al. 1989. *Cell* 56:271) is 41% identical and 83% similar to NhaA in this segment. This domain overlaps with part of the diffuse SOB motif previously identified (Deguchi et al. 1990. *J. Biol. Chem.* 265:21704) in various transporters that move  $\text{Na}^+$  ions across membranes (Schuldiner and Padan. 1992. In Alkali Cation Transport Systems in Prokaryotes. CRC Press, Inc., Boca Raton, FL. In press). [Supported by a grant from the United States Israel Binational Science Foundation.]

59. Morphological and Rheological Alterations Induced by *p*-Azido-benzylphlorizin in Normal and Sick Erythrocytes DANIEL M. HOEFNER,\* MICHAEL E. BLANK,\* BRIAN M. DAVIS,\* and DONALD F. DIEDRICH, Graduate Center for Toxicology and Center of Membrane Sciences, University of Kentucky, Lexington, Kentucky

When ~2 million molecules of *p*-azido-benzylphlorizin (*p*-AzBPhz) are bound to each erythrocyte to cause inhibition of anion exchange (noncompetitively) and glucose transport (competitively), this nonpenetrating membrane probe induces dose-dependent alterations in red cell morphology and volume as determined by light scattering, electronic cell-sizing, and micro-hematocrit measurements. The azide's low dose effects are also observed with 0.2  $\mu\text{M}$  diisothiocyanostilbene disulfonate (DIDS), but DIDS does not mimic what appears to be the nonspecific action of the azide at higher doses, namely, insertion into the lipid bilayer, echinocyte formation, and loss of membrane integrity. The kinetics of these changes have been characterized by digital image morphometry. Red blood cells (RBCs) were viewed with Nomarski optics and filmed with a video camera attachment; images were recorded at 30 frames/s and changes in cell circumference were computer analyzed. Biconcave structure collapsed and cell flattening occurred 1–2 s after normal (HbA) cells were exposed to the lowest  $\mu\text{M}$  *p*-AzBPhz or DIDS levels. Higher doses of either agent caused cell blebbing, but only azide caused echinocyte/spherocyte formation. These apparent cytoskeletal changes were reversed in <2 s by washing the azide from the membrane. *p*-AzBPhz-induced alteration in cell architecture was also found when RBC deformability was measured by microfiltration through polycarbonate filters (3- $\mu\text{m}$  pore). The azide increased filtration rate of both normal (HbA) and sickle (HbS) RBCs in a dose-dependent manner at low  $\mu\text{M}$  concentrations. [Supported in part by National Science Foundation and Commonwealth EPSCoR program grants.]

60. Kinetics of Na Transport through the Na-Mg Pathway of Hamster Red Cells WAN-YAN XU\* and JOHN S. WILLIS, Department of Physiology and Biophysics, University of Illinois, Urbana, Illinois; and Department of Zoology, University of Georgia, Athens, Georgia

We previously reported (Xu and Willis. 1991. *FASEB [Fed. Am. Soc. Exp. Biol.] J.* 5:A686) that all amiloride-sensitive (AS) Na influx in hamster red cells occurs through an apparent Na-Mg pathway; it is activated by Mg loading of the cell and inhibited by the usual activators of Na-H exchange as well as by quinidine and by ATP depletion. We now report the activation kinetics for unidirectional Na influx as measured by isotopic  $^{24}\text{Na}$  uptake and for Mg efflux measured as Mg loss into Mg-free medium

from Mg-loaded cells. Using the same kinetic analysis as Ludi and Schatzmann (1987, *J. Physiol. [Lond.]*, 390:367) we found that activation of AS Na influx and AS Mg efflux by intracellular Mg (as estimated from the equilibration concentration with A23187) had a  $K_m$  between 2 and 4 mM with a Hill coefficient of 3. Activation of AS Na influx and AS Mg efflux by extracellular Na had a  $K_m$  between 74 and 80 mM and fit a simple Michaelis-Menten hyperbola. With either Mg or Na in the medium, AS Na efflux from cells loaded with 10, 50, or 150 mM was nil, either when cells were replete with or were depleted of ATP. This last result argues against the pathway being a simple exchanger, and is in direct conflict with results of Gunther et al. (1990, *Biochim. Biophys. Acta*, 1023:455) who found a large amiloride- and quinidine-inhibitable Na efflux from Na-loaded rat red cells.

61. Structure and Function of the Low-Affinity  $\text{Na}^+$ /Glucose Cotransporter from Human Kidney YOSHIKATSU KANAI, WEN-SEN LEE, GUOFENG YOU, and MATTHIAS A. HEDIGER, *Department of Medicine, Renal Division, Brigham and Women's Hospital and Harvard Medical School, Boston, Massachusetts* (Sponsor: Steven R. Gullans)

Efficient substrate transport in the kidney is provided by low- and high-affinity transporters arranged in series along the tubule. A brush-border high-affinity  $\text{Na}^+$ -glucose cotransporter (SGLT1) was previously cloned from rabbit small intestine (Hediger et al. 1987, *Nature [Lond.]*, 330:379). We have used low-stringency screening with high-affinity SGLT1 to isolate a 2271-nucleotide cDNA from human kidney (Wells et al. 1992, *Am. J. Physiol.* In press). This clone, which codes for a 672-residue protein (SGLT2), is 59% identical at the amino acid level to SGLT1 and has a similar number and arrangement of predicted membrane-spanning regions. Using *Xenopus* oocytes injected with in vitro transcribed cRNA, we demonstrated that SGLT2 induces a two- to threefold increase in the  $\text{Na}^+$ -dependent and phlorizin-sensitive uptake of  $^3\text{H}$ - $\alpha$ -methyl-D-glucopyranoside ( $\alpha\text{MeGlc}$ ) uptake. This uptake was reproducible, statistically significant, and saturable. The  $K_m$  for  $\alpha\text{MeGlc}$  was 1.6 mM, which is representative of low-affinity transport. There was a 1.8-fold stimulation of  $^3\text{H}$ -D-galactose but no evidence of statistically significant transport of uridine, *myo*-inositol, fructose, mannose, or L-proline. Northern blot analysis and in situ hybridization using the SGLT2 rat homologue R36 (You, Wells, and Hediger unpublished sequence) as a probe demonstrated specific expression in the kidney proximal tubule S1 segment. We conclude that SGLT2 codes for the kidney-specific low-affinity  $\text{Na}^+$ /glucose cotransporter characterized in the past by studies using brush-border membrane vesicles and perfused tubule segments.

62. Differential Activation of Na Reabsorption and Cl Secretion by Forskolin in the Epithelial Cell Line A6 MICHAEL L. CHALFANT,\* BRIGITTE COUPAYE-GERARD,\* MORTIMER CIVAN, and THOMAS R. KLEYMAN, *Departments of Physiology, Bioengineering, and Medicine, University of Pennsylvania and the Veterans Affairs Medical Center, Philadelphia, Pennsylvania*

cAMP activates Na reabsorption and Cl secretion in the epithelial cell line A6. We recently observed that, in contrast to previous observations, forskolin (10  $\mu\text{M}$ ) elicited a biphasic increase in short circuit current ( $I_{sc}$ ). The kinetics of this increase in Na and Cl transport were characterized in A6 cells grown on polycarbonate membranes bathed with an amphibian Ringer's solution. After an initial rapid increase within 15 s of addition of forskolin,  $I_{sc}$  reached a peak value after  $\sim 75$  s.  $I_{sc}$  then underwent a rapid, transient fall, followed by a secondary slow increase which approached a plateau in  $\sim 10$ –20 min, remaining elevated and relatively stable for  $> 40$  min. To differentiate the response of different transport pathways to forskolin, amiloride (10  $\mu\text{M}$ ) was added to the apical compartment to inhibit Na absorption before application of forskolin. The initial rapid rise of  $I_{sc}$  was present. After the initial peak,  $I_{sc}$  fell and stabilized at a value greater than baseline amiloride-insensitive  $I_{sc}$ . The secondary rise in  $I_{sc}$  was blocked. The response to forskolin was also examined with a Cl-free solution. The initial response to forskolin was largely blunted. A small, rapid increase in  $I_{sc}$  was followed by a slow increase which approached a plateau at 10–20 min. In conclusion, activation of Cl secretion and Na reabsorption by forskolin follows distinct kinetics and is responsible for the biphasic  $I_{sc}$  response. The

initial rapid rise and first peak of  $I_{\text{sc}}$  are primarily results of Cl secretion. The slow increase in  $I_{\text{sc}}$  reflects at least two distinct transport processes: a gradual increase in Na reabsorption and a stable Cl secretion. [Supported by grants from the Veterans Administration, and the NIH (HL-07027 17 and DK-40145), and an EI award from the American Heart Association.]

63. Differential Arrival of Newly Synthesized Plasma Membrane Proteins in the Epithelial Cell Line A6 BRIGITTE COUPAYE-GERARD\* and THOMAS R. KLEYMAN. *Departments of Medicine and Physiology, University of Pennsylvania and Veterans Affairs Medical Center, Philadelphia, Pennsylvania*

The delivery of newly synthesized proteins to the apical or basolateral cell surface was examined in the amphibian epithelial cell line A6. Metabolic labeling of newly synthesized proteins with [ $^{35}\text{S}$ ]methionine was performed with a pulse (15 min)-chase protocol. At varying times during the chase, proteins at the apical or basolateral cell surface were labeled with biotin in order to examine the flow of newly synthesized proteins to the plasma membrane. Labeled, biotinylated proteins were precipitated with streptavidin agarose and then identified by SDS-PAGE and autoradiography. Recovery of newly synthesized proteins at the apical cell surface reached a maximum after a 5-min chase, and then fell slowly over the remainder of a 2-h chase. In contrast, the recovery of newly synthesized proteins from the basolateral membrane was relatively constant during the first 45 min of the chase, and then slowly rose to a maximum after ~90 min. Similar results were obtained if proteins were separated on the basis of hydrophobicity with the detergent Triton X-114. The differential arrival of newly synthesized proteins at the apical and basolateral membrane may reflect the subapical localization of the Golgi apparatus in epithelial cells. [Supported by a grant from the National Kidney Foundation and an EI Award from the American Heart Association.]

64. Hypo-osmotically Activated  $\text{Cl}^-$  Conductance in Cultured Chick Heart Cells JIAN-PING ZHANG,\* RANDALL L. RASMUSSEN,\* SARAH K. HALL,\* and MELVYN LIEBERMAN, *Department of Cell Biology, Division of Physiology, Duke University Medical Center, Durham, North Carolina*

Cultured chick heart cell aggregates subject to hypo-osmotic swelling undergo an initial increase in spontaneous contractile activity followed by eventual quiescence. Results from conventional microelectrode studies under the same experimental conditions reveal a corresponding initial increase in spontaneous electrical activity, followed by a sustained depolarization beyond threshold. The loss of spontaneous contractility and the membrane depolarization during cell swelling could be attributed to the activation of a  $\text{Cl}^-$  conductance. Furthermore,  $\text{Cl}^-$  depletion reduced the extent of regulatory volume decrease in cells exposed to hypo-osmotic swelling. The presence of a swelling-activated  $\text{Cl}^-$  conductance in chick heart cells was investigated using the whole-cell patch clamp technique.  $\text{K}^+$  currents were blocked by 1 mM  $\text{Ba}^{2+}$  or by substitution of  $\text{K}^+$  with  $\text{Cs}^+$  in both bath and pipette solutions. Changes in membrane current during cell swelling were monitored by applying voltage ramps (-90 to +60 mV,  $dV/dt = 0.5 \text{ V/s}$ ) at 10-s intervals from a holding potential of -40 mV. Exposure of cells to hypo-osmotic solution (70% NaCl) resulted in rapid osmotic swelling followed by a substantial increase in whole-cell current (5-10-fold). The current persisted for the duration of the volume perturbation and was partially reversed by return to isosmotic bath solution. Ionic selectivity of this swelling-activated current was determined by varying the external and internal  $\text{Cl}^-$  concentrations. For a variety of  $\text{Cl}^-$  concentrations, the reversal potentials of the measured swelling-activated current ( $V_{\text{rev}}$ ) closely followed the calculated  $\text{Cl}^-$  equilibrium potential ( $E_{\text{Cl}}$ ) with a slope of linear regression of 0.82 (Zhang et al. 1991. *Biophys. J.* 61:A441). The permeability ratio of this swelling-activated conductance to chloride, methanesulfonate (MSA), and aspartate (Asp) was  $P_{\text{Cl}}:P_{\text{MSA}}:P_{\text{Asp}} = 60:21:1$ . Application of a  $\text{Cl}^-$  channel blocker, diphenylamine-2-carboxylate (DPC; 200  $\mu\text{M}$ ), substantially suppressed the swelling-activated current ( $50 \pm 4\%$ ,  $n = 4$ ) without shifting the  $V_{\text{rev}}$  of this current. This swelling-activated current was further characterized at the single channel level in a cell-attached configuration. The pipette was filled with  $\text{K}^+$ -free saline solution with 1 mM  $\text{Ba}^{2+}$  to

minimize any  $K^+$  conductance. Single channel activity was observed upon hypo-osmotic swelling of the cell. The open-channel current displayed an outward rectification, which was consistent with the properties of the macroscopic currents obtained from whole-cell recording. The unitary conductance at zero current potential was 31 pS and its reversal potential was very close to the calculated  $E_{Cl}$ . From this evidence, we conclude that hypo-osmotic swelling of cultured chick heart cells activates a channel-mediated  $Cl^-$  conductance which may be involved in regulation of cell volume. [Supported by NIH grants HL-27105 and HL-07063 and AHA grant NC-91-F-3.]

65. Partial Purification and Reconstitution of the Human Multidrug Resistance Pump: Characterization of the Drug-stimulated ATPase SURESH V. AMBUDKAR,\* ISABELLE LELONG,\* JIAPING ZHANG,\* CAROL O. CARDARELLI,\* IRA PASTAN,\* and MICHAEL M. GOTTESMAN,\* *Department of Medicine, The Johns Hopkins University School of Medicine, Baltimore, Maryland; and Laboratory of Cell Biology and Laboratory of Molecular Biology, National Cancer Institute, National Institutes of Health, Bethesda, Maryland* (Sponsor: I. S. Ambudkar)

The development of resistance to multiple natural cytotoxic drugs in certain tumors in vivo and in cultured cells in vitro is associated with overexpression of the *MDR1* gene product, P-glycoprotein (Pgp), which is believed to function as an ATP-dependent multidrug efflux pump. In this study we have partially purified Pgp from the human multidrug resistant carcinoma cell line, KB-V1, and reconstituted it in phospholipid vesicles. KB-V1 plasma membranes were solubilized with 1.4% octylglucoside in the presence of 0.4% lipid and 20% glycerol and the detergent extract was chromatographed on DEAE Sepharose CL6-B. 0.1 M NaCl eluate enriched in Pgp was reconstituted by the detergent-dilution method. Pgp constituted ~25–30% of reconstituted protein and was incorporated in proteoliposomes (PL) with predominantly (>90%) inside-out orientation. ATP hydrolysis by PL was stimulated 3.5-fold by the addition of vinblastine, but it was unaffected by another hydrophobic antitumor agent, camptothecin, which is not transported by Pgp. The stimulation of ATP hydrolysis by vinblastine was observed only if the protein was reconstituted in PL, suggesting that the conformation of the soluble Pgp might not be suitable for substrate-induced activation. Several substrates enhanced the ATPase activity in a dose-dependent manner with relative potencies as follows: doxorubicin = vinblastine > daunomycin > actinomycin D > verapamil > colchicine. Although vinblastine enhanced the maximal activity, it did not change the apparent  $K_m$  for ATP (0.3 mM). The "basal" and vinblastine-stimulated ATPase activities were inhibited by vanadate but were not affected by treatment with ouabain, azide, oligomycin, *N*-ethylmaleimide, fluoride, and EGTA. These data demonstrate that Pgp, like other members of the superfamily of ABC transporters, catalyzes ATP hydrolysis which is enhanced by its substrates.

66. Identification of the Putative Na:K:Cl Cotransporter in Avian Salt Gland: Phosphorylation by VIP and Carbachol JOSEPH TORCHIA,\* CHRISTIAN LYTLE,\* BLISS FORBUSH III, and A. K. SEN, *Department of Pharmacology, University of Toronto, Toronto, Ontario, Canada; and Department of Cellular and Molecular Physiology, Yale University School of Medicine, New Haven, Connecticut*

We have previously shown that the addition of carbachol to radiolabeled salt gland cells stimulates the protein kinase C-mediated phosphorylation of a membrane-bound protein (pp170) (Torchia et al. 1991. *Am. J. Physiol.* 261:C543). In the present study we assessed the involvement of a vasoactive intestinal peptide (VIP)/adenylate cyclase pathway in the phosphorylation of pp170. The addition of VIP, in the presence of 100  $\mu$ M IBMX, resulted in a concentration-dependent increase in phosphorylation of pp170. This effect was rapid and transient with a three- to fivefold increase in phosphorylation occurring 1 min after the addition of VIP. Under similar incubation conditions, VIP stimulated a 4.6-fold increase in cAMP accumulation that paralleled the increase in phosphorylation observed. The addition of either forskolin or 8-Br-cAMP resulted in a five- to eightfold increase in the phosphorylation of pp170. pp170 was characterized further using a monoclonal antibody (Q3).

Western blotting using Q3 antibody recognized a single protein band corresponding to the molecular weight of pp170. Immunoprecipitation of pp170 from salt gland cells stimulated with either carbachol or VIP resulted in the selective extraction of a single phosphoprotein band whose phosphorylation was increased approximately fivefold in stimulated cells. The identity of pp170 was determined using two criteria. First, immunoblots of affinity-purified Na:K:Cl cotransporter preparations from shark rectal gland membranes probed with Q3 detected a single band corresponding to the molecular weight of the shark rectal gland cotransporter. Second, pp170 was selectively immunoprecipitated by a monoclonal antibody (J4) directed against a specific epitope of the shark rectal gland cotransporter (Lytle and Forbush, 1990, *J. Cell Biol.* 111:312a [Abstr.]). These results suggest that pp170 is homologous to the shark rectal gland Na:K:Cl cotransporter and thus both proteins may be functionally similar. Furthermore, phosphorylation of pp170 involves multiple second messenger pathways suggesting that the regulation of this protein may be a principal control point determining NaCl secretion. [Supported by the Canadian Cystic Fibrosis Foundation.]

67. Expression of CFTR Results in the Appearance of an ATP Channel I. L. REISIN,\* A. G. PRAT,\* E. H. ABRAHAM,\* J. AMARA,\* R. GREGORY,\* D. A. AUSIELLO, and H. F. CANTIELLO, *Renal Unit and Department of Radiation Oncology, Massachusetts General Hospital, and Department of Medicine, Harvard Medical School, Boston, Massachusetts; and Genzyme Corporation, Framingham, Massachusetts*

Cystic fibrosis is characterized by defects in cystic fibrosis transmembrane regulator (CFTR) which belongs to a superfamily of proteins implicated in the transport of ions and proteins. Recent studies demonstrated that CFTR is a protein kinase A-sensitive  $\text{Cl}^-$  channel that is regulated by ATP. The nature of this regulation is unknown. Mouse mammary carcinoma, C127, cells were transfected with CFTR-cDNA, WT2, or mock-transfected, BPV cells. CFTR expression correlated with a cAMP-dependent increase in  $^{125}\text{I}$  efflux in WT2 cells. The nature of the cAMP-dependent anionic pathway was assessed by patch-clamp techniques. cAMP-dependent whole-cell  $\text{Cl}^-$  currents of WT2 cells were  $838 \pm 514\%$  ( $n = 5$ ) higher than for BPV cells, and inhibited by 100  $\mu\text{M}$  DPC. 8-Br-cAMP stimulation under cell-attached conditions or PKA plus ATP under excised, inside-out conditions activated a nonrectifying, DPC-inhibitable  $\text{Cl}^-$  channel with a mean conductance of  $9.86 \pm 0.07$  pS ( $n = 3$ ) in WT2 cells. CFTR transfection was also associated with the presence of a cAMP-inducible steady-state release of ATP that was  $344 \pm 112\%$  ( $n = 3$ ) higher in WT2 than in BPV cells. This was further studied by patch-clamp techniques. Under symmetrical ATP, single nonrectifying ATP channels,  $9.60 \pm 0.23$  pS ( $n = 3$ ), were observed after either cAMP activation in cell-attached conditions (ATP in pipette), or PKA addition under excised, inside-out conditions. A link between the cAMP-inducible  $\text{Cl}^-$  and ATP currents was then sought. External ATP also elicited  $\text{Cl}^-$  and ATP channel activation in cell-attached patches of WT2 cells. The data indicate that CFTR expression is associated with the presence of both a  $\text{Cl}^-$  and an ATP channel.

68. The Multidrug Resistance (*mdr1*) Gene Product Functions as an ATP Channel A. G. PRAT,\* E. H. ABRAHAM,\* L. GERWECK,\* T. SENEVERATNE,\* R. J. ARCECI,\* R. KRAMER,\* G. GUIDOTTI,\* and H. F. CANTIELLO, *Renal Unit and Department of Radiation Oncology, Massachusetts General Hospital and Harvard Medical School, Boston, Massachusetts; Department of Biochemistry & Molecular Biology, Harvard University, Boston, Massachusetts; Dana Farber Cancer Institute and The Children's Hospital, Boston, Massachusetts; and Joint Center for Radiation Therapy, Cambridge, Massachusetts*

The ATP transfer mechanism through the *mdr1* gene product, P-glycoprotein (GP170), was studied with patch-clamp techniques in cells transfected with the intact *mdr1* gene, EX4N, the *mdr1* gene mutated in the ATP binding domains, 88-8, and the human lung tumor cell line, SW-1573, with no detectable GP170. When cells were internally perfused with ATP (100 mM;  $\text{Mg}^{2+}$  or Tris salts) and external 140 mM NaCl, similar, strongly rectifying, whole-cell currents were observed in the direction of chloride entering the cell for the three cell lines (reversal potential  $< -50$  mV). In contrast, in

symmetrical ATP only cells over-expressing GP170 (EX4N) showed an anionic conductance (0 mV) of  $2.03 \pm 0.04$  nS/cell compared with SW-1573 cells devoid of GP170,  $0.42 \pm 0.16$  nS/cell (indistinguishable from zero),  $P < 0.005$ . Cells expressing a mutated form of GP170 (88-8) displayed a conductance only 57% of that of EX4N cells,  $P < 0.001$ . Replacement of ATP by ADP resulted in a lower conductance, while replacement of ATP by phosphate elicited no conductance. 36 of 54 (67%) excised, inside-out patches of EX4N cells (symmetrical ATP) displayed single ATP channel currents. A single ionic conductance was calculated between 0 and 100 mV of  $13.0 \pm 0.1$  pS ( $n = 8$ ) and -100 and 0 mV of  $37.3 \pm 0.2$  pS ( $n = 8$ ). Addition of anti-GP170 antibodies to excised, inside-out patches of EX4N cells inhibited ATP channel activity by  $36 \pm 6\%$  ( $n = 3$ ),  $P < 0.05$ . The data indicate that a channel-like behavior is associated with GP170, a novel nucleotide-carrying structure.

69. Expression of the Multidrug Resistance (*mdr1*) Gene Product Is Associated with a Novel ATP-transporting Mechanism E. H. ABRAHAM,\* L. GERWECK,\* T. SENEVER-ATNE,\* R. J. ARCECI,\* R. KRAMER,\* A. G. PRAT,\* H. F. CANTIELLO, and G. GUIDOTTI, *Department of Biochemistry & Molecular Biology, Harvard University; Renal Unit and Department of Radiation Oncology, Massachusetts General Hospital and Harvard Medical School; Dana Farber Cancer Institute and The Children's Hospital, Boston, Massachusetts; and Joint Center for Radiation Therapy, Cambridge, Massachusetts*

The *mdr1* gene product, P-glycoprotein (GP170) is associated with multidrug resistance in tumor cells; however, its mechanism of action has not been elucidated. To assess the role of ATP in GP170 function, the spontaneous ATP release from Chinese hamster ovary (CHO) cells induced to over-express GP170 (CH<sup>R</sup>C5) and from uninduced (AUX B1) CHO cells was compared using HPLC measurements. ATP release was 314% higher in CH<sup>R</sup>C5 cells ( $0.42 \pm 0.07$  fmol ATP min<sup>-1</sup> cell<sup>-1</sup> vs.  $0.13 \pm 0.02$  fmol ATP min<sup>-1</sup> cell<sup>-1</sup> [ $n = 7$ ],  $P < 0.01$ ). Moreover, using the luciferin-luciferase assay, the steady-state ATP release was 2.4-fold greater in CH<sup>R</sup>C5 cells than in AUX B1 cells,  $P < 0.001$ . To correlate GP170 expression with ATP release, two different cells lines were induced to express various amounts of GP170. In CHO cells grown in the presence of colchicine, 0.2  $\mu$ g/ml and 30  $\mu$ g/ml, GP170 expression measured by immunofluorescence cell-surface staining was proportional to the ATP released,  $r = 0.98$  ( $n = 3$ ). Similar results were observed when the lung tumor cell line SW-1573, devoid of GP170, was induced to over-express GP170 with 5 and 7  $\mu$ g/ml adriamycin,  $r = 0.94$  ( $n = 3$ ). A link between GP170 expression and ATP release was also found on CHO cells transfected with the intact (EX4N) and mutated *mdr1* gene (88-8). EX4N cells had a 5.5-fold increase in the ATP release compared with 88-8 cells,  $P < 0.001$ . These results indicate that GP170 is associated with spontaneous ATP efflux from cells under physiological conditions.

70. Cloning of Partial Length cDNAs Homologous to the Human NHE-1 Antiporter from Reptilian Colon SAMANTHA P. HARRIS,\* NEIL W. RICHARDS,\* CRAIG D. LOGSDON,\* JACQUES POUYSSEGUR,\* and DAVID C. DAWSON, *Department of Physiology, The University of Michigan Medical School, Ann Arbor, Michigan; and The University of Nice, Nice, France*

Amiloride-inhibitable Na/H antiport is expressed at high levels in the basolateral membrane of turtle colon epithelial cells. In addition, a Na-selective conductance is expressed in association with the Na/H exchange activity (Post and Dawson, 1992. *Am. J. Physiol.* 262: C1089). Current and Na/H exchange activity have the same ion selectivity and sensitivity to amiloride analogues and both are activated by osmotic shrinkage. To confirm that this novel conductance represents an activity of the Na/H antiporter protein, we undertook the cloning of the Na/H antiporter cDNA from turtle colon. The recently cloned human NHE-1 antiporter (Sardet et al. 1989. *Cell*. 56:271) provided a starting point for these studies. A 1.1-kb PCR product from the human cDNA, encoding amino acids 115-499, was radiolabeled by random primer extension and used to identify a 6.0-kb transcript in Northern blots of turtle colon mRNA. To clone this transcript a turtle colon cDNA library was constructed in Lambda Zap (Stratagene Inc., La Jolla, CA) and screened with the 1.1-kb human

probe. A 0.7-kb cDNA clone was isolated and sequenced by dideoxy chain termination. The 0.7-kb clone spans a region corresponding to nucleotides 839–1,535 of the human cDNA and is highly similar to the human sequence (>80% nucleotide identity). A second partial length turtle colon cDNA clone was obtained by PCR. Degenerate oligonucleotide primers based on the human NHE-1 antiporter sequence were constructed and used to amplify reverse transcribed turtle colon mRNA. The resulting clone, TC550, corresponds to nucleotides 1,648–2,144 of the human cDNA and is again highly similar to the human sequence. TC550 was used as a probe to screen the turtle colon cDNA library and two additional clones were obtained, one of which is 1.2 kb and probably represents a region corresponding to the cytoplasmic domain of the human cDNA. We conclude that turtle colon epithelial cells express a transcript that is highly similar to the human NHE-1 antiporter and probably encodes a basolateral Na/H antiporter. [Supported by NIH grant DK-29786.]

71. Reduced Sensitivity of CFTR Mutants to Activation by cAMP and Catalytic Subunit of Protein Kinase A. DANIEL J. WILKINSON, MITCHELL L. DRUMM,\* LISA S. SMIT,\* MONIQUE K. MANSOURA,\* THERESA V. STRONG,\* MICHAEL D. UHLER,\* FRANCIS S. COLLINS,\* and DAVID C. DAWSON, *Departments of Physiology, Human Genetics, and Biological Chemistry, University of Michigan Medical School, Ann Arbor, Michigan*

The symptoms of cystic fibrosis (CF) appear to be largely attributable to impaired salt transport, and the basic defect has been identified with altered Cl<sup>-</sup> channel function. The disease is caused by mutations in the gene coding for CFTR, a membrane protein that appears to function as a gated ion channel. Activation of CFTR by drugs that elevate cytosolic cAMP has been demonstrated in a variety of heterologous expression systems, but the molecular basis for defective Cl<sup>-</sup> channel function in CF has not been identified. We used *Xenopus* oocytes to study Cl<sup>-</sup> conductance associated with expression of wild-type (wt) CFTR and several variants containing disease-related mutations in the first nucleotide binding fold (NBF1). We found that  $\Delta F508$  and other NBF1 mutants exhibited an activatable Cl<sup>-</sup> conductance with reduced sensitivity to activation by forskolin (10  $\mu$ M) and increasing doses of 3-isobutyl-1-methylxanthine (IBMX, 0.02–5 mM). The reduction in sensitivity was correlated with the severity of CF in patients homozygous for the mutations (Drumm et al. 1991. *Science (Wash. DC)*. 254:1797). To more directly ascertain the effect of NBF1 mutations on altered sensitivity to elements of the cAMP signaling pathway, we compared the sensitivity of wt and mutant CFTRs to activation by direct injection of 8-Br-cAMP or catalytic subunit of protein kinase A (pkA C-subunit). Membrane currents were assayed using a two-electrode voltage clamp, and a third pipette was inserted for direct injection of mediators. As little as 20 fmol of 8-Br-cAMP activated wt CFTR, but activation of the less sensitive mutant G551S required > 1 pmol and activation of the least sensitive mutant  $\Delta F508$  required > 10 pmol. Injection of 100 fmol of pkA C-subunit also activated these CFTR variants, but the activation rate was slower for the mutants, in the order wt > G551S >  $\Delta F508$ . These results are consistent with a model for the activation of CFTR that requires two steps: pkA-mediated phosphorylation of the R domain, and the binding and hydrolysis of ATP at one or both of the NBFs. Activation by increased levels of cAMP and pkA is consistent with the notion that reduced sensitivity due to NBF1 mutations can be overcome by increasing the steady-state level of phosphorylated CFTR. [Supported by the NIH and CF Foundation.]

72. Mechanisms of Current Flow via the Basolateral Na-H Antiporter. MARC A. POST\* and DAVID C. DAWSON, *Department of Physiology, The University of Michigan, Ann Arbor, Michigan*

We used sheets of turtle colon, apically permeabilized with amphotericin-B, to identify a basolateral Na-H antiporter. Cation exchange (Na-H, Na-Li, Na-Na) was activated in shrunken cells and was blocked by amiloride. Outwardly directed Na<sup>+</sup> or Li<sup>+</sup> gradients were associated with an outward current that was identical to cation exchange with regard to cation selectivity, sensitivity to amiloride analogues, and activation by cell shrinkage. These observations suggested that Na<sup>+</sup> conduction was a property of the basolateral antiporter (Post and Dawson. 1992. *Am. J. Physiol.* 262:C1089). We

considered three possible mechanisms for conductive cation flow: slip, electrodiffusion via a channel-like conformation of the antiporter, and a nonunity exchange stoichiometry. Imposition of an outward proton gradient (cell pH 6.0, ecf pH 8.5) induced an anomalous inward current that was selective for  $\text{Na}^+$  and  $\text{Li}^+$  (but not  $\text{K}^+$ ,  $\text{Rb}^+$ , or  $\text{Cs}^+$ ) and was blocked by amiloride, dimethylamiloride, and ethylisopropylamiloride, as expected for an antiporter-mediated exchange stoichiometry of greater than  $1\text{Na}^+$  per  $1\text{H}^+$ . The activation of outward currents by cytosolic  $\text{Na}^+$  exhibited sigmoidal kinetics that could be rationalized as the binding and translocation of more than one  $\text{Na}^+$  per transport cycle. These observations are consistent with the hypothesis that a nonunity exchange stoichiometry accounts for at least a portion of the charge translocation via the basolateral  $\text{Na-H}$  antiporter. [Supported by NIH grant DK-29786.]

73. Comparison of the Translation of Rabbit  $\alpha$ -Globin and  $\beta$ -Globin mRNAs RICHARD T. TIMMER,\* KAREN S. BROWNING,\* LISA WEILL,\* and JOANNE M. RAVEL.\*  
*Department of Chemistry and Biochemistry, The University of Texas at Austin, Austin, Texas*  
(Sponsor: Robert B. Gunn)

In this study,  $\alpha$ -globin and  $\beta$ -globin mRNAs were prepared by in vitro transcription of the cDNA clones for these mRNAs and their translation was studied in vitro.  $\alpha$ -Globin mRNA is translated at 60–80% the rate of  $\beta$ -globin mRNA in a rabbit reticulocyte lysate system, in a wheat germ S30 system and in a partially purified system from wheat germ. The concentrations of the translation initiation factors (eIF) required to obtain a half-maximal rate of translation ( $C_{0.5}$ ) of  $\alpha$ -globin and  $\beta$ -globin mRNAs were determined in a highly fractionated system from wheat germ. In addition, the efficiency of binding of  $\alpha$ -globin and  $\beta$ -globin mRNAs to 40 S ribosomal subunits and 80 S initiation complexes was measured in the presence of highly purified eIF-2, eIF-3, eIF-4A, eIF-4B, eIF-4C, eIF-4F, and eIF-5. No difference was observed in the rate of elongation of  $\alpha$ - and  $\beta$ -globin polypeptides starting with preformed 80 S initiation complexes. The results of this investigation indicate that the difference in the rate of translation of  $\alpha$ - and  $\beta$ -globin mRNAs is due to a difference in the ability of these mRNAs to form 48 S initiation complexes resulting from differences in the requirement for specific translation initiation factors. These results are discussed in the context of the competition model of translation which postulates that mRNAs at high concentrations are in competition for a limited supply of initiation factors and that those mRNAs with the greatest affinity for the initiation factors will be translated preferentially.

74. Functional Expression of Human Band 3, the Anion Exchange Protein 1, in *Dictyostelium discoideum* KANG LIU, PAULINE SMITH,\* and ROBERT B. GUNN.  
*Department of Physiology, Emory University School of Medicine, Atlanta, Georgia*

This is the first functional expression of a mammalian membrane protein in the cellular slime mold, *Dictyostelium discoideum* (Dd), a unicellular eucaryote. The cDNA of erythroid human band 3 (HB3) was mutated in the first five codons to favor those used by Dd, and was inserted into pBS18, an expression vector with the neomycin resistance gene. Dd, strain Ax3, was transfected with this construct using  $\text{CaHPO}_4$ , and transformants were selected in media with G418 and dinitro stilbene disulfonate (DNDS). Cells from two polyclonal cultures were positive by Southern and Northern analysis but without detectable HB3 protein by Western analysis. Function was demonstrated as follows: (a) There was a  $36\text{-Cl}$  influx that was two to eight times that in untransfected controls ( $1\text{--}2\text{ pmol}/\mu\text{g}$  protein per min at  $20^\circ\text{C}$ ) or cells transfected with pBS18 containing no HB3 cDNA; (b) This added flux was inhibited by phloretin; (c) The added flux had an activation energy of only  $11\text{ kcal/mol}$ ; (d) This added flux was inexplicably insensitive to DNDS inhibition unless the cells were grown for 24 h in the absence of DNDS before the flux. Several cell lines with positive Southern but negative Northern analyses had control fluxes. Untransfected cells treated for 3 h at  $30^\circ\text{C}$  to induce heat shock proteins (also induced by stilbenes) had slightly lower  $\text{Cl}$  influx values. Control cells treated with sucrose to block endocytic vesicle cycling had control fluxes. The two expressing cultures had elevated chloride fluxes for 3 mo. [Supported by NIH grant HL-28674.]

75. Anion-selective Channel Activity of P-Glycoprotein GUILLERMO A. ALTENBERG,\* JULIO A. COPELLO,\* YIN ZHANG,\* JAMES BELLI,\* and LUIS REUSS, *Departments of Physiology and Biophysics and Radiation Therapy, University of Texas Medical Branch, Galveston, Texas*

P-glycoprotein (P-Gp) is overexpressed in many mammalian cells that exhibit multidrug resistance (MDR), and is thought to be an ATPase that actively extrudes liposoluble substrates from the cells, including chemotherapeutic agents. P-Gp belongs to the same superfamily as the cystic fibrosis transmembrane conductance regulator. Recent measurements of whole-cell currents suggest that P-Gp is a  $\text{Cl}^-$  channel (Valverde et al. 1992. *Nature [Lond.]*, 355:830). Here, the patch clamp technique was used to measure single-channel currents in wild type (V79) and MDR (LZ-8) Chinese hamster lung fibroblasts. P-Gp accounts for 1 and 20% of the total plasma membrane protein in V79 and LZ-8 cells, respectively. Anion-selective channels were found in both cell lines. The channels were active in cell-attached patches, and were found more frequently in LZ-8 cells (85 vs. 25% of high-resistance seals). In inside-out patches with 150 mM KCl in the pipette and 145 mM NaCl plus 5 mM KCl in the bath, current was zero at a membrane voltage ( $V_m$ ) of 0 mV. Replacing cytosolic  $\text{Cl}^-$  with gluconate changed the reversal potential to approximately -60 mV, indicating that this is a  $\text{Cl}^-$ -selective anion channel. The channel is an outward rectifier; its conductance was ~50 pS for positive  $V_m$  and ~25 pS for negative  $V_m$ . There was no effect of cytosolic  $[\text{Ca}^{2+}]$  (1 mM or 0.3  $\mu\text{M}$ ) on channel activity, and the data do not support voltage dependence of the open probability or gating differences between V79 and LZ-8 cells. P-Gp purified from LZ-8 plasma membranes (Belli et al. 1990. *Cancer Res.* 50:2191) by SDS electrophoresis and elution techniques (all of the purified protein can be immunoprecipitated with the anti P-Gp monoclonal antibody C219) was incorporated into artificial planar lipid bilayers. Single-channel events were observed upon addition of ~1  $\mu\text{g}$  of purified P-Gp to the *cis* compartment. With symmetric solutions (200 mM KCl, 2 mM  $\text{MgCl}_2$ , 1 mM ATP, and 10 mM MOPS/KOH, pH 7.40) there was no current flow at 0 mV, and the single-channel conductances were 25 and 35 pS for negative and positive voltages (*trans* reference), respectively. In the presence of a salt concentration difference (220/20 mM KCl *cis/trans*), the reversal potential was ~60 mV, the value expected for an anion-selective pathway. These results indicate that  $\text{Cl}^-$  channels are found more frequently in the MDR LZ-8 cells and that the reconstituted purified P-Gp has anion channel activity. It remains to be proven that this activity is consistent with that of the P-Gp present in the plasma membrane. [Supported in part by NIH grants CA-34269 and RR-07205.]

76. Functional Imaging of the Multidrug Resistance P-Glycoprotein with an Organotechnetium Complex JAMES M. CROOP,\* MARY L. CHIU,\* MARK BUDDING,\* JAMES F. KRONAUGE,\* ROBERT KRAMER,\* and DAVID PIWNICA-WORMS, *Department of Radiology, Harvard Medical School, Brigham and Women's Hospital, and Pediatric Hematology/Oncology, Dana-Farber Cancer Institute, The Children's Hospital, Boston, Massachusetts; and Lederle Laboratories, American Cyanamid, Pearle River, New York*

P-glycoprotein (Pgp), a 170-kD plasma membrane protein encoded by the mammalian multidrug resistance gene (MDR1), appears to function as an energy-dependent efflux pump of some of the most potent chemotherapeutic drugs. To test the hypothesis that the gamma-emitting organotechnetium complex, hexakis(2-methoxyisobutylisonitrile)technetium(I) ( $^{99\text{m}}\text{Tc}$ -SESTAMIBI), a lipophilic cationic radiopharmaceutical useful in perfusion imaging, could also be a suitable Pgp transport substrate, we examined the cellular pharmacological profile of  $^{99\text{m}}\text{Tc}$ -SESTAMIBI in Chinese hamster V79 lung fibroblasts and the 77A and LZ derivative cell lines which express modestly low, intermediate, and very high levels of Pgp, respectively. Steady-state contents of  $^{99\text{m}}\text{Tc}$ -SESTAMIBI in V79, 77A, and LZ cells were  $10.0 \pm 0.5$  ( $n = 9$ ),  $3.6 \pm 0.5$  ( $n = 8$ ), and  $0.4 \pm 0.02$  ( $n = 9$ ) fmol (mg protein) $^{-1}$  ( $\text{nM}_0$ ) $^{-1}$ , respectively, consistent with enhanced extrusion of the imaging agent by Pgp-enriched cells. To ascertain if  $^{99\text{m}}\text{Tc}$ -SESTAMIBI cell content could be increased by inhibition of Pgp, concentration-effect curves of the reversing agents verapamil and cyclosporin A were generated. Maximal doses (>100  $\mu\text{M}$ ) of these reversing agents enhanced  $^{99\text{m}}\text{Tc}$ -SESTAMIBI accumulation in V79, 77A, and LZ cells by ~10-, 25-, and 200-fold, respectively. The  $\text{IC}_{50}$  values for tracer

accumulation in the presence of verapamil in V79, 77A, and LZ cells were 4, 100, and 200  $\mu\text{M}$ , respectively. The  $\text{IC}_{50}$  values for cyclosporin A were 0.9, 3, and  $>25$   $\mu\text{M}$ , respectively. Furthermore, compared with V79 cells in control buffer, the initial efflux rate of  $^{99\text{m}}\text{Tc}$ -SESTAMIBI (determined at 2 min) was  $\sim 2.5$  times slower in the presence of the Pgp modulator verapamil (10  $\mu\text{M}$ ), consistent with Pgp-mediated efflux of  $^{99\text{m}}\text{Tc}$ -SESTAMIBI. Eadie-Hofstee analysis of verapamil-enhanced  $^{99\text{m}}\text{Tc}$ -SESTAMIBI accumulation as a function of ATP concentration was consistent with Michaelis-Menten kinetics displaying an apparent  $K_m$  of 59  $\mu\text{M}$  for ATP, similar to values for the ATP dependence of Pgp-mediated vinblastine transport. The interaction of carrier-added  $^{99\text{m}}\text{Tc}$ -SESTAMIBI with Pgp was directly examined by displacement of the Pgp photo-affinity probe [ $^{125}\text{I}$ ]iodoaryl azidoprazosin (IAP) from plasma membrane preparations derived from drug-resistant LZ cells or human leukemia CEM/VBL cells.  $^{99\text{m}}\text{Tc}$ -SESTAMIBI inhibited photolabeling of Pgp by IAP in a concentration-dependent manner; half-maximal effect was observed at  $\sim 100$ - to 1,000-fold molar excess  $^{99\text{m}}\text{Tc}$ -SESTAMIBI. The utility of tracer  $^{99\text{m}}\text{Tc}$ -SESTAMIBI to functionally image Pgp expression in human tumors in vivo was demonstrated by gamma camera scintigraphy. Bilateral tumor xenographs were produced in opposite flanks of nude mice with drug-sensitive KB human carcinoma cells or drug-resistant KB/8.5 cells. In four animals tested with paired tumor xenographs, the  $^{99\text{m}}\text{Tc}$ -SESTAMIBI accumulation was  $35 \pm 4\%$  lower in Pgp-enriched tumors compared with parental tumors implanted in the opposite flank. These experiments demonstrate the feasibility of scintigraphically imaging Pgp expression in vivo with  $^{99\text{m}}\text{Tc}$ -SESTAMIBI. Functional imaging with these organotechnetium complexes may provide a novel mechanism to rapidly characterize Pgp expression in human tumors in vivo and ultimately provide a means to target patients for specific cancer therapies. [Supported by NIH grants HL-42966, CA-011227, and CA-48162. D. Pownall-Worms is an Established Investigator of the American Heart Association.]

77. Amino Acid Substitutions at Codons 338 and 339 of P-Glycoprotein Strongly Modulate Anthracycline and Colchicine Resistance while Having Little Effect on Either Actinomycin D or Vincristine Resistance SCOTT E. DEVINE\* and PETER W. MELERA.\*  
*Department of Biological Chemistry, Graduate Program in Molecular and Cell Biology, and the Cancer Center, University of Maryland School of Medicine, Baltimore, Maryland* (Sponsor: Donald R. Matteson)

P-glycoprotein (Pgp) is a putative plasma membrane transporter that, when expressed in eukaryotic cells, confers resistance to a variety of cytotoxic agents. Pgp is proposed to have 12 transmembrane and two ATP-binding domains and is thought to mediate drug efflux via an ATP-dependent mechanism; the lethal toxicities of these compounds are avoided with the reduction of their intracellular concentrations. One aspect of Pgp that remains a mystery is its ability to both recognize and mediate the efflux of many structurally and functionally dissimilar compounds. Our recent work (Devine et al. 1992. *Proc. Natl. Acad. Sci. USA*. In press) suggests that the sixth transmembrane (tm6) domain of Pgp is involved in the mechanism of drug recognition and efflux. We report here the construction and preliminary analysis of Chinese hamster DC-3F cell lines stably expressing high levels of either normal or tm6-mutant Pgp. Comparison of cell lines with equivalent levels of normal and mutant Pgp expression suggests that, although the tm6 domain is strongly implicated in the mechanisms of colchicine and anthracycline efflux, it does not play the same role in the efflux of actinomycin D nor vincristine. These data are consistent with two possible models proposing that either (a) Pgp has a single drug efflux mechanism for all drugs, involving a single complex drug binding site which combines several, but distinct, drug recognition capabilities, or (b) the drug efflux mechanism used by Pgp involves spatially distinct drug recognition sites. [Supported by NCI grant CA-44678.]

78. Electrogenic Properties of the Cloned System  $\gamma^+$  Basic Amino Acid Transporter Expressed in *Xenopus* Oocytes MICHAEL P. KAVANAUGH\* and R. ALAN NORTH.  
*Vollum Institute, Oregon Health Sciences University, Portland, Oregon*

The voltage dependence of substrate flux mediated by the cloned murine system  $\gamma^+$  basic amino acid transporter was studied in *Xenopus* oocytes expressing the transporter. Voltage-clamped oocytes

displayed inward currents in response to application of arginine, lysine, and ornithine; the currents increased exponentially with hyperpolarization in the voltage range +40 to -120. The apparent  $K_m$  for arginine decreased and approached a minimum with hyperpolarization. Outward flux of substrate through the transporter was measured after loading of the cells by long applications of arginine; outward currents increased exponentially with membrane depolarization. A computer simulation of transport kinetics was developed based on a four-state model of facilitated transport. The simulation suggests a marked ion-well effect for substrate binding to the intracellular site. In addition, hyperpolarization increased the rate constant governing the conformational transition of the loaded carrier from outside to inside as well as the return of the binding site on the unloaded carrier to the extracellular face. In summary, the results show that voltage affects system  $y^+$  transport kinetics in addition to affecting the Nernst equilibrium, suggesting that membrane potential may provide a means for regulating intracellular levels of basic amino acids.

79. Immunological Identification of Na-K-Cl Cotransport Proteins in Avian Salt Gland and Human Colonic (T84) Cells CHRISTIAN LYTLE, JOSEPH TORCHIA, and BLISS FORBUSH III, *Department of Cellular and Molecular Physiology, Yale University School of Medicine, New Haven, Connecticut; and Department of Pharmacology, University of Toronto, Toronto, Ontario, Canada*

We have developed a panel of monoclonal antibodies that recognize the basolateral membrane glycoprotein responsible for Na-K-Cl cotransport in the dogfish shark rectal gland (Lytle et al. 1990. *J. Gen. Physiol.* 96:44a [Abstr.]). Members of this panel selectively recognize one of four different structural domains of the 195-kD cotransporter. Three of these antibodies (J3, J4, and J7) also recognize a 170-kD glycoprotein in duck salt gland membranes. Because these two glycoproteins (a) share immunological identity at multiple sites, (b) are phosphorylated in response to secretagogues (Torchia et al. 1991. *Am. J. Physiol.* 261:C543; Lytle and Forbush. 1990. *J. Cell Biol.* 111:312a [Abstr.]), and (c) selectively bind the photoreactive loop diuretic [ $^3$ H]BSTBA, they appear to represent homologous forms of the Na-K-Cl cotransporter. A monoclonal antibody (Q3) raised against this 170-kD duck salt gland protein has proven suitable for immunoprecipitation, immunoblotting, and immunolocalization. Four different antibodies (Q3, J3, J4, J7) recognize the 170-kD duck protein and the 195-kD shark cotransporter. J3, J7, and J25 also detect a 195-kD protein in membranes isolated from another chloride-secreting epithelium, the human colonic adenocarcinoma (T84 cell). After enzymatic (N-glycanase) removal of N-linked oligosaccharide, the immunoreactive proteins in T84 cells, rectal gland, and salt gland exhibit similar molecular masses (~135 kD). We propose that these three chloride-secreting epithelia possess similar 135-kD Na-K-Cl cotransport core proteins.

80. Cloning and Expression of the Na-K-Cl Cotransporter of Shark Rectal Gland JIAN-CHAO XU,\* CHRISTIAN LYTLE, TRACEY ZHU,\* EDWARD BENZ, JR., and BLISS FORBUSH III, *Departments of Cellular and Molecular Physiology and Internal Medicine, Yale University School of Medicine, New Haven, Connecticut*

We have screened a shark rectal gland cDNA expression library with monoclonal antibodies that selectively recognize the Na-K-Cl cotransport protein. Three clones (3B, 9C, and 24A) were isolated. DNA restriction maps, Southern blot analysis, and sequence analysis demonstrated that the three cDNAs overlapped. An Eco RI/Eco RI fragment (~1.4 kb) from the 5' end of 24A was used to rescreen the cDNA library, and another clone (16-2) containing the entire coding sequence of the cotransporter was obtained. The predicted protein is 1,191 amino acids long with a molecular mass of 129,787 D. Hydrophobicity analysis identified ~12 hydrophobic segments within the central region of the protein long enough to form membrane-spanning domains, and sequence analysis revealed nine potential sites for N-linked glycosylation. The protein bears no substantial homology with sequences currently listed in the Genbank database, suggesting that it represents an entirely new family of membrane transporters. Northern blot analysis of mRNA isolated from shark rectal gland and brain detected a single band of 7.5 kb. Stable transformation of human embryonic kidney (HEK-293) cells with 16-2 cDNA resulted in the expression of a 160-kD protein recognized by four

different anti-cotransporter antibodies. When N-linked oligosaccharides were removed from the expressed protein with *N*-glycanase, its molecular mass matched that of the deglycosylated rectal gland cotransporter (135 kD); thus, the entire core cotransport protein is expressed and partially glycosylated. Immunofluorescence microscopy localized the expressed protein along the plasma membrane of the HEK-293 cell. After preincubation in a Cl-free medium, cells transformed with the 16-2 cDNA took up  $^{86}\text{Rb}$  six times faster than control cells. This expressed  $^{86}\text{Rb}$  influx absolutely required external sodium and chloride and was inhibited by bumetanide with an affinity ( $\text{IC}_{50} = 0.37 \mu\text{M}$ ) 10 times lower than that exhibited by the endogenous HEK-293 cell Na-K-Cl cotransporter.

**81. Characterization of a Cation-selective Channel Activated by Extracellular ATP in Epithelial Cells** TIMOTHY J. TURNER and STEPHEN P. SOLT OFF, *Department of Physiology, Tufts University School of Medicine, Boston, Massachusetts*

Extracellular ATP elevates  $[\text{Ca}^{2+}]_i$  and stimulates multiple  $\text{Ca}^{2+}$ -dependent ion transport mechanisms (including  $\text{Cl}^-$  and  $\text{K}^+$  channels) that are involved in fluid secretion in rat parotid acinar cells. The effects of ATP require extracellular  $\text{Ca}^{2+}$ , and ATP stimulates an extracellular Na-sensitive uptake of  $^{45}\text{Ca}^{2+}$ . These isotopic flux studies and other measurements suggested that ATP activates a  $\text{Na}^+$ - and  $\text{Ca}^{2+}$ -permeable cation channel (Solt off et al. 1992, *Am. J. Physiol.* 262:C934-C940). We now demonstrate that ATP activates a distinct ion channel in parotid acinar cells. In whole cell patch clamp electrophysiological studies, extracellular ATP (10–1,000  $\mu\text{M}$ ) activated an inward current (peak amplitude =  $396 \pm 31 \text{ pA}$ ,  $n = 43$ ) in a concentration-dependent fashion. The current was reduced by extracellular Mg as we previously demonstrated for alterations in  $[\text{Ca}^{2+}]_i$ , suggesting that the active nucleotide form was  $\text{ATP}^{4-}$ . The current was also blocked by Coomassie brilliant blue and DIDS (4,4'-diisothiocyanostilbene disulfonate), compounds that blocked the binding of ATP to intact parotid cells. The removal of extracellular  $\text{Ca}^{2+}$  from cells exposed to physiological concentrations of  $\text{Na}^+$  did not appreciably affect the peak current amplitude, suggesting that the majority of current was due to  $\text{Na}^+$  entry. The reversal potential for ATP-stimulated currents was  $\sim -5 \text{ mV}$ , consistent with activation of a nonselective cation channel. When cells were dialyzed with 2 mM BAPTA/5 mM EGTA, the current was still activated by ATP, consistent with other studies that suggested that the channel was not activated by an elevation of  $[\text{Ca}^{2+}]_i$ . ATP analogue studies indicated a selectivity sequence of the following: benzylbenzyl ATP >  $\text{ATP}\alpha\text{S}$  > ATP > 2-CH<sub>3</sub>-SATP >  $\text{ATP}\gamma\text{S}$  >  $\beta,\gamma$ -methylene ATP, ADP >  $\alpha,\beta$ -methylene ATP. These studies suggest that the elevation of  $[\text{Ca}^{2+}]_i$  by ATP is due to the activation of a nonselective cation channel. Since ATP is costored and cosecreted with neurotransmitters, it itself may function as a neurotransmitter and play a role in the initiation of fluid secretion in these cells.

**82. Role of Calcium in cAMP-induced Activation of Hepatic  $\text{Na}^+$ /Taurocholate Cotransport** STEFAN GRÜNE\* and M. SAWKAT ANWER, *Departments of Medicine and Pharmacology, Tufts University School of Veterinary Medicine, North Grafton, Massachusetts*

Cellular mechanisms by which glucagon and cAMP stimulate hepatic  $\text{Na}^+$ /TC uptake is not clear, and may involve cAMP-induced increases in cytosolic  $[\text{Ca}^{2+}]$  ( $[\text{Ca}^{2+}]_i$ ). This hypothesis was tested by studying the effect of dibutyryl cAMP (DBcAMP) on  $[\text{Ca}^{2+}]_i$  and  $\text{Na}^+$ /TC uptake in isolated rat hepatocytes. DBcAMP increased the maximal rate of  $\text{Na}^+$ /TC uptake without affecting apparent  $K_m$  and  $\text{Na}^+$ -independent uptake. A number of agents were used to determine if the effect of DBcAMP is mediated via  $\text{Ca}^{2+}$ . These agents included a  $\text{Ca}^{2+}$  buffering agent (MAPTA), a blocker of intracellular  $\text{Ca}^{2+}$  release (TMB8), an inhibitor of phospholipase C (U73122), and a phorbol ester known to activate protein kinase C (PMA). All these agents decreased DBcAMP-induced increases in  $[\text{Ca}^{2+}]_i$ , as well as DBcAMP-induced stimulation of  $\text{Na}^+$ /TC uptake. Since these agents act via different mechanisms and yet produce the same effect on DBcAMP-induced increases in  $[\text{Ca}^{2+}]_i$  and  $\text{Na}^+$ /TC uptake, it is likely that the effect of cAMP is mediated via intracellular  $\text{Ca}^{2+}$ . However, other  $\text{Ca}^{2+}$  mobilizing agents (thapsigargin and vasopressin) failed to stimulate  $\text{Na}^+$ /TC uptake. Calmidazolium, an inhibitor of calmodulin, inhibited DBcAMP-induced  $\text{Na}^+$ /TC uptake without affecting DBcAMP-

induced increases in  $[Ca^{2+}]_i$ . Calmidazolium also decreased DBcAMP-induced hyperpolarization of hepatocytes. Since hepatic  $Na^+/TC$  cotransport is believed to be electrogenic, these result may indicate that cAMP stimulates  $Na^+/TC$  cotransport by calcium/calmodulin-mediated changes in membrane potential. However, why other  $Ca^{2+}$  mobilizing agents failed to stimulate  $Na^+/TC$  uptake remains unexplained. [Supported by NIH grant DK-33436.]

83.  $Na^+-Ca^{2+}-K^+$  Exchanger and cGMP-gated Channel of the Vertebrate Photoreceptor Are Associated PAUL J. BAUER\* and BERTHOLD HUPPERTZ,\* *Institut für Biologische Informationsverarbeitung, Forschungszentrum Jülich, Jülich, Germany*

In the outer segments of vertebrate photoreceptors  $Ca^{2+}$  enters the cell through the cGMP-gated channels and is extruded by  $Na^+-Ca^{2+}-K^+$  exchange. We addressed the question of whether or not these two proteins are distributed independently of each other in the plasma membrane. Both proteins are localized exclusively in the plasma membrane of the outer segment (Bauer, 1988, *J. Physiol. [Lond.]*, 401:309; Cook et al. 1989, *J. Biol. Chem.* 264:6996; Reid et al. 1990, *Biochemistry*, 29:1601) which in bovine rod outer segments constitutes ~6% of the total membrane area. Fusion of disk and plasma membrane resulted in a distribution of channels and exchangers over ~35% of the total membrane, consistent with a channel density of ~300  $\mu m^{-2}$  in the plasma membrane (i.e., before membrane fusion). However, channels and exchangers did not distribute independently of each other but were localized on the same vesicle fraction. Even after solubilization of the membrane proteins in 3-([3-cholamidopropyl]-dimethylammonio)-1-propanesulphonate (CHAPS) and reconstitution in soybean phosphatidylcholine, both proteins were almost exclusively in the same vesicle fraction. Therefore, we conclude that both proteins are associated in the membrane and, moreover, that there are at least as many exchangers as channels. We could, however, not determine the stoichiometry of this association. The association of channel and exchanger enabled us to investigate quantitatively the  $Na^+-Ca^{2+}$  exchange in normal and reversed direction with the vesicle technique since right side-out and inside-out oriented channels will also have right side-out and inside-out oriented exchangers, respectively, but only inside-out oriented channels can be opened upon adding cyclic GMP. The fractions of vesicles containing right side-out and inside-out oriented exchangers were about similar. In the absence of  $K^+$ , both modes of  $Na^+-Ca^{2+}$  exchange showed only little  $Na^+-Ca^{2+}$  exchange. In the presence of  $K^+$ , normal and reversed mode  $Na^+-Ca^{2+}$  exchange had similar  $Na^+$  concentrations of ~70 mM for half-maximal activation and cooperativity parameters,  $n_{Hill}$ , of ~2.0; the two modes of  $Na^+-Ca^{2+}$  exchange differed, however, in the exchange rate, the normal mode being about a factor of two faster than the reversed mode.

84. Novel Protein Motif Describes the Transmembrane Domain of Single Span Membrane Proteins CAROLINA LANDOLT\* and REINHART A. F. REITHMEIER,\* *Medical Research Council Group in Membrane Biology, Departments of Medicine and Biochemistry, University of Toronto, Toronto, Ontario, Canada (Sponsor: Luis Reuss)*

Analyses of the transmembrane domains of 115 single span type I (amino terminus extracellular, carboxyl terminus cytoplasmic) human plasma membrane proteins demonstrated that the distribution of hydrophobic amino acids within the transmembrane domain was not random, with isoleucine preferred at the amino terminus followed by a valine-rich domain and leucine favored at the carboxyl-terminal region. Similarly, the distribution of amino acids in both flanking segments was not random with helix initiators (Pro, Asn, and Ser) favored at the amino-terminal flank and basic residues (Lys and Arg) localized to the carboxyl-terminal flank. Aromatic amino acids (Tyr, Trp, and Phe) were localized to the membrane/aqueous interface. Single span type II (opposite orientation from type I) transmembrane segments appear to have a similar distribution of hydrophobic amino acids with respect to the lipid bilayer with leucine now localized to the amino-terminal region and isoleucine favored at the carboxyl-terminal region. Tyrosine and tryptophan were again localized at the membrane interface, with positively charged residues favored at the amino-terminal, cytoplasmic flank. The first transmembrane segment of multi-span membrane proteins with a cytoplasmic amino

terminus has a type II topology while the second transmembrane segment has a type I topology with respect to the lipid bilayer. Preliminary results suggest that these transmembrane segments share some common features with single span membrane proteins with equivalent topology. Isoleucine was preferred in the amino-terminal half of the second transmembrane domain while proline was favored at the amino-terminal flank of these transmembrane segments. Positively charged residues were localized to the cytoplasmic flanking domain of both the first and second transmembrane segments. [Supported by a group grant from the Medical Research Council of Canada.]

85. A Method for Identification of a Thymidine Transport Protein by Functional Complementation in Yeast DOUGLAS HOGUE,\* MICHAEL ELLISON,\* and CAROL E. CASS,\* *Department of Biochemistry, University of Alberta, Edmonton, Alberta, Canada*

The transport of physiological and some pharmacologically relevant nucleoside analogues into mammalian cells is mediated by a family of nucleoside transport (NT) proteins. Identification of these NT proteins by classical biochemical techniques has proven difficult; hence we have attempted to identify cDNA that encode NT proteins by using a functional expression approach in *Saccharomyces cerevisiae*, a eukaryotic cell that lacks a thymidine (dThd) influx mechanism. Our procedure involves the rescue of *S. cerevisiae* grown in the presence of methotrexate (MTX) and sulfanilimide (SAA) by expression of a mammalian NT protein. MTX and SAA act synergistically to inhibit the conversion of deoxyuridylate to thymidylate (dTTP) by thymidylate synthetase, thereby blocking the only route of dTTP synthesis and eliciting cell death. An obstacle to our approach was the absence of thymidine kinase (TK) in *S. cerevisiae*, the mechanism by which dTTP would be generated from dThd that enters the cell via a NT protein. We have created a strain that expresses functional TK and grows in the presence of MTX, SAA, and high concentrations of dThd, presumably due to diffusional entry of dThd. Cloning of NT proteins should be possible because this growth is absent at lower dThd concentrations, a condition under which a functional NT protein should circumvent cell death. A murine cDNA plasmid expression library was transformed into this TK-containing strain and growth of transformants was assayed on plates containing MTX, SAA, and a low concentration of dThd. Several clones, containing an identical cDNA insert, were isolated and shown to confer plasmid-mediated dThd-dependent growth in the presence of MTX and SAA. Sequence analysis of this clone has revealed a putative protein product that contains potential membrane-spanning hydrophobic domains. This ability to functionally screen for dThd transport activity should be applicable for the identification of other members of the nucleoside transporter family.

86. Evidence for an Eosin Site Separate from the ATP Site in the Human Red Cell Calcium Pump CRAIG GATTO\* and MARK A. MILANICK, *Department of Physiology, University of Missouri-Columbia, Columbia, Missouri*

Fluorescein-5-isothiocyanate (FITC) may label a lysine in the ATP site of P-type pumps. We characterized inhibition of the plasma membrane Ca pump produced by eosin (tetrafluoroeosin), eosin-5-isothiocyanate (EITC), and 5-iodoacetamidoeosin (IAE). ATP-dependent  $^{45}\text{Ca}$  uptake into inside-out vesicles (IOVs) was measured. We found that eosin and ATP did not compete in the Ca pump, suggesting that they do not share the same site. The  $K_i$  for eosin was 0.05–0.2  $\mu\text{M}$ . The inactivation rate ( $k$ ) of EITC, FITC, and IAE irreversible inhibition was determined at several different inhibitor concentrations. IOVs were preincubated in the absence of substrates for 0, 1, 2, and 3 min at 37°C at pH 7.4. The suspension was diluted ~10-fold into media containing albumin and substrates and Ca uptake was determined. The time course of inhibition was fit to a single exponential function (and was not constrained to be zero inhibition at  $t = 0$ ; i.e., a fast phase may also have been present). The plot of  $k$  vs. inhibitor concentration saturated for all three compounds, suggesting that reversible binding preceded the irreversible reaction. Surprisingly, the  $K_{1/2}$  for IAE (1–2  $\mu\text{M}$ ) was ~10-fold less than the  $K_{1/2}$  for EITC (20–25  $\mu\text{M}$ ), suggesting that IAE and EITC bind reversibly at different sites before labeling those sites. The  $K_{1/2}$  for EITC was similar to  $K_{1/2}$  for FITC (~25 and 50  $\mu\text{M}$ , respectively), whereas the  $K_i$  for eosin differed from fluorescein (<0.2 and ~1,000  $\mu\text{M}$ , respectively).

It may be that IAE labels a site that binds eosin better than fluorescein. We propose that IAE and eosin bind to a site distinct from the ATP and FITC site(s). [Supported by Marion-Merrell Dow, Inc. and NIH grant DK-37512. M. A. Milanick is the recipient of a Research Career Development Award from the NIH.]

87. Multiple Site Optical Recording of Action Potential Propagation in Patterned Monolayer Sheets of Heart Cells in Culture STEPHAN ROHR\* and B. M. SALZBERG, Departments of Neuroscience and Physiology, University of Pennsylvania School of Medicine, Philadelphia, Pennsylvania

Structural complexities at the macroscopic level (e.g., branching of muscle bundles, Spach et al. 1982, *Circ. Res.* 50:175) can alter normal propagation and produce conduction disturbances in the heart. With the goal of establishing a model system in which propagation anomalies can be investigated at the microscopic level, we adapted the technique of multiple site optical recording of transmembrane voltage (MSORTV) to patterned monolayer sheets of neonatal rat heart cells in culture (Rohr et al. 1991, *Circ. Res.* 68:114). Cultures having defined geometries (photolithographically patterned substrate) were stained with voltage-sensitive styryl dyes (RH423, Di-8-ANEPPS) and mounted in a temperature-controlled bath fixed to the stage of an inverted microscope (model IM-35; Carl Zeiss, Inc., Thornwood, NY). Cell assemblies were stimulated using an extracellular electrode sufficiently distant that only propagated action potentials invaded the region of interest. An image of this area was projected onto a  $12 \times 12$  photodiode array. Photocurrents from the 124 central elements were converted to voltages, amplified, and processed by an analogue-to-digital converter (1.6-kHz frame rate). A subset of 16 freely selectable channels was monitored in parallel by a faster data acquisition system (62.5-kHz frame rate). Control conduction velocities, measured optically over multiple cells grown as monolayer strands of varying width (50–100  $\mu\text{m}$ ), were in the range of 0.3–0.5 m/s. When the width of a continuous strand was increased abruptly from 60 to 2,800  $\mu\text{m}$ , impulse propagation from the narrow to the wider region became discontinuous in a frequency-dependent manner: increasing stimulation rates gave rise to longer delays and the appearance of foot potentials at the transition boundary. Eventually, at stimulation rates  $\geq 2$  Hz, preparations exhibited intermittent conduction failures and complex propagation patterns such as those characteristic of Wenckebach periodicity. Altering the discontinuity to a funnel-like widening with an angle of  $120^\circ$  between the funnel sides generally did not affect the blocking phenomenon. The experiments demonstrate that the combination of MSORTV and reproducible geometric patterning of monolayer sheets of heart cells in culture provide improved spatial and temporal resolution over conventional methods and permit the study of the structural origin of propagation disturbances at cellular and subcellular levels. [Supported by Swiss NSF grant 823-A-028424 and USPHS grant NS-16824.]

88. Whole-Cell Analysis of Electrogenic Neurotransmitter Transport in Transfected HeLa Cells STEFANIA RISSO,\* LOUIS J. DeFELICE,\* and RANDY D. BLAKELY,\* Department of Anatomy and Cell Biology, Emory University, Atlanta, Georgia (Sponsor: R. DeHaan)

The rapid removal of extracellular neurotransmitter after release is mediated by a large family of homologous  $\text{Na}^+$ /cotransport proteins encoded by single RNAs. HeLa cells transfected with cDNAs encoding monoamine and amino acid neurotransmitter transporters exhibit transport activities virtually identical to that observed with brain membrane preparations. Membrane vesicle and whole cell studies suggest that several of these transporters conduct electrogenic transport, providing the opportunity to obtain single measurements of transporter activity and regulation. We have explored this possibility by performing whole-cell patch clamp measurements of HeLa cells expressing the cloned GABA transporter. The GABA transporter was isolated by PCR techniques and cloned into the plasmid pBluescript SKII- in a sense orientation downstream of the T7 RNA polymerase promoter. HeLa cells infected with a vaccinia virus encoding the T7 RNA polymerase (10 pfu/cell) were transfected with the GABA transporter plasmid and whole-cell patch clamp recordings were conducted 16–24 h later. Control cells were either given virus alone or were transfected with the expression plasmid lacking the transporter cDNA. GABA transporter transfected cells, but not control

cells, exhibited an inward current in response to micromolar (1–100  $\mu\text{M}$ ) GABA concentrations in the extracellular medium. The GABA-induced current is typically in the range of 50–100 pA at  $-60$  mV and 50  $\mu\text{M}$  GABA. Voltage ramps ( $-90$  to  $10$  mV from a holding potential of  $-40$  mV) at fixed concentrations indicate a linear dependence of GABA-induced currents on membrane potential, with a reversal potential between  $0$  and  $10$  mV, consistent with the inward cotransport of  $n\text{Na}^+$  and  $\text{Cl}^-$  with GABA. These findings indicate that both kinetic and steady-state properties of native and mutant neurotransmitter transporters can be monitored in single transfected mammalian cells. [Supported by NIH grant HL-27385 (L. J. DeFelice and S. Risso) and NIDA grant DA-07390 (R. D. Blakely).]

89. pH Regulation in Frog Skeletal Muscle Membrane Domains: Transverse Tubular Membrane Vesicles ROBERT W. PUTNAM, *Department of Physiology and Biophysics, Wright State University School of Medicine, Dayton, Ohio*

Microelectrode studies have suggested that the two pH-regulating transport systems in frog (*Rana pipiens*) skeletal muscle fibers, the  $\text{Na}/\text{H}$  and  $(\text{Na} + \text{HCO}_3)/\text{Cl}$  exchangers, are localized to the surface membrane (SM) and not the transverse tubular membrane (TTM). To further study the distribution of these exchangers, pH regulation was studied in small membrane vesicles enriched in TTM. TTM vesicles were isolated by a modification of the technique of Hidalgo et al. (1986. *Biochim. Biophys. Acta*. 855:79). Compared with the crude muscle homogenate, this vesicle fraction was enriched 175-fold in  $\text{Na}/\text{K}$  ATPase ( $27.7 \pm 5.4$   $\mu\text{mol}/\text{mg} \cdot \text{h}$ ) and 65-fold in  $\text{Mg}$  ATPase ( $182 \pm 42$   $\mu\text{mol}/\text{mg} \cdot \text{h}$ ) activities, indicating enrichment of this fraction for plasmalemma.  $\text{Ca}$  ATPase activity was absent from the TTM vesicle fraction ( $0.12 \pm 0.12$   $\mu\text{mol}/\text{mg} \cdot \text{h}$ ), indicating little contamination by sarcoplasmic reticular membrane. That the TTM fraction is distinct from the SM is shown by the marked enrichment (290-fold) of nitrendipine binding (a TTM marker) in these vesicles compared with crude homogenate. The majority of the TTM vesicles appear to be well sealed and in an inside-out configuration, as shown by the 50–85% increase in  $\text{Na}/\text{K}$  ATPase activity and ouabain binding induced by the detergent saponin. These vesicles could be loaded with the pH-sensitive dye pyranine by preinjecting the hind limbs of frogs with pyranine and including 500  $\mu\text{M}$  pyranine in the homogenization media. Creation of a large inward  $\text{Na}$  gradient (in nominally  $\text{CO}_2$ -free solution) had no effect on intravesicular pH. Vesicles acidified by exposure to nigericin (a  $\text{K}/\text{H}$  exchanging ionophore) showed a marked alkalization in the presence of a large inward  $\text{Na}$  gradient, but this alkalization was unaffected by amiloride. Upon exposure to propionic acid or dimethyl-2,4-oxazolidinedione the vesicles acidified, but no pH recovery was observed even in the presence of a large inward  $\text{Na}$  gradient. In summary, the vesicle data seem to confirm the lack of a  $\text{Na}/\text{H}$  exchanger in the TTM of frog skeletal muscle. [Supported by NIH grant AR-38881.]

90. Role of  $\text{Na}/\text{H}$  Exchange in Volume Regulation in Primary Rat Astrocytes and C6 Glioma Cells LAMARA D. SHRODE,\* MICHAEL McMANUS,\* and ROBERT W. PUTNAM, *Department of Physiology and Biophysics, Wright State University, Dayton, Ohio; and Department of Anesthesiology, Children's Hospital, Boston, Massachusetts*

Intracellular pH ( $\text{pH}_i$ ) and volume regulation were studied in primary rat astrocytes and C6 glioma cells.  $\text{pH}_i$  was measured with the pH-sensitive dye BCECF and cell volume was measured with a near right angle laser light-scattering technique (Strange and Morrison. 1992. *Am. J. Physiol. [Cell Physiol.]* In press). Both measurements were made on monolayers of cultured cells grown on glass chips. Steady-state  $\text{pH}_i$  ( $\text{pH}_o = 7.4$ ,  $\text{CO}_2$ -free,  $37^\circ\text{C}$ ) in primary astrocytes was  $7.01 \pm 0.03$  ( $n = 58$ ) (mean  $\pm$  SE) and in C6 cells was  $7.28 \pm 0.02$  ( $n = 83$ ). After a 5-min prepulse of 30 mM  $\text{NH}_4\text{Cl}$ , both types of cells acidified to  $\sim 6.0$ . The  $\text{pH}_i$  recovery from this acidification was somewhat faster in C6 cells ( $0.31 \pm 0.03$  pH unit/min) than in primary astrocytes ( $0.21 \pm 0.02$  pH unit/min). This recovery was completely abolished by 1 mM amiloride or by  $\text{Na}$ -free solutions in both cell types, indicating the presence of the  $\text{Na}/\text{H}$  exchanger. Jean et al. (1986. *J. Biochem. [Tokyo]*. 160:211) have shown activation of the  $\text{Na}/\text{H}$  exchanger upon exposure of C6 cells to a hyperosmotic solution. We observed a  $0.65 \pm 0.02$  pH unit alkalization (rate of  $0.24 \pm 0.02$  pH unit/min) upon exposure of glioma cells

to hypertonic mannitol solutions (HEPES buffer + 250 mM mannitol,  $\pi = 450$  mosM). This alkalinization was fully inhibited by 1 mM amiloride. We have now demonstrated a similar response in primary rat astrocytes. Upon exposure to a hyperosmotic solution, pH<sub>i</sub> increased by  $0.44 \pm 0.03$  pH unit at a rate of  $0.16 \pm 0.03$  pH unit/min. Furthermore, in primary astrocytes this alkalinization was dose dependent, increasing with increasing hyperosmolarity. Volume measurements showed that glioma cell shrinkage, induced upon the removal of NH<sub>4</sub>Cl, is markedly increased when Na/H exchange is inhibited by amiloride. In summary, the Na/H exchanger is present in both C6 cells and primary astrocytes, and plays a major role in pH<sub>i</sub> recovery and regulatory volume increase in both types of cells.

91. Molecular Biology of Osmolyte Transporters in MDCK cells: Na/myo-Inositol and Na/Cl/Betaine Cotransporters H. MOO KWON,\* ATSUSHI YAMAUCHI,\* SHINICHI UCHIDA,\* AGNES S. PRESTON,\* and JOSEPH S. HANDLER,\* *Department of Medicine, The Johns Hopkins University, Baltimore, Maryland* (Sponsor: Gerda Breitwieser)

Cells in the hypertonic mammalian renal medulla are protected from the deleterious effects of high electrolyte concentrations by accumulating high concentrations of nonperturbing osmolytes including myo-inositol (MI) and betaine (B). When kidney-derived MDCK cells are cultured in hypertonic medium, they accumulate MI and B up to 1,000 times their medium concentration. This results from hypertonicity-induced high rates of MI and B transport into cells. We have recently isolated cDNAs encoding Na/MI cotransporter (SMIT) and Na- and Cl-dependent B transporter (BGT-1) using expression in *Xenopus* oocytes (Kwon et al. 1992. *J. Biol. Chem.* 267:6297; Yamauchi et al. 1992. *J. Biol. Chem.* 267:649). The SMIT predicts a protein of 718 amino acids with an extensive amino acid sequence similarity to the Na/D-glucose (SGLT1) and Na/nucleoside (SNST1) cotransporters, identifying it as a member of the Na-coupled transporter gene family. Northern analysis indicated that transporter mRNA is present in kidney medulla > kidney cortex > brain. BGT-1 encodes a protein of 614 amino acids that exhibits highly significant sequence and topographic similarity to the brain neurotransmitter (GABA, noradrenaline, dopamine, and serotonin) transporters, indicating that it is a member of the Na/Cl-coupled transporter gene family. To investigate the mechanisms by which hypertonicity evokes increases in MI and B transport in MDCK cells, we used the cDNAs to measure the abundance of the mRNAs for the transporters and their rates of transcription after changes in osmolality. When MDCK cells were switched from isotonic to hypertonic medium, mRNA abundance of both transporters rose >10-fold in 24 h and remained elevated. The increase in mRNA levels preceded the increase in respective transporter activities. Transcription of the transporter genes rose as early as 2 h and reached a peak ~20- (SMIT) and 13-fold (BGT-1) those in isotonic cells 16 h after the switch. When cells were switched back to isotonic medium, mRNA abundance and transcription of the transporter genes returned to isotonic levels in 12 h. Thus, transcription appears to be the primary step in regulation of MI and B transports by hypertonicity. [Supported by NIH grant DK-42479.]

92. The Three Forms of NaCl Neutral Entry Are All Present in the Apical Membrane of Rabbit Gallbladder Epithelium DARIO CREMASCHI, CRISTINA PORTA,\* DANIELA RICCARDI,\* GUIDO BOTTA,\* and GIULIANO MEYER,\* *Department of General Physiology and Biochemistry, University of Milan, Milan, Italy*

The double ion exchange and a K<sup>+</sup>/bumetanide-insensitive Na<sup>+</sup>-Cl<sup>-</sup> symport sustain NaCl absorption in rabbit gallbladder incubated with bicarbonate-saline; conversely, only the second is operant with bicarbonate-free bathing salines. Under the latter conditions (plus 10<sup>-4</sup> M acetazolamide) transepithelial fluid (and NaCl) net flux was measured gravimetrically every 30 min, adding hydrochlorothiazide (HCTZ) at different luminal concentrations to check the symport sensitivity to the drug. Maximum inhibition (~70% of the control transport) was apparently obtained with 10<sup>-5</sup> M HCTZ. The residual transport (~30%) was sensitive to luminal 10<sup>-4</sup> M bumetanide, in contrast to the control transport, but was insensitive to stilbenes. Thus, HCTZ seems to have inhibited all the original

transport, a new bumetanide-sensitive transport having been elicited by the inhibition, partially masking the inhibition itself. All this makes approximate the HCTZ dose-response curve. It remains, however, that if phosphates and sulfates (17.1 mM) were eliminated from the bicarbonate-free salines (Tris buffer saline), a 10-fold lower HCTZ concentration was sufficient to obtain the same result. An electrical method was also used to measure fluid (and NaCl) absorption with improved temporal resolution (6-min periods). With the Tris buffer saline, fluid absorption, so measured, was insensitive to bumetanide but was abolished by  $10^{-4}$  M HCTZ already in the first 6-min period; therefore, a correct dose-response curve could be obtained in this phase. The bumetanide-sensitive transport was homeostatically activated after 12–30 min. When this process was also inhibited by bumetanide, no absorption was measured again for 12–30 min; afterwards, a second new transport was elicited which proved insensitive to bumetanide and even to  $2 \times 10^{-4}$  M HCTZ, but which was abolished by  $3 \times 10^{-4}$  M HCTZ. These results show that: (a) all three forms of NaCl neutral entry are present in the apical membrane, (b) the bumetanide-sensitive process is activated only upon inhibition of the other two transport systems, (c) a second homeostatic reaction consists of a reactivation of the HCTZ-sensitive symport upon a decrease in its sensitivity to the drug, and (d) the symport sensitivity to HCTZ is reduced in the presence of bivalent anions in the bathing saline.

93. Intracellular Calcium Regulation in Snail Neurons: A Role for Na:Ca Exchange?  
HELEN J. KENNEDY\* and ROGER C. THOMAS, *Department of Physiology, University of Bristol, Bristol, United Kingdom*

Intracellular calcium ( $aCa_i$ ) was measured in large unidentified neurones of *Helix aspersa* in isolated ganglia using the fluorescent indicator fura2 and calcium-sensitive microelectrodes (Thomas and Kennedy, 1992. *J. Physiol. [Lond.]*, 446:134P). Separate quartz light guides were used to illuminate a selected, dye-injected cell and to collect the emitted fluorescence. Cells were voltage clamped to a potential of  $-60$  mV and superfused with snail Ringer containing 80 mM NaCl, 7 mM  $CaCl_2$ , 5 mM  $MgCl_2$ , 4 mM KCl, and 20 mM HEPES to a pH of 7.5. Average resting values for  $aCa_i$  were  $\sim 30$ – $100$  nM as determined by fluorescence or calcium-sensitive microelectrodes. Depolarizations to 0 mV for 16 s caused large increases in  $aCa_i$ , which recovered to resting values; no such increase was observed in Ca-free Ringer. We monitored the rate of recovery from such depolarizations to assess the contribution of various regulating processes in  $Ca^{2+}$  homeostasis. We used sodium orthovanadate in the voltage clamp electrode (100 mM) to block the  $Ca^{2+}$ -ATPase of the plasma membrane (DiPolo et al. 1979. *Nature. [Lond.]*, 281:228). This caused a rise in resting  $aCa_i$ , which did not return to control values. Recovery from depolarizations was slower and returned only to the elevated level of  $aCa_i$ . We have made many attempts to demonstrate the presence of a Na:Ca exchange in the plasma membrane. Removing extracellular Na had no effect on the resting  $aCa_i$ , or the rate of recovery of  $aCa_i$  from 16-s depolarizations to 0 mV. We also used K-free Ringer or ouabain (100  $\mu$ M), which are known to raise intracellular  $Na^+$ . This had no effect on the resting  $aCa_i$ . Hence, we conclude that there is probably a  $Ca^{2+}$ -ATPase present in the plasma membrane which contributes to the regulation of  $aCa_i$ . However, as yet we have been unable to demonstrate the presence of a Na:Ca exchanger in snail neurons. [Supported by the Medical Research Council.]

94. Structure, Regulation, and Function of ProP: An Osmoregulated and Osmoregulatory Proline/Betaine Transporter from *Escherichia coli* K-12 DOREEN E. CULHAM,\* KATHERINE S. EMMERSON,\* CARLTON GYLES,\* DANIEL MAMELAK,\* BRIAN STEER,\* and JANET M. WOOD,\* *Departments of Microbiology, Veterinary Microbiology and Immunology, and Chemistry and Biochemistry, University of Guelph, Guelph, Ontario, Canada*

*Escherichia coli* cells that are exposed to hypertonic environments can resist dehydration and growth inhibition by accumulating such solutes as potassium ions, trehalose, amino acids (such as glutamate or proline), and/or amino acid derivatives (such as glycine betaine and proline betaine). Proline and glycine betaine are actively accumulated via transporters encoded in genetic loci *proP* and *proU*. ProP and ProU are present and expressed in clinical *E. coli* isolates. Betaines facilitate the growth of such

strains in artificial urine. Proline transport via ProP is activated by a hyperosmotic shift in whole cells and in cytoplasmic membrane vesicles derived from *E. coli* (Milner et al. 1988, *J. Biol. Chem.* 263:14900). ProP is activated only by membrane-impermeant osmolytes, implying that its activity is determined by cell turgor. DNA sequence analysis suggests that ProP is a 500-amino acid, hydrophobic protein similar in structure to the superfamily of enzymes that catalyze facilitated diffusion or ion-linked transport of organic solutes. Members of the transporter family are integral membrane proteins, many of which are thought to possess cytoplasmic amino and carboxyl termini and to cross the cytoplasmic membrane 12 times. ProP is most similar to KgtP (an alpha ketoglutarate transporter from *E. coli*) and to citrate transporters from *E. coli* and *Klebsiella pneumoniae*. Neither citrate nor alpha ketoglutarate is an osmoprotectant and neither transporter is known to be osmoregulated. Sequence alignments indicate that ProP differs from those systems by including a carboxyl terminal extension that is strongly predicted to participate in the formation of an alpha helical coiled coil. We propose that the carboxyl terminus of ProP may be involved in its response to turgor. We have prepared antibodies that recognize a synthetic peptide corresponding to the carboxyl-terminal ProP sequence. Those antibodies are being used to test our predictions regarding the membrane localization, topology, and function of the ProP protein. [Supported by the Kidney Foundation of Canada.]

95.  $\text{Ca}^{2+}$ -activated  $\text{K}^{+}$  Channel of Human and Rabbit Red Cells: Ligand Binding and Transport Inhibition by Synthetic Scorpion Toxins CARLO BRUGNARA, LUCIA DE FRANCESCHI,\* and SETH L. ALPER. *Department of Pathology, Brigham and Women's Hospital; Molecular Medicine and Renal Units, Beth Israel Hospital; and Department of Cellular and Molecular Physiology, Harvard Medical School, Boston, Massachusetts*

We have investigated the interactions of charybdotoxin (ChTX), iberiotoxin (IbTX), and mutant ChTX analogues with the  $\text{Ca}^{2+}$ -activated  $\text{K}^{+}$  channel (Gardos pathway) in human and rabbit erythrocytes. We measured the binding of  $^{125}\text{I}$ -ChTX to erythrocytes and its displacement by unlabeled analogues, and compared these data with electrical and isotopic indices of channel activity. We found that a major portion of  $^{125}\text{I}$ -ChTX bound to red cells was displaceable by excess unlabeled ChTX (50 nM). The specific  $^{125}\text{I}$ -ChTX binding to human red cells is markedly increased in low ionic strength conditions as compared with that measured at physiological ionic strength, and at alkaline pH as compared with normal pH. In medium containing 18 mM NaCl, 2 mM KCl, 10 mM Tris-Cl, pH 8.0, 230 mM sucrose, and  $1 \times 10^7$  cells/ml, this specific component can be described most simply as a single class of sites of  $K_d = 75$  pM and  $B_{\max} = 105$  sites per cell.  $\text{Ca}^{2+}$ -activated  $^{86}\text{Rb}$  influx measured under identical conditions revealed an  $\text{ID}_{50}$  for ChTX of 25 pM at low ionic strength and 1,500 nM at physiological ionic strength. Similar studies in rabbit erythrocytes at low ionic strength revealed a  $K_d$  for  $^{125}\text{I}$ -ChTX = 75 pM, with 125 binding sites/cell and an  $\text{ID}_{50}$  for inhibition of  $^{86}\text{Rb}$  influx = 25 pM. Whereas IbTX neither inhibited  $\text{Ca}^{2+}$ -activated  $^{86}\text{Rb}$  influx nor displaced  $^{125}\text{I}$ -ChTX in human red cells, it partially displaced  $^{125}\text{I}$ -ChTX and inhibited  $^{86}\text{Rb}$  influx in rabbit red cells. Studies with synthetic analogues of ChTX showed that the mutant toxin K27Q was inactive as a transport inhibitor and displayed a large reduction in ability to displace  $^{125}\text{I}$ -ChTX. The mutation K31Q resulted in abolition of ionic strength dependence of the inhibitory effect on the  $\text{Ca}^{2+}$ -activated  $\text{K}^{+}$  permeability. In spite of the similarities between the radioligand binding constants and the inhibition constants of unlabeled ChTX, we examined the potency of  $^{125}\text{I}$ -ChTX as a transport inhibitor. We found that the radioligand was 20–60-fold less potent than the unlabeled parent compound. [Supported by NIH grants P60-HL-15157, DK-39249, and Z124 from the Cystic Fibrosis Foundation.]

96. Ca Influx Oscillates during  $[\text{Ca}]_i$  Oscillations Induced by Thapsigargin (TG) in Salivary Acinar Cells J. KEVIN FOSKETT and DAVID WONG,\* *Hospital for Sick Children, Toronto, Ontario, Canada*

Depletion of  $\text{IP}_3$ -sensitive Ca stores in parotid salivary acinar cells by microsomal Ca-ATPase inhibition activates plasma membrane Ca influx and induces sinusoidal, slow (period 3–7 min)

caffeine- and ryanodine-sensitive  $[Ca]_i$  oscillations. To explore the link between activation of Ca influx and generation of oscillations, we examined the dependence of  $[Ca]_i$  oscillations on extracellular Ca ( $Ca_o$ ) influx. Acute removal of  $Ca_o$  immediately abolished oscillations. Membrane depolarization by elevated extracellular K, or exposure to 10 mM Ni, 100  $\mu$ M Gd, or 500  $\mu$ M Mn, also rapidly terminated oscillations. Acute  $Ca_o$  removal or rapid introduction of inorganic Ca channel blockers during the upstroke of an oscillation immediately terminated any further  $[Ca]_i$  rise. The subsequent rate of decline of  $[Ca]_i$  was similar to the rate associated with the normal downstroke of the preceding oscillation. The data suggest that  $[Ca]_i$  oscillations are associated with oscillating plasma membrane Ca influx, which varies 6–30-fold during an oscillation cycle. Elevating  $[Ca]_o$  enhanced the likelihood of oscillations, and the extent of  $IP_3$ -sensitive Ca store depletion correlated with the ability to oscillate. Thus, the likelihood of generating oscillatory behavior was proportional to the magnitude of Ca influx.  $[Ca]_i$  may feed back to regulate Ca entry, since acutely changing  $[Ca]_o$  between 1.2 and 3 mM caused rapid over- and undershoots of  $[Ca]_i$ . We propose that the plasma membrane Ca permeability activated by depletion of the  $IP_3$ -sensitive Ca store oscillates. However, Ca influx oscillations are not linked to oscillations of the Ca content of the  $IP_3$ -sensitive pool since that pool is continuously depleted in the presence of TG, but rather may be due in part to negative feedback by elevated  $[Ca]_i$  on Ca influx.

97. Expression of CFTR Chloride Channels in Heart PAUL C. LEVESQUE,\* PADRAIG J. HART,\* JOSEPH R. HUME, JAMES L. KENYON,\* and BURTON HOROWITZ,\*  
*Department of Physiology, University of Nevada School of Medicine, Reno, Nevada*

cAMP-dependent chloride channels modulate changes in resting membrane potential and action potential duration in response to autonomic stimulation in heart. A growing body of evidence suggests that there are marked similarities in the properties of the cAMP-dependent chloride channels in heart and CFTR (cystic fibrosis transmembrane regulator) chloride channels found in airway epithelia or in cells expressing the CFTR gene product. These similarities raise the important question of whether or not CFTR chloride channels and cardiac cAMP-dependent chloride channels are structurally equivalent proteins. The objective of this study was to determine whether CFTR, whose amino acid structure is known, is expressed and is responsible for the cAMP-activated chloride conductance in heart. Poly A<sup>+</sup> mRNA was isolated from rabbit ventricle and converted to cDNA for amplification using the polymerase chain reaction. A fragment corresponding to the nucleotide-binding domain 1 (NBD1) of the CFTR transcript was cloned. Comparison of the amino acid sequence of NBD1 of human CFTR with the deduced sequence of the rabbit heart PCR product indicated 98% identity. Northern blot analysis, using the heart amplification product as a cDNA probe, demonstrated expression of homologous transcripts in human atrium, guinea pig and rabbit ventricle, and dog pancreas. *Xenopus* oocytes injected with poly A<sup>+</sup> mRNA extracted from rabbit and guinea pig ventricle or dog pancreas expressed similar time-independent, outwardly rectifying chloride currents in response to an elevation of cAMP which were not observed in noninjected control oocytes. These results provide strong molecular and electrophysiological evidence supporting the hypothesis that the cAMP-activated chloride channel from heart is the same as the CFTR chloride channel. [Supported by NIH grants HL-30143 and HL-08505.]

98. Basolateral Glucose Transport Development in Porcine Kidney (LLC-PK<sub>1</sub>) and Opossum Kidney (OK) Cell Lines PAMELA J. GALLOWAY and JOHN S. COOK,  
*University of Tennessee-Oak Ridge Graduate School of Biomedical Sciences and Biology Division, Oak Ridge National Laboratory, Oak Ridge, Tennessee*

Differentiated LLC-PK<sub>1</sub> and OK cells are useful models of the proximal tubule in that they possess both apical (Na<sup>+</sup>-dependent) and basolateral (Na<sup>+</sup>-independent) glucose transporters. The former is assayed as the capacity for Na<sup>+</sup>-dependent, phlorizin-sensitive, concentrative uptake of  $\alpha$ -methylglucoside, while the latter is assayed as the Na<sup>+</sup>-independent, phlorizin-insensitive uptake of 2-deoxyglucose under either zero-trans or infinite-trans (50 mM 3-O-methylglucose) conditions. In both cell lines

the kinetics of basolateral glucose transport are altered as a function of development. In proliferating cells, before the apical transport function is expressed, the  $K_m$  for 2-deoxyglucose uptake is low, suitable for moving glucose into the cells in support of metabolism and growth. As the cells differentiate and express  $\text{Na}^+$ -dependent hexose uptake at their apical surface, they acquire basolateral transport characterized by an increase in  $K_m$ . The  $V_{\max}$  for low  $K_m$  transport is significantly decreased as high  $K_m$  transport appears. These modified kinetics may facilitate transepithelial glucose transport by facilitating glucose exit from the basolateral surface into a glucose-containing environment. In OK cells, Western blots suggest that the alterations in  $K_m$  may be the result of the presence of transporters recognized by GLUT1 (low  $K_m$ ) and GLUT2 (high  $K_m$ ) antisera. Immunofluorescence microscopy has been used to study the changing pattern of distribution of these transporters as a function of the cells' development. [Supported by USDOE under contract DE-AC05-84OR21400 with Martin Marietta Energy Systems, Inc., and by NCI T32 CA09104.]

99. Discovery of a High Affinity, Sodium-dependent L-Proline Transporter Expressed in Subpopulations of Putative Glutamatergic Neurons ROBERT T. FREMEAU, JR.,\* MARC G. CARON,\* and RANDY D. BLAKELY,\* *Departments of Pharmacology, Neurobiology, Cell Biology, and Howard Hughes Medical Institute, Duke University Medical Center, Durham, North Carolina; and Department of Anatomy and Cell Biology, Emory University School of Medicine, Atlanta, Georgia* (Sponsor: George J. Augustine)

Rapid chemical signaling between neurons and target cells is dependent upon the precise control of the magnitude and duration of neurotransmitters in synaptic spaces. High affinity,  $\text{Na}^+$ -dependent reuptake of neurotransmitters into presynaptic nerve terminals or surrounding glial cells by pharmacologically distinct membrane transport proteins is widely regarded as the principal means for rapidly inactivating synaptic neurotransmitters. We have used PCR with degenerate oligonucleotides derived from two conserved regions of the norepinephrine and  $\gamma$ -aminobutyric acid transporters to identify novel  $\text{Na}^+$ -dependent transporters in rat brain. One PCR product hybridized to a 4.0-kb RNA concentrated in subpopulations of putative glutamatergic neurons including mitral cells of the olfactory bulb, pyramidal cells of layer V of the cerebral cortex, pyramidal cells of the piriform cortex, and pyramidal cells of field CA3 of the hippocampus. In contrast, background labeling was observed over granule cells of the dentate gyrus, caudate-putamen, choroid plexus, ependymal cells of the cerebral ventricles, and white matter tracts. Transient expression of the cognate cDNA conferred  $\text{Na}^+$ -dependent L-proline uptake in HeLa cells which was saturable ( $K_m = 9.7 \mu\text{M}$ ) and exhibited a pharmacological profile similar to that for high affinity L-proline transport in rat brain slices. The cloned transporter cDNA predicts a 637-amino acid protein with 12 putative transmembrane domains and exhibits 44–45% amino acid sequence identity with other members of the emerging family of neurotransmitter transporters. These findings support a synaptic role for L-proline in specific excitatory pathways in the central nervous system and provide the basis for a direct molecular analysis of the presynaptic components of these excitatory projections.

100. In Vivo Measurements of Endosome Acidification in ADH-stimulated Toad Bladder Granular Cells F. EMMA,\* H. W. HARRIS, and K. STRANGE, *Division of Nephrology, Children's Hospital, Boston, Massachusetts*

ADH stimulation induces the insertion of water channels into the apical membrane of tight urinary epithelia such as the toad bladder and renal collecting duct. Hormone removal or application of a mucosa-to-serosa osmotic gradient results in rapid endocytic retrieval of water channels. The intracellular processing and ultimate fate of endocytosed water channels is incompletely understood. In vitro measurements, however, have demonstrated that endosomes isolated shortly after retrieval (10 min) contain functional water channels, whereas endosomes isolated later (60 min) apparently lack this transporter (Zeidel et al. *Am. J. Physiol.* In press). In many cells, endosome acidification plays an important role in the processing and sorting of endocytosed proteins. We therefore examined endosome acidification by fluorescence ratio microscopy in intact toad bladders after induction of

water channel retrieval in the presence of the pH-sensitive fluid phase marker, BCECF-dextran. Granular cells were imaged at 100× using an intensified CCD camera and digital image processing methods. The pH of individual endosomes was determined by measuring the ratio of the intensities of emitted light after excitation at 495 and 440 nm. A complete calibration curve for BCECF-dextran was obtained by imaging single, isolated organelles clamped at various pH values. A one-point in vivo calibration of BCECF was obtained at the end of each experiment by brief treatment of bladders with digitonin at pH 7. In bladders imaged 60 min after water channel retrieval, we observed that the vast majority of endosomes had a pH near 7. Exposure of bladders to 60 mM  $\text{NH}_4\text{Cl}$  had little effect on endosome pH, confirming the absence of acidification. 4–5 h after retrieval, however, virtually all endosomes were acidic (pH < 5.5) and alkalized dramatically in the presence of  $\text{NH}_4\text{Cl}$ . We conclude that endosome acidification plays little role in the early processing and sorting of retrieved water channels. [Supported by NIH grants RR-06725 and DK-38774 and an AHA grant-in-aid.]

101. Mechanism and Control of Volume Regulatory Inositol Efflux in Cultured Glioma Cells K. STRANGE, R. MORRISON,\* L. SHRODE,\* and R. PUTNAM, *Division of Nephrology, Children's Hospital, Boston, Massachusetts; and Department of Physiology and Biophysics, Wright State University, Dayton, Ohio*

C6 glioma cells regulate their volume during chronic (>8 h) exposure to hypertonicity by inositol accumulation. When returned to isotonic media, the cells swell and volume-regulate slowly and inositol levels return to control values in 18–24 h. Inositol loss is mediated by a three- to fivefold increase in the rate of inositol efflux. This enhanced efflux occurs immediately upon swelling and is terminated rapidly by returning cells to hypertonicity. Large changes in transmembrane  $\text{Na}^+$  gradients, complete removal of external  $\text{Na}^+$ , or exposure to 1 mM phlorizin had little effect on inositol efflux, demonstrating that it was not mediated by reversal of the  $\text{Na}^+$ /inositol cotransporter. The phorbol ester PMA (20 nM) had no effect on baseline inositol efflux, but enhanced swelling-induced efflux by 230%. Downregulation of PKC had no effect on baseline or swelling-induced inositol efflux, but completely blocked stimulation by 200 nM PMA. 0.5 mM cAMP or 0.05 mM forskolin did not alter baseline efflux, but increased swelling-induced efflux by 200 and 300%, respectively. Fura-2 measurements indicated no change in cell  $\text{Ca}^{2+}$  upon swelling. 0.1  $\mu\text{M}$  ionomycin dramatically elevated cell  $\text{Ca}^{2+}$ , but did not alter inositol efflux. 100  $\mu\text{M}$  eicosatetraynoic acid, an inhibitor of arachidonic acid (AA) metabolism, inhibited swelling-induced efflux by 46%. The cytochrome P-450 inhibitor ketoconazole (100  $\mu\text{M}$ ) inhibited baseline inositol efflux by 55% and completely blocked swelling-induced efflux. Taken together, these results demonstrate that inositol efflux in C6 cells is mediated by a pathway distinct from the  $\text{Na}^+$ /inositol cotransporter. Regulation of the efflux pathway may be mediated by metabolites of AA, possibly products of the cytochrome P-450 pathway. Phosphorylation induced by PKC or PKA may also modulate inositol efflux. [Supported by NIH grant NS-30591 and by an ADA grant.]

102. Pharmacology of Biogenic Amine Transporters GARY RUDNICK\* and STEPHEN C. WALL,\* *Department of Pharmacology, Yale University School of Medicine, New Haven, Connecticut* (Sponsor: Bliss Forbush III)

The plasma membrane transporters for serotonin, norepinephrine, and dopamine are members of the rapidly expanding family of  $\text{Na}^+$ - and  $\text{Cl}^-$ -dependent cotransport carriers. In addition to sharing primary sequence homology, the biogenic amine transporters share a common sensitivity to psychoactive compounds which distinguishes them from the other members of this family. Drugs used clinically to treat depression are potent inhibitors of the biogenic amine transporters. The serotonin transporter is thought to be the primary target for this class of compounds. Binding of the tricyclic antidepressant imipramine to the serotonin transporter is stimulated by both  $\text{Na}^+$  and  $\text{Cl}^-$ .  $\text{Na}^+$  increases the rate of [ $^3\text{H}$ ]imipramine binding and its affinity, but  $\text{Cl}^-$  increases affinity with no effect on rate. Cocaine inhibits all three biogenic amine transporters, although the dopamine transporter is

thought to be the primary target for the behavioral effects of cocaine. Binding of cocaine analogues to the serotonin and dopamine transporters is stimulated by  $\text{Na}^+$  but not  $\text{Cl}^-$ . Moreover, cocaine analogue binding is reduced at low pH ( $< 7$ ), in contrast to serotonin and dopamine binding, which are stimulated by  $\text{Cl}^-$  and relatively insensitive to pH. Despite these differences in binding characteristics, binding of cocaine analogues to the serotonin transporter is competitive with both serotonin and imipramine. Amphetamine and its congeners represent a third class of drugs which interact with these transporters. The neurotoxic amphetamine derivatives 3,4-methylenedioxymethamphetamine (MDMA) and *p*-chloroamphetamine (PCA) are both substrates for the serotonin transporter, and release serotonin from membrane vesicles containing the transporter by a process of transporter-mediated exchange. This exchange process provides a model for amphetamine-mediated biogenic amine release in vivo. [Supported by NIDA grant DA-07259.]

103. Organic Cation Transport in the Proximal Kidney Tubule of the *Ambystoma Tigrinum* MARK R. WEBER and EMILE L. BOULPAEP, *Department of Cellular & Molecular Physiology, Yale University School of Medicine, New Haven, Connecticut*

Organic cations are secreted from the serosal side to the mucosal side of proximal kidney tubules as determined by isotope flux measurements in perfused and collapsed tubules (Schäli et al. 1983. *Am. J. Physiol.* 245:F238) and in vesicles (Wright and Wunz. 1987. *Am. J. Physiol.* 253:F1040). This study examines the mechanisms of tetramethylammonium (TMA) transport in isolated perfused proximal kidney tubules by using simultaneous recordings of intracellular TMA-selective electrodes (Cotton et al. 1989. *J. Gen. Physiol.* 93:649) and intracellular Ling-Gerard electrodes. This arrangement enables the simultaneous measurement of apical and basolateral membrane voltages and cellular TMA concentrations ( $[\text{TMA}]_{\text{cell}}$ ) with high spatial and temporal resolutions. TMA is readily taken up from the bath but not from the lumen. When  $[\text{TMA}]_{\text{bath}}$  is between 0.5 and 4 mM, the steady-state  $[\text{TMA}]_{\text{cell}}/[\text{TMA}]_{\text{bath}}$  ratio is 4.84 ( $\pm 0.46$  SE,  $n = 8$ ) and the TMA influx has an exponential rate constant of  $2.05 \times 10^{-3} \text{ s}^{-1}$  ( $\pm 2.30 \times 10^{-4}$ ,  $n = 8$ ). When TMA is added to the bath, the basolateral membrane depolarizes and the TMA-induced depolarization ( $\Delta V_{\text{TMA}}$ ) decays as the basolateral influx ( $J_{\text{TMA}}$ ) decays and the TMA cell/bath concentration ratio increases. Both  $J_{\text{TMA}}$  and  $\Delta V_{\text{TMA}}$  are immediately abolished upon the addition of either 1 mM amiloride or cimetidine to the bath.  $J_{\text{TMA}}$  is independent of both bath Na and bath Cl. The combined bath and lumen TMA efflux has an exponential rate constant of  $3.41 \times 10^{-3} \text{ s}^{-1}$  ( $\pm 1.21 \times 10^{-3}$ ,  $n = 3$ ) and is partially inhibited when 1 mM amiloride or cimetidine is applied to either or both membranes. The above results indicate (a) that TMA is rheogenically transported across the basolateral membrane into the cell, and (b) that it is secreted into the lumen. [Supported by NIH grants DK-17433 and 5 T32 GM-07527.]

104. Interaction of Structurally Similar Substrates with Organic Anion Transport in Winter Flounder Proximal Tubule MARGARET A. DAWSON\* and J. LARRY RENFRO.\* *Marine/Freshwater Biomedical Sciences Center, The University of Connecticut, Storrs, Connecticut; and National Marine Fisheries Service, Milford Laboratory, Milford, Connecticut* (Sponsor: J. L. Roberts)

We used primary monolayer cultures of winter flounder renal proximal tubules to study the interaction with organic anion transport of anionic herbicides structurally related to the known transport substrate, 2,4-dichlorophenoxyacetic acid (2,4-D). We measured unidirectional *p*-aminohippuric acid (PAH) fluxes for 2-h periods at a PAH concentration of 10  $\mu\text{M}$  and herbicide concentrations ranging from 0.1  $\mu\text{M}$  to 1.0 mM. 2-(2-Methyl 4-chlorophenoxy) propionic acid (mecoprop) inhibited PAH secretion at concentrations of 0.1 and 1.0 mM. At concentrations of 0.1 and 1.0  $\mu\text{M}$  mecoprop, PAH secretion increased throughout the experiment, reaching levels of  $139 \pm 8.3$  and  $132 \pm 8.9\%$  of control, respectively, within 2 h. It appears that mecoprop inhibits PAH secretion at the outer face of the peritubular membrane. The stimulation of secretion at the lower mecoprop concentrations is consistent with an increase of anion exchange after the buildup over time of

intracellular mecoprop. This is similar to the biphasic effect observed with glutarate (Pritchard, 1988, *Am. J. Physiol.* 255:F597) and suggests the ability of mecoprop to support anion exchange in place of glutarate. The biphasic effect was also demonstrated over time at 10  $\mu$ M mecoprop; PAH secretion of mecoprop-treated cultures was significantly less than that of controls at 60 min, increasing to the control level within 90 min. [Supported by NIH/NIEHS grant P30ES03948 and Connecticut Department of Environmental Protection grant CWR 227-R.]

105. Evidence That MDR Protein Is Not an Active Drug Transporter, But Indirectly Alters the Steady-State Level of Chemotherapeutic Drug Efflux by Altering Intracellular pH PAUL D. ROEPE,\* DIANE CARLSON, HENRI SCOTT, and LI-YONG WEL, *Laboratory of Membrane Biophysics, Memorial Sloan-Kettering Cancer Center, New York* (Sponsor: Olaf S. Andersen)

Human multidrug resistance protein (P-glycoprotein) is a homologue of components of bacterial active transport systems and has been shown to be responsible for "increased efflux" of various chemotherapeutics from multidrug resistant (MDR) tumor cells. Since photoaffinity analogues of some chemotherapeutics bind to MDR protein, and since increased MDR protein is correlated qualitatively with increased steady-state levels of efflux, it has been proposed that MDR protein is an active drug transporter that has the un-Mitchellian ability to recognize and transport diverse substrates. However, photolabeling studies did not quantitate the specific activity of labeled MDR protein relative to other integral membrane proteins, and it has yet to be unequivocally shown that MDR protein transports drugs against a concentration gradient and/or imparts rate enhancement to the drug efflux process. This laboratory has investigated the kinetic parameters of drug efflux as well as other properties for several series of sequentially derived MDR cells (i.e., sibling cells exhibiting increased resistance concomitant with increased MDR expression), and the following conclusions have been reached: (a) Although the steady-state level of anthracycline efflux is qualitatively related to the level of MDR protein expression for  $\leq 120$ -fold resistant cells, when attention is paid to altered levels of exchangeable substrate in various cells, the apparent initial rate of transport is found to be virtually identical in all sensitive and resistant cells examined, regardless of relative MDR protein expression. (b) The relative steady-state of drug efflux correlates quantitatively with intracellular pH ( $pH_i$ ), increasing as  $pH_i$  increases for increasingly resistant MDR cells. Various treatments that affect efflux also affect  $pH_i$ . (c)  $Na^+/H^+$  antiport is increased in MDR cells, but it is unclear if this correlates with relative MDR expression, and verapamil dramatically affects  $Na^+/H^+$  antiport for the resistant cells. (d)  $Cl^-/HCO_3^-$ -dependent reacidification mechanisms are severely impaired in MDR cells, and MDR cells have dramatically altered permeability to  $Cl^-$  and  $HCO_3^-$ . This property may correlate with levels of MDR protein. The data in their entirety suggest that MDR protein modulates the level of exchangeable drug by altering  $pH_i$ , and other parameters such as intrinsic phosphorylation/dephosphorylation which then impact on additional  $pH$  stasis mechanisms, but does not perform active drug transport per se. This hypothesis is consistent with observed phenomenology, basic pharmacologic principles, and chemiosmotic theory. [Supported by the Raymond & Beverly Sackler Foundation and the Society of Sloan-Kettering.]

106. Regulation of Hexose Transporter GLUT-1 by Glucose in Fibroblasts PHILLIP A. ORTIZ\* and HOWARD C. HASPEL,\* *Department of Physiology and Biophysics, State University of New York, Stony Brook, New York* (Sponsor: Ira S. Cohen)

We are investigating the membrane compartments and glucose (Glc) metabolites involved in the posttranslational regulation of the functional expression of hexose transporter GLUT-1 by Glc in cultured rodent fibroblasts (Haspel et al. 1991, *Mol. Endocrinol.* 5:61; Ortiz et al. 1992, *Biochemistry*. In press). We localized GLUT-1 by both immunoblotting of subcellular membrane fractions and immunofluorescence microscopy. We found that Glc deprivation induces the selective accumulation of GLUT-1 in the plasma membrane of fibroblasts. We propose that this accumulation of GLUT-1 is a

consequence of specific translocation of the carrier from intracellular compartments to the cell surface. We suggest that this recruitment may indirectly decrease GLUT-1 degradation. To test this hypothesis we examined the effects of inhibitors of lysosomal protein degradation on hexose transport and GLUT-1 accumulation in Glc-fed and -deprived fibroblasts. Acidotropic amines or the endopeptidase inhibitor leupeptin cause GLUT-1 accumulation, but, unlike Glc deprivation, do not stimulate hexose transport. These inhibitors of lysosomal function do not augment Glc deprivation-induced increases in hexose transport or GLUT-1 content. In contrast, these agents diminish the loss of accumulated GLUT-1 from Glc-deprived fibroblasts upon Glc refeeding, but do not alter the return of hexose transport to control levels. We conclude that lysosomal degradation of GLUT-1 is not directly regulated by Glc. We suggest that the ability of Glc to downregulate the functional expression of the carrier may involve internalization into compartments that are distinct from acidified organelles such as lysosomes and endosomes. The role of Glc metabolism in Glc deprivation-induced increases in hexose transport and GLUT-1 content was examined by using Glc analogues and phosphoglucose isomerase-deficient (PGI<sup>-</sup>) fibroblasts. The nonmetabolizable Glc analogue, 3-O-methylglucose (MeGlc) is transported by GLUT-1. MeGlc prevents the stimulation of hexose transport observed in Glc-deprived fibroblasts but fails to prevent GLUT-1 accumulation. We conclude that hexose transport and GLUT-1 content are differentially regulated by Glc metabolism. The role of hexose phosphates in these phenomena was examined with PGI<sup>-</sup> cells. Relative to wild type cells, PGI<sup>-</sup> cells are refractory to Glc deprivation-induced increases in hexose transport and GLUT-1 content. These differences correlate well with Glc-6-P levels. The ability of substrates for GLUT-1 and glucose metabolites to recruit GLUT-1 from intracellular compartments to the cell surface needs to be reevaluated and requires further study. [Supported by the American Diabetes Association and a W. Burghardt Turner Dissertation Fellowship.]

107. Cloning, Chromosomal Mapping, and Polymorphic Analysis of a Human Apical Epithelial Na<sup>+</sup>/H<sup>+</sup> Exchanger (NHE-3) Isoform STEVEN R. BRANT,\* ETHYLIN W. JABS,\* JOHN WASMUTH,\* MICHAEL BERNSTEIN,\* XIANG LI,\* SUSAN WALKER,\* JACQUES POUYSSEGUR,\* MARK DONOWITZ, and CHUNG-MING TSE,\* *Departments of Medicine, Physiology, and Pediatrics, The Johns Hopkins University School of Medicine, Baltimore, Maryland; Department of Biochemistry, University of California, Irvine, California; and the Centre de Biochimie-Centre National de la Recherche Scientifique, Nice, France*

As previously reported, we have cloned and expressed three rabbit Na<sup>+</sup>/H<sup>+</sup> exchanger isoforms. NHE-1 is the housekeeping isoform. It is expressed in almost all tissues and is located on the basolateral membrane of ileal villus cells. NHE-1 was first cloned in the human and its gene is located on human chromosome 1. NHE-2 and NHE-3 are epithelial specific isoforms, with NHE-3 the most likely isoform responsible for apical Na<sup>+</sup>/H<sup>+</sup> exchange activity of ileal villus cells. Using a <sup>32</sup>P-labeled probe constructed from NHE-2 cDNA, a human kidney cortex cDNA library was screened. A 1,351-bp clone (HKC-3) that had 94% amino acid identity (98% similarity) to rabbit NHE-3 over its amino acid sequences 130-505 was isolated and sequenced. Thus HKC-3 represents a partial cDNA encoding the human NHE-3 isoform. To localize the human NHE-3 gene, HKC-3 was <sup>32</sup>P-labeled and hybridized to Southern blots of hybrid DNAs from the NIGMS Human/Rodent Somatic Cell hybrid mapping panel #1 restricted with EcoRI. Under wash conditions of high stringency, 7.2- or 6.8-, 2.7- or 2.3-, and 1.5- or 1.4-kb polymorphic bands were detected by autoradiography. There was 100% concordance between the presence of these bands and human chromosome 5. To analyze the EcoRI RFLPs seen in the hybrids, Southern blot analysis was performed on human genomic DNAs of CEPH (Centre d'Etude du Polymorphisme Humain, Paris, France) pedigrees and digested with EcoRI. The observed heterozygosity in unrelated individuals was 71%. By segregation analysis, it was determined that HKC-3 detects three polymorphic sites containing a total of nine alleles that segregate in a Mendelian fashion. No recombination was observed among the sites (i.e., there was complete linkage disequilibrium). In conclusion, (a) a partial cDNA (HKC 3) representing human NHE-3 has been cloned; (b) human and rabbit NHE-3 are highly homologous; (c) the NHE-3 gene is

located on human chromosome 5; and (d) analysis of CEPH pedigrees shows that HKC-3 detects three EcoRI polymorphic sites that segregate in a Mendelian fashion.

108. GLUT1 Glucose Transporters and the Long-Term Regulation of Glucose Uptake ANNA GUMA,\* NAVA BASHAN,\* ELENA BURDETT,\* HARI HUNDAL,\* TOOLSIE RAMLAL,\* and AMIRA KLIP, *Division of Cell Biology, The Hospital for Sick Children, Toronto, Ontario, Canada*

Glucose transport in muscle is regulated by stimuli as diverse as hormones, exercise, impairment of oxidative metabolism, and anti-diabetic drugs. The L6 line of skeletal muscle cells has been used amply as an in vitro model of uninnervated muscle. In these cells, glucose transport responds to both acute and chronic stimuli. GLUT1 and GLUT4 glucose transporter isoforms are expressed in differentiated L6 myotubes. The acute (<1 h) response to insulin consists of translocation of GLUT4 glucose transporters to the plasma membrane. In contrast, the chronic (4–24 h) response to the hormone involves biosynthesis of GLUT1 transporters. In both instances there is an elevation in glucose uptake. The purpose of this work was to compare the molecular mechanism by which glucose transport and transporters are regulated upon prolonged exposure of L6 cells to diverse stimuli. We observed that prolonged (4–24 h) exposure of L6 cells to low (3%) atmospheric oxygen levels or to uncouplers and inhibitors of the respiratory chain elevates glucose transport. The need for this response may be to produce ATP through increased anaerobic glucose metabolism. This response included synthesis of GLUT1 transporters; however, in the case of dinitrophenol (DNP) and rotenone, translocation of GLUT1 transporters was sufficient to sustain elevated transport. The biguanide metformin is used in the treatment of type 2 diabetes to reduce hyperglycemia, but its mechanism of action is unknown. In L6 cells, metformin elevated glucose influx after several hours. As with the effects of DNP and rotenone, metformin caused translocation of GLUT1 transporters; however, in contrast to DNP and rotenone, this occurred in the absence of changes in total content of GLUT1 proteins. In neither case was the GLUT4 isoform affected, suggesting that the intracellular pools of each isoform are distinct and the isoforms are regulated differentially. In summary, these results suggest that GLUT1 transporters in L6 cells can be regulated by chronic exposure to different effectors. Both translocation and biosynthesis are involved in these responses. Given the importance of regulation of glucose transport by anti-diabetic drugs in vivo and that transport is abnormal in diabetes, we have initiated studies to investigate the pools of GLUT1 and GLUT4 glucose transporters using isolated human muscle membranes.

109. Expression of P-Glycoprotein Genes That Confer Drug Resistance in Primary Culture of Rat Hepatocytes CHOW HWEE LEE\* and VICTOR LING,\* *Division of Molecular and Structural Biology, Ontario Cancer Institute, Toronto, Ontario, Canada*

Three classes of P-glycoprotein (Pgp) genes, termed class I, II, and III, have been identified. Class I and II Pgp genes can confer multidrug resistance (MDR), while the class III gene cannot confer this phenotype. A recent study from this laboratory showed that the rat also contains three Pgp genes (Deuchars et al. 1992. *Biochim. Biophys. Acta.* 1130:157). Cloned putative 3' untranslated regions of rat Pgp genes were used to generate gene-specific probes. We report here the detection of significant mRNA levels of class II Pgp gene in adult rat hepatocytes with time in culture. A modest increase in class I gene was also seen, while class III gene showed a somewhat opposite effect. These data suggest that the MDR phenotype can be induced in rat hepatocytes by simply plating the cells in culture without any prior exposure to foreign chemicals. The influence of cell-cell and cell-matrix interactions on this phenotype was investigated. Our results show that Pgp expression can be attenuated when hepatocytes are sandwiched between two layers of collagen gel, or when plated at high density on hydrated collagen—both culture conditions that favor liver-specific gene expression. We are currently investigating whether transcriptional or posttranscriptional mechanisms are responsible for the changes in the levels of Pgp transcripts. [Supported by National Cancer Institute of Canada and by NIH grant CA-37130.]

110. Modulation of the Chronotropic Actions of the (Na-K-Cl) Cotransporter ALEXANDER A. HARPER,\* JULIAN P. L. DAVIS,\* and ALAN R. CHIPPERFIELD,\* *Department of Anatomy and Physiology, University of Dundee, Dundee, Scotland, United Kingdom*

The (Na-K-Cl) cotransporter can function as an inwardly directed chloride pump, and, by making  $[Cl]_i$  closer to  $[Cl]_o$ , can act as a depolarizing influence, e.g., in vascular smooth muscle (Davis et al. 1991. *Clin. Sci.* 81:73; Davis et al. 1992. *J. Physiol. [Lond.]*. In press. (Abstr.)). To examine whether regulation of membrane potential by the cotransporter might be a more widespread phenomenon, we investigated the effects of the loop diuretic bumetanide, a specific inhibitor of the (Na-K-Cl) cotransport system, on pacemaker activity in the isolated rat heart. Application of this agent (10  $\mu$ M) clearly increased the rate of discharge of the sino-atrial node from 3.19 Hz ( $\pm 0.63$  SD) to 3.71 Hz ( $\pm 0.87$ ,  $n = 12$ ,  $P < 0.001$ ). Pharmacological maneuvers indicate that the positive chronotropic action of loop diuretics is associated with catecholamine release, and that this action is not due to the effects of these agents on chloride channels is confirmed by the negative chronotropic action of 4,4'-dinitrostilbene-2,2'-disulphonic acid (10  $\mu$ M), an anion channel blocker (Bahinski et al. 1989. *Nature [Lond.]*. 340:718) that decreased sino-atrial node discharge to 81% ( $\pm 3$ ,  $n = 3$ ) of control values. Cotransporter functioning is modulated by several neuroactive peptides, including angiotensin II (Haas. 1989. *Annu. Rev. Physiol.* 51:443), and the elements of an intrinsic cardiac renin-angiotensin system have recently been characterized (Lindpaintner and Ganten. 1991. *Circ. Res.* 68:905). Angiotensin II (10 nM) also had a positive chronotropic effect in the isolated sino-atrial node preparation, increasing the frequency of spontaneous action potentials to 121% ( $\pm 17$ ,  $n = 7$ ) of control. The positive chronotropic effects of bumetanide and angiotensin II were nonadditive; thus application of angiotensin II in the presence of bumetanide evoked no further elevation of pacemaker discharge beyond that produced by bumetanide. The functional role of the cotransporter and its regulation in the control of cardiac performance merits further investigation.

111. Regulatory Interaction of Intracellular ATP,  $Na^+$ , and  $Cl^-$  with the NaK2Cl Cotransporter NORMAN WHISENANT,\* MAHROOZ KHADEMAZAD,\* and SHMUEL MUALLEM, *Department of Physiology, University of Texas Southwestern Medical Center, Dallas, Texas*

To probe the mechanism(s) by which intracellular ATP,  $Na^+$ , and  $Cl^-$  regulate the activity of the NaK2Cl cotransporter we measured bumetanide-sensitive (BS)  $^{86}Rb$  fluxes in the osteosarcoma cell line UMR-106-01. Under physiological gradients of  $Na^+$ ,  $K^+$ , and  $Cl^-$ , depleting ATP by incubation with deoxyglucose and antimycin A (DOG/AA) for 20 min at 37°C reduced BS- $^{86}Rb$  uptake from 6 to 1 nmol/mg P per min. Similar incubation with 0.5 mM ouabain had no effect on the uptake, excluding the possibility that DOG/AA inhibited the uptake by collapsing the  $Na^+$  and  $K^+$  gradients. Loading the cells with  $Na^+$  and depleting of  $K^+$  by 2–3-h incubation with ouabain or DOA/AA or by 5-min incubation with monensin and nigericin increased the rate of BS  $^{86}Rb$  uptake to 12–15 nmol/mg P per min. The increased uptake due to ouabain was insensitive to cellular ATP and was accompanied by a matching increase in BS- $^{86}Rb$  efflux rate. The stimulated fluxes required extracellular  $Na^+$ ,  $K^+$ , and  $Cl^-$ . Thus, loading the cells with  $Na^+$  induced a rapid  $K^+/K^+$  exchange which was insensitive to cellular ATP. Therefore, ATP regulates a step in the turnover cycle which is required for net, but not  $K^+/K^+$  exchange fluxes. Since the exchange required all three ions, the most likely step regulated by ATP is the conformational transition of the empty carrier. Depleting cells from  $Na^+$  or  $Cl^-$  increased net BS- $^{86}Rb$  uptake from medium containing physiological  $Na^+$  and  $K^+$  concentrations to 15 nmol/mg P per min without affecting exchange flux. On the other hand, increasing  $Na^+$  above 60 mM inhibited net and stimulated exchange fluxes. Thus,  $Na^+$  appears to regulate the cotransporter by interacting at least twice with internal sites during each turnover cycle. Interaction with a high affinity site (saturated at  $\sim 10$  mM) reduces net uptake threefold without triggering exchange, whereas interaction with a low affinity site (saturation above 140 mM) inhibits net and, in parallel, stimulates exchange fluxes. An increase in  $Cl^-$  inhibited net without affecting exchange fluxes. We conclude that low  $Na^+$  and  $Cl^-$  can regulate the availability or the conformational transition of the empty carrier on the cytosolic site. High  $Na^+$  appears to stimulate one of the reversal reactions needed for exchange and as a consequence, inhibits net forward uptake. [Supported by NIH grant DK-38938.]

112. Cell Volume Reduction of Mouse Erythroleukemia (MEL) Cells during Differentiation Is Primarily Mediated by a Reduction in Na-K-2Cl Cotransport ERIC DELPIRE and STEVEN R. GULLANS, *Renal Division, Brigham and Women's Hospital, Harvard Medical School, Boston, Massachusetts*

Differentiation of proerythroblasts into mature erythrocytes involves a profound reduction in cell volume. Maturation of reticulocytes into erythrocytes is known to be associated with a loss of KCl which appears to be mediated by increased activity of  $K^+$  efflux pathways. MEL cells are proerythroblasts that can be induced to differentiate successively into reticulocytes and erythrocytes. We evaluated the changes in cell volume and  $K^+$  transport in MEL cells during the transition from proerythroblast to reticulocyte. When exposed to 1.8% dimethyl sulfoxide, the cells differentiated to the reticulocyte stage in ~7 d. During that period, they synthesized hemoglobin, reduced their total protein content by 40%, and exhibited a 56% decrease in cell volume. To evaluate the role of various transport pathways in the volume reduction, we performed Rb-86 uptakes in the presence or absence of selected inhibitors. In undifferentiated cells, a total Rb(K) influx of  $1,642 \pm 8$  attomol/cell per min was measured. Of this, 53% was mediated by bumetanide-sensitive Na-K-2Cl cotransport, 34% by ouabain-sensitive Na/K pump, 8% by barium- and quinidine-sensitive  $K^+$  channel, and 5% by furosemide-sensitive K-Cl cotransport. After 4 d of differentiation, the Rb uptake was reduced by 57% ( $714 \pm 35$  attomol/cell per min), mainly due to a dramatic decrease in Na-K-2Cl cotransport activity (from  $878 \pm 18$  to  $102 \pm 32$  attomol/cell per min). The  $Na^+$ -independent K-Cl cotransport activity also dramatically decreased by 90%. In contrast, Na/K pump activity was unchanged after 4 d in DMSO ( $446 \pm 26$  vs.  $474 \pm 40$  attomol/cell per min). In conclusion, cell volume reduction occurring during MEL cell differentiation is mainly due to a reduction in Na-K-2Cl cotransport activity (inward leak) rather than an increase in the activity of an outwardly poised  $K^+$  transport mechanism.

113. The Effect of Varying Membrane Potential on K:Cl Cotransport in Human Erythrocytes D. KAJI, *Veterans Administration Medical Center, Bronx, New York; and Mount Sinai School of Medicine, New York*

The stoichiometry of K:Cl transport has been reported to be 3:2 in *Necturus* gall bladder. In erythrocytes, K:Cl stoichiometry (and therefore electroneutrality) of this cotransport system has not been established. The aim of the present investigation was to investigate the effect of varying membrane potential ( $V_m$ ) on K flux mediated by this cotransport pathway in human erythrocytes. We used hemisodium, a new selective Na ionophore, in the presence of a Na gradient to shift  $V_m$  away from  $E_{Cl}$  toward  $E_{Na}$  at constant extracellular and intracellular K and Cl concentrations. KCl cotransport was measured as the difference in K ( $^{86}Rb$ ) influx over 3 min in isosmotically swollen and nonswollen Na-loaded cells (100 mM Na, 50 mM K using the nystatin method) incubated in media with 1 mM NaCl, 50 mM KCl, 99 mM N-methyl glucamine Cl, and various concentrations of hemisodium.  $V_m$  was measured in parallel experiments by the change in fluorescence of the carbocyanine dye diS-C<sub>3</sub>-5. The baseline  $V_m$  in swollen cells (-8 mV) was not different from that in nonswollen cells (-9.5 mV). With increasing hemisodium concentrations,  $V_m$  shifted toward  $E_{Na}$  (-122 mV) and reached -63 mV with 0.1 mM hemisodium. Over the 3-min time period of influx, cell volume changed by <2% and  $V_m$  remained constant. Swelling-activated K flux was 5.5 and 3.5 mmol/liter original cells per h in two normal subjects and remained constant with increasing hemisodium concentrations. Thus, K:Cl cotransport was independent of membrane potential over this range. Thus, unlike the cotransport in *Necturus* gallbladder, KCl cotransport in human erythrocytes is unaffected by varying  $V_m$ , and by inference is electroneutral with a 1:1 stoichiometry. [Supported by a Merit Review Grant, Veterans Affairs.]

114. Biphasic Stimulation of Glucose Transport in Response to Inhibition of Oxidative Phosphorylation MANGALA SHETTY,\* KAREN VIKSTROM,\* JOHN N. LOEB, and FARAMARZ ISMAIL-BEIGI, *Departments of Medicine and of Microbiology and Immunology, Columbia University, and Albert Einstein College of Medicine, New York*

Inhibition of oxidative phosphorylation by azide in the rat liver cell line, Clone 9, markedly stimulates glucose transport in a "biphasic" fashion (Shetty et al. 1992. *Am. J. Physiol.* 262:C527). In

the "early" phase (0–2 h) an eightfold stimulation of glucose transport is mediated entirely by posttranslational mechanisms, whereas in the "late" phase (8–24 h) the further stimulation of transport is associated with 8- and 2.5-fold increments in cell erythroid/brain glucose transporter (GLUT-1) mRNA and GLUT-1 content, respectively. (These cells express only the GLUT-1 isoform under both basal and stimulated states.) To determine the contribution of translocation of GLUT-1 sites to the plasma membrane versus activation of sites preexisting in the plasma membrane, quantitative Western blot analysis of GLUT-1 content was performed on homogenates and plasma membrane fractions, and the results were normalized against Na,K-ATPase  $\alpha$ -subunit content. An eightfold stimulation of specific 3-O-methylglucose uptake after 2 h of exposure to azide occurred in the absence of any change in total cell GLUT-1 content and was accompanied by a modest (1.8-fold) increment in plasma membrane GLUT-1 content. In contrast, after 24 h of exposure to azide, a 12-fold stimulation of glucose transport was associated with a 2-fold increase in total cell GLUT-1 content and a 6.5-fold increment in the GLUT-1 content of plasma membranes. Immunofluorescence microscopy yielded results consistent with the above findings, showing only minimal changes in the fluorescence pattern of cells exposed to azide for 2 h, and a substantial enhancement of cell fluorescence, especially at the cell periphery, after 24 h of exposure to azide. The results suggest that the early stimulation of glucose transport in response to azide is largely mediated by activation of GLUT-1 sites preexisting in the plasma membrane, whereas the late response is accompanied by increased cell GLUT-1 content as well as a translocation of GLUT-1 sites to the plasma membrane. [Supported by NIH grant HD-05506 and a Grant-in-Aid from the American Heart Association, New York Affiliate.]

**115. Na/K/Cl Cotransport in Rat Red Blood Cells of Different Cell Age** HEIMO MAIRBÄURL and JOSEPH F. HOFFMAN, *Department of Cellular and Molecular Physiology, Yale University Medical School, New Haven, Connecticut*

Cells of different buoyant density were separated from whole blood of erythropoietin-treated rats by density gradient centrifugation.  $^{22}\text{Na}$  efflux was measured on cells containing 50 mmol Na, and K<sub>i</sub>/liter cells in media containing (mM): 100 NaCl, 5 KCl, 5 glucose, 20 HEPES (pH 7.4), and 5 mM ouabain together with sucrose to achieve the desired osmolarity (240, 300, or 360 mosmol/liter). Na/K/Cl cotransport was taken as the bumetanide (50  $\mu\text{M}$ )–inhibitable fraction of Na efflux. The reticulocyte content in the two cell fractions (top and bottom) studied was, respectively, 96 and 0.2%, the mean cellular hemoglobin concentration was 280 and 356 g/l, and the total red cell Mg was 6.9 and 2.0 mmol/liter cells. In the top fraction red cells, Na/K/Cl cotransport (millimoles/liter cells per hour) was 0.6 at normal cell volume, was reduced to 0.2 by swelling, but was increased to 2.5 by shrinkage, whereas in bottom cells, the flux at normal cell volume was 1.4 and changed to 1.1 and 1.9 after swelling and shrinkage, respectively. Cotransport in cells of normal or shrunken cell volume was stimulated by okadaic acid (1  $\mu\text{M}$ ) to be about eight in cells from the top and about two in the bottom fraction. In contrast, staurosporine completely inhibited cotransport in normal and shrunken red cells. The results indicate that reticulocytes compared with mature cells have increased cotransport capacity and that this is probably due to an increased number of cotransporters per cell. The maturation-related differences may represent changes (loss) either in the cotransport protein and/or in the mechanism(s) controlling the phosphorylated state of the system. [Supported by NIH grant HL-09906.]

**116. Mechanism of Inhibition of Chloride Secretion in T<sub>84</sub> Cells by Stimulation of Protein Kinase C** B.-Q. SHEN,\* W. SKACH,\* R. A. BARTHELSON,\* D. C. GRUENERT,\* E. SIGAL,\* R. J. MRSNY,\* and J. H. WIDDICOMBE,\* *Cystic Fibrosis Research Center and the Cardiovascular Research Institute, University of California Medical Center, San Francisco, California; and the Department of Pharmaceutical Research and Development, Genentech Incorporated, South San Francisco, California* (Sponsor: Leslie C. Timpe)

We have investigated how stimulation of protein kinase C leads to an inhibition of cAMP-dependent Cl secretion in T<sub>84</sub> cells. Specifically, we tested the hypothesis that the inhibition was due to loss of the

cystic fibrosis transmembrane conductance regulator (CFTR), an apical membrane Cl channel. As described by others (Trapnell et al. 1991. *J. Biol. Chem.* 266:10319), we found that treatment with the phorbol ester, phorbol myristate acetate (PMA), reduced CFTR mRNA levels by 80% with a  $t_{1/2}$  of 2 h. Chloride secretion, measured as forskolin-induced short circuit current, was abolished with a  $t_{1/2}$  of ~2 h. However, CFTR levels, determined by immunoprecipitation and phosphorylation, showed negligible change over 48 h of treatment with PMA. Nor did 12-h exposure to PMA affect the forskolin-stimulated efflux of  $^{125}\text{I}$  into high K medium, a measure of anion channel activity. Thus, we conclude that CFTR has a turnover time of > 24 h, and that the effects of PMA on cAMP-dependent Cl secretion are not due to loss of CFTR. [Supported by NIH grant HL-42368.]

117. Vasopressin Activates Cation-selective Channels and Increases Cytosolic Sodium Concentration in Hepatocytes STEVEN D. LIDOFKY,\* MING-HONG XIE,\* BRUCE F. SCHARSCHMIDT,\* and J. GREGORY FITZ.\* *Department of Medicine and Liver Center, University of California, San Francisco, California; and Department of Medicine, Duke University, Durham, North Carolina* (Sponsor: David Copenhagen)

Vasopressin and other hormones that signal via the phosphoinositide cascade increase  $\text{Na}^+$  entry into hepatocytes. Indirect evidence suggests that  $\text{Na}^+$  may modulate the effects of such hormones on hepatocellular gene expression (Kruijer et al. 1986. *J. Biol. Chem.* 261:7929), but the effect of such hormones on cytosolic  $\text{Na}^+$  concentration ( $[\text{Na}^+]_i$ ) has been uncertain. The aim of this study was to determine the effect of vasopressin on  $[\text{Na}^+]_i$  and to characterize the mechanism of  $[\text{Na}^+]_i$  alteration.  $[\text{Na}^+]_i$  and intracellular pH ( $\text{pH}_i$ ) were measured in single hepatocytes using the cation-sensitive dyes SBFI and BCECF, respectively, and dual wavelength microfluorimetry. In parallel studies, single channel currents were measured using patch clamp recording techniques. Under basal conditions,  $[\text{Na}^+]_i$  averaged  $13.1 \pm 1.5$  mM and was increased  $8.3 \pm 0.9$  mM ( $n = 21$ ) by vasopressin. The increase in  $[\text{Na}^+]_i$  was not attributable to inhibition of the  $\text{Na}^+/\text{K}^+$  pump and was dependent on the presence of extracellular  $\text{Na}^+$ , suggesting that it was due to hormonal activation of  $\text{Na}^+$  influx. It was not dependent on the presence of extracellular bicarbonate, amino acids, or taurocholate, solutes known to enter hepatocytes via  $\text{Na}^+$  coupling, suggesting that  $\text{Na}^+$  influx did not occur via known cotransport processes. Vasopressin had no effect on  $\text{pH}_i$ , suggesting that it did not activate  $\text{Na}^+/\text{H}^+$  antiport. In parallel studies in the cell-attached configuration with NaCl in the patch pipette, no spontaneous ion channel activity was identified in 14 cells under basal conditions. Exposure to vasopressin (100 nM) initiated single channel activity within 1–3 min in 11 of the 14 cells. At the resting membrane potential currents were inward, consistent with the movement of positive charge into the cell. Slope conductance averaged 30 pS. Currents were unaffected by removal of  $\text{Cl}^-$  from the pipette or substitution of  $\text{K}^+$  for  $\text{Na}^+$  but were eliminated by substitution of the impermeant cation choline for  $\text{Na}^+$ . After excision of the membrane patch, the single channel currents reversed near 0 mV in symmetric cation solutions, and ion substitutions showed a permeability sequence of  $\text{Na}^+ \approx \text{K}^+ \gg \text{Cl}^-$ . We conclude that vasopressin activates cation-selective channels in the plasma membrane of hepatocytes and increases  $[\text{Na}^+]_i$ . Activation occurs rapidly and appears to represent an early step in signal transduction which mediates hormone-activated  $\text{Na}^+$  entry.

118. A 3.5-kb mRNA Encodes for a Hepatic Organic Cation Transport Protein MING-HONG XIE,\* MARY COCHRAN,\* STEVEN LIDOFKY,\* and BRUCE SCHARSCHMIDT,\* *Department of Medicine, University of California, San Francisco, California* (Sponsor: David Copenhagen)

Organic cations include a variety of xenobiotics as well as endogenous compounds. They are believed to be taken up and metabolized by liver via two or more transport mechanisms that appear to exhibit broad specificity for a variety of organic cations. However, little is known about the functional characteristics of hepatic organic cation uptake, and the responsible transport proteins have not been identified. In the present studies we have explored the utility of *Xenopus laevis* oocytes for heterologous expression, characterization, and cloning of the proteins that mediate hepatic

organic cation uptake. Tetraethylammonium (TEA), a monovalent, aliphatic quaternary amine, was used as a prototype organic cation. Rat liver total mRNA (50 ng) or H<sub>2</sub>O (50 nl) was injected into oocytes, and the uptake rate of [<sup>14</sup>C]TEA was measured 72 h after injection. As compared with H<sub>2</sub>O-injected oocytes, the uptake of [<sup>14</sup>C]TEA by mRNA-injected oocytes was increased twofold ( $2.78 \pm 0.28$  vs.  $1.28 \pm 0.30$  pmol/oocyte per h). When total mRNA was size-fractionated by sucrose density gradient centrifugation, injection into oocytes of mRNA in the range of 3.5 kb selectively enriched [<sup>14</sup>C]TEA uptake ~5–10-fold. These findings indicate that a 3.5-kb mRNA encodes for a protein that mediates hepatic uptake of TEA and presumably other organic cations. They further demonstrate the potential utility of *Xenopus laevis* oocytes for expression cloning of hepatic organic cation transport protein(s).

**119. Aldosterone-induced Proteins in Model Renal Epithelia: Molecular Weight Isoforms and Heteromeric Complex Formation** BONNIE L. BLAZER-YOST and ROBERT W. YOST, *University of Pennsylvania School of Medicine and Veterans Affairs Medical Center, Philadelphia, Pennsylvania; and Camden County College, Blackwood, New Jersey*

Aldosterone-stimulated Na<sup>+</sup> transport is dependent on new protein synthesis. We have previously identified and characterized a constellation of electrophoretically polymorphic (*M*<sub>r</sub> 65,000 and 70,000) and microheterogeneous (*pI* = 5.6–6.4) aldosterone-induced proteins (AIPs) in model renal epithelia such as the urinary bladder of the toad *Bufo marinus* and the A6 cell line. The AIPs copurify with an amiloride-sensitive Na<sup>+</sup> channel and appear to be the only channel component induced by aldosterone. It is possible, therefore, that these polypeptides act as regulatory subunits modulating channel function during aldosterone-stimulated Na<sup>+</sup> transport. Alternatively, they may comprise an integral part of the transporting site. The possible significance of isoform heterogeneity was investigated by subjecting a Triton X-100-solubilized membrane fraction from aldosterone-treated toad urinary bladder to gel filtration under nonreducing conditions. Procedures were optimized to preserve the integrity of subunit interactions found in complexes such as heteromeric channels. Under these conditions no AIPs were detected in fractions having molecular masses <120 kD, indicating that, in their native configuration, the AIPs are part of larger complexes. By size fractionation the 70-kD isoforms are part of a complex with a molecular mass >500 kD. The size of this complex is consistent with that of a heteromeric Na<sup>+</sup> channel previously described by D. Benos. In contrast, the 65-kD isoforms elute at a lower (130–380 kD) molecular mass. The identity of the complex containing the 65-kD AIP isoforms is unknown. It could represent a precursor form of the Na<sup>+</sup> channel, a Na<sup>+</sup> channel with distinct physical characteristics, or an unrelated protein complex. [Supported by a V.A. Merit Review grant.]

**120. Cloned Na/GABA Cotransporter: Electrophysiological Analysis Yields Turnover Number of 5–10 per Second** SELA MAGER,\* JANIS NAEVE,\* MICHAEL QUICK,\* BRUCE N. COHEN,\* NORMAN DAVIDSON,\* and HENRY A. LESTER, *Division of Biology 156-29, California Institute of Technology, Pasadena, California*

cRNA from the rat brain Na/GABA/Cl cotransporter GAT-1 (Guastella et al. 1990. *Science* [Wash. DC]. 249:1303) was synthesized with (a) either the alfalfa mosaic virus untranslated region or a modified Shaker sequence at the 5' end, and (b) a poly(A) tail at the 3' end and expressed in *Xenopus* oocytes. *Equilibria*: 100 μM GABA produces inward currents of several hundred nanoamperes at -140 mV, ~10-fold smaller at -20 mV. Dose-response relations change with voltage; half-maximal [GABA] varies between 20.7 μM at -140 mV and 6.5 μM at -20 mV. GABA currents are nearly absent without Na (Li, Tris) and reduced (ninefold at -20 mV, only twofold at -140 mV) without Cl (acetate, methanesulfonate). GABA uptake inhibitors were as follows: (a) nipecotic acid, ACHC, and DABA are actually substrates, producing 40–80% of the maximal GABA currents; (b) SKF-89976-A blocks the GABA currents and produces no currents. *Kinetics*: (a) After a voltage jump with GABA, Na, and Cl present, currents reach a new steady state within <10 ms (our temporal resolution). (b) Without GABA, voltage jump currents begin at roughly the same amplitude, then decay to zero with a time constant of ~100 ms; (c) without Na, the transient currents are absent. In case (b), the transients

probably represent either (1) an incomplete transport cycle or (2) voltage-dependent Na binding. The integrated transients represent charge movements; these are half complete at  $-30$  mV, begin to saturate at  $\sim -120$  and  $+20$  mV, and change  $e$ -fold for  $\sim 25$  mV. Assuming 1 elementary charge per transporter, each oocyte expresses up to  $5 \times 10^{11}$  transporters, or  $\sim 20,000/\mu\text{m}^2$ . There is a linear relation between maximum GABA currents and integrated transients among oocytes; the slope yields a turnover number of  $5 \text{ s}^{-1}$  at  $-80$  mV, consistent with the voltage jump relaxation rates. [Supported by NS-11756, Synaptic Pharmaceuticals, NRSA (J. Naeve), and AHA (S. Mager).]

121. Purification of P-Glycoprotein and Reconstitution of Drug Transport ADAM B. SHAPIRO\* and VICTOR LING,\* *Molecular and Structural Biology, Ontario Cancer Institute, Toronto, Ontario, Canada*

P-glycoprotein (Pgp) was highly purified from multidrug-resistant Chinese hamster ovary cells grown in culture under colchicine selection. A monoclonal antibody affinity column was used to purify the Pgp from a Zwittergent 3-12 or 3-14 extract of a crude membrane preparation. The protein was eluted gently and in high yield by a synthetic peptide containing the epitope of the antibody. The Pgp is nearly pure and active in ATP hydrolysis in detergent solution. Further purification was obtained by hydroxylapatite chromatography. Reconstitution of active drug transport will be attempted.

122. Cloning and Functional Characterization of an Epithelial Cell-specific and Amiloride-resistant  $\text{Na}^+/\text{H}^+$  Exchanger Isoform (NHE-3) CHUNG-MING TSE,\* SUE LEVINE,\* MARSHALL MONTROSE,\* STEVEN BRANT,\* SUSAN WALKER,\* JACQUES POUYSEUR, and MARK DONOWITZ, *Departments of Medicine and Physiology, The Johns Hopkins University, Baltimore, Maryland; and Department of Biochemistry, University of Nice, Nice, France*

Epithelial cells from ileal villus and kidney cortex have  $\text{Na}^+/\text{H}^+$  exchangers on both apical (ap) and basolateral (bl) membranes. In both tissues, the ap  $\text{Na}^+/\text{H}^+$  exchangers are distinguished from the bl isoform by being relatively amiloride resistant. We previously cloned and expressed two  $\text{Na}^+/\text{H}^+$  exchanger isoforms (NHE-1 and NHE-2). NHE-1 is the bl isoform. Although they are both sensitive to amiloride inhibition ( $K_i = 1 \mu\text{M}$ ), NHE-2 is 50-fold more resistant to ethylisopropylamiloride (EIPA) than is NHE-1. We now report the cloning of a third  $\text{Na}^+/\text{H}^+$  exchanger isoform (NHE-3). Using a Styl-Styl fragment of rabbit NHE-2 cDNA as a probe (encoding amino acid residues 42–632), a rabbit ileal villus cell cDNA library and a rabbit kidney cortex cDNA library were screened under low stringency conditions. This yielded a full-length NHE-3 cDNA which encodes a protein of 832 amino acids with  $M_r = 92747$ . NHE-3 exhibits 41 and 44% amino acid identity with NHE-1 and NHE-2, respectively. Overall, these three  $\text{Na}^+/\text{H}^+$  exchangers have 28% amino acid identity. They are all predicted to have 10–12 membrane-spanning domains and a long cytoplasmic tail which contains putative protein kinase phosphorylation motifs. Northern blot analysis of poly(A<sup>+</sup>) RNA isolated from rabbit ileum using NHE-3 cDNA as a probe hybridized to a single 5.4-kb transcript. Detailed tissue distribution of message, as performed by ribonuclease protection assay, showed that the NHE-3 message is exclusively expressed in intestine and kidney. When NHE-3 cDNA was stably expressed in the PS120 fibroblast cell line deficient in endogenous  $\text{Na}^+/\text{H}^+$  exchangers, the transfected cells restored their  $\text{Na}^+/\text{H}^+$  exchange activity. Furthermore, NHE-3 is "hyper-resistant" to amiloride and EIPA inhibition with a  $K_i$  of 39 and  $8 \mu\text{M}$ , respectively. Thus, we conclude that (a) NHE-3 is a functional  $\text{Na}^+/\text{H}^+$  exchanger; (b) it is kidney and intestine specific; and (c) it is amiloride and EIPA resistant. Taken together, NHE-3 has the characteristics of the ileal villus and kidney cortex ap  $\text{Na}^+/\text{H}^+$  exchangers.

123. Control of Volume and Intracellular pH under Hypotonic Conditions in Human Promyelocytic Leukemic HL-60 Cells KENNETH R. HALLOWS,\* DIEGO RESTREPO, and PHILIP A. KNAUF, *Department of Biophysics, University of Rochester Medical Center, Rochester, New York; and Monell Chemical Senses Center, Philadelphia, Pennsylvania*

Subsequent to swelling under hypotonic conditions, human promyelocytic leukemic (HL-60) cells exhibit a compensatory regulatory volume decrease (RVD) response, which returns cell volume to

near resting levels within 30 min (Hallows et al. 1991. *Am. J. Physiol.* 261:C1154). Evidence obtained through the use of inhibitors, ion substitution, and isotope flux and equilibration techniques suggests that this RVD response is mediated by the efflux of K and Cl through separate conductive pathways in the membrane. However, if RVD occurred exclusively through KCl loss, intracellular pH ( $\text{pH}_i$ ) regulation could be compromised since the anion exchanger in these cells tends to keep  $[\text{Cl}]_i/[\text{Cl}]_o = [\text{H}]_o/[\text{H}]_i$  (Restrepo et al. 1988. *J. Gen. Physiol.* 92:489). With a large drop in  $[\text{Cl}]_i$  during RVD,  $\text{pH}_i$  would drop substantially if the anion exchanger remained active. If Na/H exchange were also activated to defend against this drop in  $\text{pH}_i$ , osmolyte accumulation would counteract the RVD phenomenon. Cells were suspended in media that were 50% isotonic with varying  $\text{HCO}_3$  concentrations present, and the contents of intracellular  $\text{H}_2\text{O}$ , Cl, and K were measured using a triple-label isotope technique and atomic absorption spectrophotometry. In all of the different media, net Cl effluxes were significantly less than net K effluxes during RVD and were insufficient to account for the degrees of volume recovery observed. Therefore, additional osmolytes must be involved in the RVD process in HL-60 cells. Moreover, since the  $[\text{Cl}]_i/[\text{Cl}]_o$  ratio changes only slightly,  $\text{pH}_i$  homeostasis is not severely challenged during RVD. Indeed, fluorometric estimates of  $\text{pH}_i$  using 2,7-bis(carboxyethyl)-5(6)-carboxyfluorescein during RVD in the different media showed only slight initial drops in  $\text{pH}_i$  ( $\leq 0.2$  pH units). [Supported by NIH grants HL-18208 and GM-42495.]

124. Effect of cAMP on Intracellular pH in Principal Cells of Frog Skin VIJAY LYALL, TAMMY S. BELCHER,\* and THOMAS U. L. BIBER, *Department of Physiology, Medical College of Virginia, Virginia Commonwealth University, Richmond, Virginia*

We have demonstrated that vasotocin in the basolateral compartment depolarized the potential across the apical cell membrane ( $V_a$ ), increased short circuit current ( $I_{sc}$ ), decreased the fractional resistance of the apical cell membrane ( $\text{FR}_a$ ), and alkalinized intracellular pH ( $\text{pH}_i$ ) in the principal cells of frog skin (Lyall et al. 1991. *J. Gen. Physiol.* 98:20a [Abstr.]). To investigate if the hormone-induced, potential-dependent changes in  $\text{pH}_i$  are a consequence of an increase in intracellular cAMP, we measured both  $V_a$  and  $\text{pH}_i$  simultaneously in frog skins with double-barreled, pH-sensitive microelectrodes in the presence and absence of basolateral cAMP (1 mM), theophylline (2.5 mM), and forskolin (10  $\mu\text{M}$ ). Skins were perfused continuously in Ringer's solution containing (mM) 110 NaCl, 2.5  $\text{KHCO}_3$ , and 1.0  $\text{CaCl}_2$  gassed with air containing 0.2%  $\text{CO}_2$  (pH 8.0) under open circuit or short circuit conditions. Theophylline, an inhibitor of phosphodiesterase, depolarized  $V_a$  by  $14 \pm 3$  mV, decreased  $\text{FR}_a$  by  $0.14 \pm 0.03$ , increased  $\text{pH}_i$  by  $0.11 \pm 0.02$ , and increased  $I_{sc}$  by  $32 \pm 5\%$  (mean  $\pm$  SEM;  $n = 6$ ,  $P < 0.01$ ). Under open circuit conditions theophylline depolarized both  $V_a$  ( $\Delta V_a = 20 \pm 4$  mV) and  $V_b$  ( $\Delta V_b = 24 \pm 5$  mV), the potential across the basolateral membrane, and increased  $\text{pH}_i$  by  $0.10 \pm 0.01$  ( $n = 3$ ). Forskolin, activator of adenylate cyclase, depolarized  $V_a$  ( $\Delta V_a = 30$  mV) and increased both  $I_{sc}$  ( $\Delta I_{sc} = 50\%$ ) and  $\text{pH}_i$  ( $\Delta = 0.12$ ;  $n = 2$ ). Bromo (Br)- or 8-chlorophenylthio (8-CPT)-cAMP increased both  $\Delta \text{pH}_i$  by  $0.14 \pm 0.02$  and  $\Delta I_{sc}$  by  $22 \pm 7 \mu\text{A}$  ( $n = 4$ ). However, Br-cAMP showed a biphasic effect. Initially  $V_a$  depolarized ( $\Delta = 8.5$  mV) with an acidification of  $\text{pH}_i$  and a decrease in  $I_{sc}$  with time followed by an increase in both  $I_{sc}$  and  $\text{pH}_i$  without change in  $V_a$ . With 8-CPT-cAMP  $V_a$  depolarized when both  $I_{sc}$  and  $\text{pH}_i$  increased without initial acidification. These data suggest that the potential-dependent changes in  $\text{pH}_i$  are regulated by cAMP. [Supported by NIH grant DK-26347.]

125. L-Alanine-induced Changes in Hepatocyte Intracellular  $\text{K}^+$  and  $\text{Cl}^-$  Activities and Water Volume KENING WANG\* and ROBERT WONDERGEM, *Department of Physiology, James H. Quillen College of Medicine, East Tennessee State University, Johnson City, Tennessee*

The purpose of this study was to use ion-sensitive, double-barreled microelectrodes (Corning 477317 and 477913; Corning Glass Inc., Corning, NY) to measure changes in hepatocyte transmembrane potential ( $V_m$ ), intracellular  $\text{K}^+$  and  $\text{Cl}^-$  activities ( $a_{\text{K}^+}$  and  $a_{\text{Cl}^-}$ ), and water volume during L-alanine uptake. Mouse liver slices were superfused with control and experimental Krebs physiological salt solutions. The experimental solution contained 20 mM L-alanine and the control solution was adjusted to the same osmolality (305 mosM) with added sucrose. Hepatocytes were also loaded with 50 mM tetramethylammonium ion ( $\text{TMA}^+$ ) for 10 min. Changes in cell water volume during L-alanine

uptake were determined by changes in intracellular, steady-state TMA<sup>+</sup> activity measured with the K<sup>+</sup> electrode (Reuss, 1985. *Proc. Natl. Acad. Sci. USA.* 82:6014). Hepatocyte control  $V_m$  was  $-35 \pm 1$  mV. L-Alanine uptake first depolarized  $V_m$  by  $2 \pm 0.2$  mV and then hyperpolarized  $V_m$  by 6 mV to  $-41 \pm 1$  mV ( $n = 16$ ) over 6–13 min. During this hyperpolarization  $a_K^i$  decreased 8% or 7 mM from the control value of  $82 \pm 7$  mM to  $75 \pm 7$  mM ( $n = 4$ ). Hyperpolarization of  $V_m$  by L-alanine uptake also resulted in a 38% decrease in  $a_{Cl}^i$  from  $20 \pm 2$  to  $12 \pm 3$  mM ( $n = 7$ ;  $P < 0.01$ ). Changes in  $V_m$  and  $V_m - V_{Cl}$  voltage traces were parallel during the time of L-alanine hyperpolarization, which is consistent with passive distribution of intracellular Cl<sup>-</sup> with the  $V_m$  in hepatocytes. Hepatocyte water volume during L-alanine uptake increased by  $10 \pm 2\%$ . This swelling accounts for the decrease in  $a_K^i$ , but it does not explain the 38% decrease in  $a_{Cl}^i$ . We conclude that hepatocyte  $a_K^i$  decreases during L-alanine uptake along with cell swelling, and that the hyperpolarization of  $V_m$  during L-alanine uptake provides electromotive force to decrease  $a_{Cl}^i$ . These ionic events may contribute to hepatocyte volume regulation during organic solute transport. [Supported by PHS 1R01-AA09967.]

126. Functional Analysis of Cystic Fibrosis Mutations Associated with Mild Disease  
DAVID N. SHEPPARD,\* DEVRA P. RICH,\* RICHARD J. GREGORY,\* DAVID W. SOUZA,\* ALAN E. SMITH,\* and MICHAEL J. WELSH, *Howard Hughes Medical Institute, University of Iowa, Iowa City, Iowa; and Genzyme Corporation, Framingham, Massachusetts*

The disease cystic fibrosis (CF) is caused by mutations in the gene encoding the cystic fibrosis transmembrane conductance regulator (CFTR), a cAMP-regulated Cl<sup>-</sup> channel. The most common mutation, deletion of phenylalanine 508 (CFTRΔF508), is associated with severe lung disease and pancreatic insufficiency. However, other mutations including CFTR-R117H, -R334W, and -R347P, are associated with mild lung disease and pancreatic sufficiency. (Mutations are named in their single letter amino acid code; for example, CFTR-R117H means that arginine 117 is mutated to histidine.) These mutations are located in the first membrane-spanning domain; CFTR-R334W and -R347P lie in the sixth transmembrane segment, while CFTR-R117H is in the extracellular loop between the first and second transmembrane segments. To understand why these mutations are associated with mild disease, we transiently expressed CFTR-R117H, -R334W, and -R347P in HeLa cells using the vaccinia virus-T7 hybrid expression system and assessed function using the fluorescent dye 6-methoxy-N-(sulfoethyl) quinolinium (SPQ) and the patch-clamp technique. The SPQ assay indicated that all of the mutants were functional; they generated cAMP-stimulated anion efflux similar to wild-type CFTR. Whole-cell patch-clamp recordings of cells expressing these mutants exhibited little or no basal Cl<sup>-</sup>-selective currents, but addition of cAMP agonists reversibly activated large Cl<sup>-</sup>-selective currents with linear current-voltage relationships; the currents showed no evidence of voltage-dependent activation or inhibition. These whole-cell properties are characteristic of wild-type CFTR Cl<sup>-</sup> channels. We are now characterizing the single-channel properties of these mutants in excised inside-out membrane patches.

127. Reconstitution of Functional Water Channels in Liposomes Containing Purified Red Cell CHIP28 Protein MARK L. ZEIDEL, SURESH V. AMPUDKAR,\* BARBARA L. SMITH,\* and PETER AGRE,\* *Department of Medicine, Harvard Medical School, Boston, Massachusetts; and Johns Hopkins University School of Medicine, Baltimore, Maryland*

Water rapidly crosses the plasma membranes of red blood cells (RBCs) through specialized highly selective water channels. However, the identity of the water channel has remained elusive. CHIP28 is an abundant integral membrane protein in RBCs and renal tubules, and *Xenopus laevis* oocytes injected with CHIP28 RNA were reported to exhibit high osmotic water permeability ( $P_f$ ). Proteoliposomes containing CHIP28 protein exclude urea and protons but exhibit marked increases in  $P_f$  compared with control liposomes (control  $P_f = 0.0097 \pm 0.004$  cm/s [SD;  $n = 3$ ]; CHIP28 proteoliposome  $P_f = 0.054 \pm 0.008$  cm/s, both at 37°C). From the increment in  $P_f$  due to CHIP28 and the densities of CHIP28 in proteoliposomes, the permeability of each CHIP28 protein molecule ( $P_f$ ) is  $11.7 \pm 1.8 \times 10^{-14}$  cm<sup>3</sup>/s. From the density of CHIP28 proteins in the RBC ( $2 \times 10^5$  copies/RBC),

the expected  $P_f$  attributable to CHIP28 in intact RBC is 0.017 cm/s, in good agreement with the observed RBC  $P_f$  of 0.018 cm/s. Like  $P_f$  of intact RBC,  $P_f$  of CHIP28 proteoliposomes is reversibly inhibited by mercurial sulfhydryl reagents such as parachloromercuribenzenesulfonate (pCMBS) and  $\text{HgCl}_2$  and exhibits a low Arrhenius activation energy of  $3.1 \pm 0.5$  kcal/mol. These results demonstrate that neither specialized lipid structure nor cytoskeletal proteins are required for water channel function and indicate that CHIP28 protein is the structure responsible for most transmembrane water movement in the RBC. The selectivity of the CHIP28 protein for water over urea and protons indicates that the protein forms an extremely narrow pore which appears to exclude positive charge. [Supported by NIH grants DK-43955, DK-36081, HL-33991, HL-48268, and AA-09012, and by grants from the Department of Veterans Affairs and the American Heart Association.]

128. Na-dependent  $\text{Cl}/\text{HCO}_3$  Exchange in Human Promyelocytic Leukemic HL60 Cells  
DIEGO RESTREPO and RUTHANNE B. SNYDER,\* *Monell Chemical Senses Center, Philadelphia, Pennsylvania; and Department of Physiology, University of Pennsylvania, Philadelphia, Pennsylvania*

When HL60 cells are suspended in mammalian Ringers containing 20 mM  $\text{HCO}_3$  with Cl replaced by gluconate, intracellular pH ( $\text{pH}_i$ ) increases exponentially by  $0.76 \pm 0.05$  ( $n = 7$ ) pH units from an initial  $\text{pH}_i$  of  $7.14 \pm 0.03$ . The initial rate of increase of  $\text{pH}_i$  in the absence of  $\text{Cl}_o$  decreases from  $0.26 \pm 0.03$  to  $0.006 \pm 0.012$  pH units/min ( $n = 7$ ) upon removal of extracellular Na. The initial Na-dependent alkalization rate measured in the absence of  $\text{Cl}_o$  is abolished when the experiment is performed in the absence of bicarbonate or with cells that have been previously depleted of intracellular Cl. On this basis, it appears that the alkalization measured in the absence of  $\text{Cl}_o$  is partially mediated by a transport system that exchanges intracellular Cl for extracellular  $\text{HCO}_3$  in a Na-dependent manner (Na-dependent  $\text{Cl}/\text{HCO}_3$  exchange). The rate of Na-dependent  $\text{Cl}/\text{HCO}_3$  exchange did not change appreciably when HL60 cells were induced to differentiate along the granulocytic pathway by addition of 1.25% DMSO for 5 d ( $0.25 \pm 0.03$  pH units/min,  $n = 7$  in undifferentiated cells and  $0.24 \pm 0.04$  pH units/min,  $n = 3$  in DMSO-differentiated cells). The Na-dependent  $\text{Cl}/\text{HCO}_3$  exchange rate was not altered by addition of the Na/H exchange inhibitor DMA, but was abolished by addition of either 1 mM  $\text{H}_2\text{DIDS}$  or 2  $\mu\text{M}$  of the oxonol dye DiBAC<sub>4</sub>(5). The Na-dependent  $\text{Cl}/\text{HCO}_3$  exchanger appears to be active at resting  $\text{pH}_i$  and contributes to the process of recovery from acute acidification in  $\text{HCO}_3$ -containing medium. [Supported by NIH grant GM-42495.]

129. Magnesium Depletion of Low K Sheep Red Blood Cells Reveals a Proton-titrable Site Controlling K:Cl Cotransport ANDREAS ERDMANN\* and PETER K. LAUF, *Department of Physiology & Biophysics, Wright State University, Dayton, Ohio*

Variations of intracellular and extracellular pH ( $\text{pH}_i$  and  $\text{pH}_o$ ) and intracellular Mg ( $\text{Mg}_i$ ) affect ouabain-resistant (OR) K and Rb fluxes in low K (LK) sheep red blood cells (SRBC) (Lauf, 1985. *Am. J. Physiol.* 249:C271; Zade-Oppen and Lauf, 1990. *J. Membr. Biol.* 118:143). To understand these observations in terms of K:Cl cotransport activation, we investigated the effect of  $\text{pH}_i$ , varied by titration with  $\text{CO}_2$  or  $\text{HCO}_3^-$ , and of  $\text{Mg}_i$ , altered by the ionophore A23187 plus extracellular Mg ( $\text{Mg}_o$ ) or a Mg chelator (EDTA) in LK SRBC equilibrated in media with Cl or with anions not cotransported, such as  $\text{NO}_3$  or methylsulfonate ( $\text{CH}_3\text{SO}_3$ ). Using sucrose on top of a 90-mM Na-buffered salt base, osmolarity was covaried with medium acidification to maintain cell volume at unity. In Cl and  $\text{NO}_3$ , the experimental slopes of osmolarity vs. pH were identical and less negative than the calculated slopes (Gunn et al. 1973. *J. Gen. Physiol.* 61:185), but were more negative for  $\text{CH}_3\text{SO}_3$ , suggesting transport in the dissociated and undissociated forms. The relationship between measured  $\text{pH}_i$  and  $\text{pH}_o$  for each anion was  $\sim 0.5$  U higher than predicted (Glaser, 1979. *J. Membr. Biol.* 51:217), but the calculated membrane potentials were not. Under these rigorous conditions, both OR K efflux and Rb influx were Cl dependent at a  $\text{pH}_o$  close to 7.1, but not at  $\text{pH}_o$  6 and 8 where Cl was inhibitory. Removal of  $\text{Mg}_i$  elevated OR K effluxes at pH 7.1 with saturation at pH 8,

suggesting a  $pK_a$  value of the protonated site of  $\sim 6.6$ , whereas Mg<sub>i</sub> loading abolished the K:Cl flux at  $pH_o$  7.1. However, OR Rb influx was activated by Mg depletion without saturation at pH 8. Mg<sub>i</sub> depletion-induced OR K (Rb) fluxes were absent in  $NO_3^-$  and  $CH_3SO_3^-$ , consistent with K:Cl cotransport activation. Thus in LK SRBC, K:Cl cotransport has a bell-shaped pH dependence with a maximum around  $pH_o$  7.1 (when  $pH_i$  is 7.5). Mg<sub>i</sub> depletion significantly altered the  $pH_o$  dependence of K:Cl cotransport by revealing a  $H^+$ -titrable site. Whether this site is identical with that shown for OR K fluxes after thiol modification or alkaline  $pH_i$  clamping remains to be established. [Supported by the American Heart Association and NIH grant RO1 37-160.]

130. Detailed Characterization of the Kinetics and Regulation of Three Cloned Rabbit Ileal  $Na^+/H^+$  Exchangers Stably Expressed in a Fibroblast Cell Line S. LEVINE,\* M. MONTROSE,\* J. POUYSSEGUR, M. TSE,\* and M. DONOWITZ, *Departments of Medicine and Physiology, The Johns Hopkins University, Baltimore, Maryland; and Department of Biochemistry, University of Nice, Nice, France*

We have identified, cloned, and sequenced three members of the mammalian  $Na^+/H^+$  exchanger gene family which differ in tissue distribution, sensitivity to amiloride, and kinase and growth factor regulatory responses. NHE-1, present on the ileal villus cell basolateral membrane and in many other tissues, is sensitive to amiloride. NHE-2 is an apical isoform expressed in intestine and also in kidney and adrenal gland, and is relatively sensitive to amiloride. NHE-3 is expressed exclusively in kidney and intestine and is the most resistant to amiloride. For kinetic studies, the cDNAs from the exchangers were stably transfected into a fibroblast cell line (PS120) selected to have no endogenous  $Na^+/H^+$  exchanger.  $Na^+/H^+$  exchange was studied fluorometrically in cells loaded with the pH-sensitive dye 2',7'-bis(2-carboxymethyl)-5,6-carboxyfluorescein. Plots of  $Na^+/H^+$  exchange vs. internal  $[H^+]$  fit a sigmoidal rather than hyperbolic response curve, with a Hill number  $> 2$  for all three exchangers, suggesting the presence of an internal  $H^+$  modifier site. The exchangers differed in regulation by growth factors and phorbol esters. Serum stimulated all three exchangers, however, with different kinetic effects. In NHE-1 serum lowered the  $K_m(H^+)$  but did not change  $V_{max}$ , while the effect on NHE-2 and NHE-3 was to increase the  $V_{max}$  without a change in  $K_m(H^+)$ . A similar stimulation was seen with phorbol myristate acetate (PMA) for NHE-1 and NHE-2; in contrast, in NHE-3 PMA caused an inhibition of Na/H exchange. We conclude that: (a) NHE-1 is apparently the "housekeeping" isoform, localized in the intestine to the basolateral membrane; (b) the function of NHE-2 is not known; however, it is distinct from NHE-1 in kinetic response to growth factors and in tissue distribution; and (c) inhibition by phorbol esters, resistance to amiloride, and tissue distribution suggest that NHE-3 has similarities to the ileal apical exchanger involved in neutral NaCl absorption.

131.  $K^+$  and  $Cl^-$  Channels Induced by Hypo-osmotic Challenge in Vestibular Dark Cells PHILINE WANGEMANN,\* NOBUYUKI SHIGA,\* and DANIEL C. MARCUS, *Boys Town National Research Hospital, Omaha, Nebraska*

Cell height was measured in dark cell epithelium. Regulatory volume decrease in response to a hypo-osmotic challenge (RVD-HYPO) was observed when the osmolarity was lowered from 300 to 150 mosM. RVD-HYPO was inhibited when the outward KCl gradient was reduced by increasing perfusate  $K^+$  or  $Cl^-$ . In the presence of 75 mM KCl, the KCl gradient became inward directed; the cells swelled due to KCl influx more than expected for a perfect osmometer. The ion selectivity of this KCl influx was  $K^+ = Rb^+ \gg Cs^+ > Na^+$  and  $Cl^- = NO_3^- = SCN^- \gg gluconate^-$ . In the presence of 50 mM  $K^+$  and 75 mM  $Cl^-$ , RVD-HYPO was inhibited by  $2 \times 10^{-2}$  M tetraethylammonium (TEA),  $10^{-3}$  M quinidine, and  $5 \times 10^{-3}$  M lidocaine, but not by  $5 \times 10^{-3}$  M barium or  $10^{-3}$  M amiloride. Evidence for two TEA-insensitive  $K^+$  channels was obtained under isosmotic conditions. Under isosmotic unswollen conditions, evidence for a barium- and lidocaine-sensitive but TEA- and quinidine-insensitive  $K^+$  channel was based on the finding that barium and lidocaine but not TEA and quinidine stimulated RVD-HYPO when added under isosmotic conditions before the hypo-osmotic challenge. Under isosmotic swollen conditions, evidence for a barium-, lidocaine-, and quinidine-sensitive, but

TEA-insensitive  $K^+$  channel has been reported earlier (Wangemann et al. 1992. *Am. J. Physiol.* In press). In the presence of 50 mM  $K^+$  and 75 mM  $Cl^-$ , RVD-HYPO was inhibited by the stilbene derivatives  $10^{-3}$  M DIDS and  $10^{-3}$  M SITS, but not by  $10^{-5}$  M NPPB,  $10^{-4}$  M acetazolamide, or  $10^{-4}$  M ethoxzolamide. Under isosmotic unswollen and swollen conditions no inhibition by DIDS was observed, suggesting the absence of DIDS-sensitive  $Cl^-$  channels. These data suggest that the hypo-osmotic challenge specifically induced a TEA-sensitive  $K^+$  channel and a DIDS-sensitive  $Cl^-$  channel. [Supported by NIH grants DC-01098 (P. Wangemann) and DC-00212 (D. C. Marcus) and the Deafness Research Foundation (P. Wangemann).]

132. Photosensitive Visceral Muscles in the Stable Fly, *Stomoxys calcitrans* B. J. COOK, U.S. Department of Agriculture, Agricultural Research Service, Food Animal Protection Research Laboratory, College Station, Texas

Extraocular photoreception has been reported in both vertebrates and invertebrates (Yoshida. 1979. In Handbook of Sensory Physiology. Springer, Berlin. VII/6A:582). Among insects this type of photoreception has generally been detected in two classes of cells: those present in endocrine organs and those found in the central and peripheral nervous system. The incidence of direct photoactivation of insect muscle, however, appears to have been an unreported phenomenon until now. Two groups of visceral muscles in the adult stable fly have shown photosensitive properties: (a) the network of stellate muscle cells that cover the surface of the ovary, and (b) the muscle layers of the lateral and common oviduct. The duration of the spontaneous contractions of the sheath that surrounds the isolated ovary ranged from 200 ms to 4 s. An impedance converter was used to detect changes in the amplitude, frequency, and tonus of these events. Isolated ovaries showed no response to light below an intensity of 1,750 Lux. However, at illuminations between 2,460 and 28,000 Lux, an 80% increase in the frequency of ovarian sheath contractions was detected. Although ovaries receive innervation from the median abdominal nerve (Cook and Peterson. 1989. *Arch. Insect Biochem. Physiol.* 12:15), no terminations could be detected above the pedicel and no peripheral nerve cells are associated with either the pedicel or the ovary. Thus, it was concluded that this photoactivation in the ovarian sheath was probably a direct response to light. Preparations of the oviduct isolated from their connections to the central nervous system and peripheral nerve cells continued to contract in a spontaneous and rhythmic manner. Both phasic contractions (1–25 s in duration) and tonic events (15–30 s in duration) were detected by means of a small load cell. Like the ovarian muscularis, the oviduct showed no response to light below 1,750 Lux, but above an illumination of 3,000 Lux a light-dependent increase in amplitude frequency and tonus was observed up to a maximum at 28,000 Lux.

133. Sequencing of a Renal cDNA Related to the  $Na^+$ /Nucleoside and  $Na^+$ /Glucose Cotransporters ANA M. PAJOR,\* Department of Physiology, University of Arizona, College of Medicine, Tucson, Arizona (Sponsor: William H. Dantzler)

The SGLT family is the family of transporters related in sequence to the  $Na^+$ /glucose cotransporter. The members of this family include mammalian intestinal and renal  $Na^+$ /glucose cotransporters (SGLT1), a renal  $Na^+$ /nucleoside cotransporter (SNST1), a renal  $Na^+$ /myoinositol cotransporter (SMIT), and bacterial  $Na^+$ -dependent cotransporters for proline and pantothenate. To date, no other proteins show significant sequence homology with the members of the SGLT family. A 2-kb cDNA, RK-D, was isolated from the same rabbit renal library from which the  $Na^+$ /nucleoside cotransporter was isolated (Pajor and Wright. 1992. *J. Biol. Chem.* 267:3557). The mRNA for RK-D was ~2.1 kb and was found in both heart and kidney (Pajor and Wright, 1992). The RK-D cDNA was sequenced and found to contain a single open reading frame encoding a protein of 597 amino acids, considerably smaller than SNST1 and SGLT1. However, Kyte-Doolittle analysis predicts 12 membrane-spanning domains, in common with both SNST1 and SGLT1. There is a single putative glycosylation site, in the same location as the one seen in SNST1 and SGLT1. RK-D is equally related to SNST1, SGLT1, and SMIT with ~50% sequence identity and 70% sequence similarity to all three transporters. Because of the high sequence similarity and conservation of "signature" family features, it is very likely that RK-D

encodes a  $\text{Na}^+$ -dependent cotransporter. Expression studies to determine the function of RK-D are currently underway. [Supported by startup funds from the University of Arizona.]

**134. Involvement of Band 3 in Volume-activated Taurine Efflux in Skate Erythrocytes** MARK MUSCH\* and LEON GOLDSTEIN, *Department of Medicine, University of Chicago, Chicago, Illinois; Section of Physiology, Brown University, Providence, Rhode Island; and Mount Desert Island Biological Laboratory, Salsbury Cove, Maine*

Swelling of skate erythrocytes produces a marked increase in taurine (a major cell osmolyte) efflux, which is inhibited by the stilbene DIDS, an agent known to covalently bind to the erythrocyte anion exchanger, band 3. We used DIDS binding to determine if band 3 was directly involved in the volume-activated taurine efflux. Using the radiolabeled analogue [ $^3\text{H}$ ]dihydroDIDS( $\text{H}_2\text{DIDS}$ ) we determined that exposure to hypotonic medium (460 vs. 940 mosmol/liter) stimulated a rapid increase in the binding to the erythrocytes. This increased  $\text{H}_2\text{DIDS}$  binding was also observed when the permeant solute ethylene glycol replaced half of the medium NaCl. The initial rate of covalent binding was not altered under these conditions, suggesting that total binding but not the affinity of the  $\text{H}_2\text{DIDS}$  for the covalent binding site was altered. Since a variety of signals stimulate taurine efflux and the formation of diacylglycerol, we determined whether hypotonicity stimulated band 3 phosphorylation. Erythrocytes were prelabeled with [ $^{32}\text{P}$ ] $_i$ , and subsequently exposed to hypotonic medium; then cells were removed and plasma membranes rapidly isolated. Three membrane proteins (molecular masses 99, 65, and 32 kD) showed increased phosphorylation after hypotonic exposure. The 99-kD protein was immunoprecipitated with human band 3 antibody. The phosphate associated with this band increased significantly after hypotonic exposure. The results suggest that hypotonicity affects taurine efflux through actions on band 3, possibly through a phosphorylation event. [Supported by a NSF grant.]

**135. In Vitro Assembly of the  $\text{Na}^+/\text{K}^+$  ATPase from Subunits** JIA YEU LIU\* and GUIDO GUIDOTTI, *Department of Biochemistry and Molecular Biology, Harvard University, Cambridge, Massachusetts*

The  $\text{Na}^+/\text{K}^+$  ATPase belongs to a large family of enzymes known as the P-type ATPases, which are present in bacterial, mammalian, plant, and yeast cells (Jorgensen and Anderson, 1988, *J. Membr. Biol.* 103:95).  $\text{Na}^+/\text{K}^+$  ATPase is an integral plasma membrane protein composed of two different polypeptide subunits. The large subunit, the alpha chain (100 kD), is believed to be the major catalytic subunit. The small subunit, the beta chain (50 kD), is a glycoprotein with an as yet undefined function. Numerous studies on the  $\text{Na}^+/\text{K}^+$  ATPase have shown that both the alpha and beta subunits are necessary for successful expression of functional enzyme in cells (Noguchi et al. 1987, *FEBS [Fed. Eur. Biochem. Soc.] Lett.* 225:27; Horowitz et al. 1990, *J. Biol. Chem.* 265:4189). The beta subunit could be required for: (a) catalysis, (b) synthesis, assembly, and correct transport to the plasma membrane, or (c) both. We present evidence that: (a) the alpha subunit, when expressed in yeast cells, can insert into the membrane in the absence of the beta subunit; and (b) this alpha subunit is correctly folded. The experimental rationale has been to find conditions where the native enzyme can reversibly dissociate into alpha and beta subunits. We used this assay to show that the alpha subunit expressed in the absence of a beta subunit is capable of association in vitro with the beta subunit.

**136. Purification of ATPase-active P-Glycoprotein: Lipid Interactions and Functional Reconstitution** CARL A. DOIGE,\* XIAO-HONG YU,\* and FRANCES J. SHAROM,\* *Department of Chemistry and Biochemistry, University of Guelph, Guelph, Ontario, Canada*

P-glycoprotein is a 180-kD protein that is proposed to mediate multidrug resistance by acting as an ATP-driven drug efflux pump. Little is currently known about either the mechanism of transport or the way in which ATP hydrolysis is coupled to drug efflux. To obtain biochemical information on P-glycoprotein function at the molecular level, we set out to isolate and reconstitute the protein in

functional form. Plasma membrane from multidrug-resistant CHRC5 Chinese hamster ovary cells was subjected to a two-step selective extraction with the detergent 3-[(3-cholamidopropyl)dimethylammonio]-1-propanesulfonate to obtain a fraction enriched in P-glycoprotein (30% pure), with ATPase activity of  $0.55 \mu\text{mol min}^{-1} \text{mg}^{-1}$ . This extract was further purified by affinity chromatography on lentil lectin-Sepharose, producing a P-glycoprotein preparation that was homogeneous on SDS-PAGE. The resulting preparation has a very high ATPase activity ( $1.5 \mu\text{mol min}^{-1} \text{mg}^{-1}$ ), and probably retains native functionality. P-glycoprotein ATPase activity was lost over time with incubation at  $22^\circ\text{C}$ . Certain lipids, especially phosphatidylethanolamine (PE), were able to protect the ATPase from inactivation, while others had little effect, suggesting that the ATP binding domain of P-glycoprotein is stabilized by association with membrane PE. In addition, certain species of PE and phosphatidylcholine (PC) were able to restore the ATPase function of deoxycholate-delipidated P-glycoprotein. ATPase-active P-glycoprotein was reconstituted into mixtures of PC and PE by gel filtration chromatographic removal of detergent. The resulting proteoliposomes showed ATPase activity, which doubled on detergent permeabilization, suggesting that P-glycoprotein was reconstituted symmetrically. Proteoliposomes containing P-glycoprotein demonstrated ATP-stimulated uptake of  $[^3\text{H}]\text{colchicine}$  over a time of 1–5 min, which was not seen in liposomes of lipid alone. [Supported by a grant from the National Cancer Institute of Canada.]

137. Interaction of Multidrug-resistant Chinese Hamster Ovary Cells with the Peptide Ionophore Gramicidin D DOUG W. LOE\* and FRANCES J. SHAROM,\* *Department of Chemistry and Biochemistry, University of Guelph, Guelph, Ontario, Canada*

Multidrug resistance (MDR) results from the overexpression of a 170-kD membrane protein called P-glycoprotein (Pgp). MDR Chinese hamster ovary (CHO) cells are cross-resistant to gramicidin D (GmD), a small peptide ionophore proposed to form helical dimeric channels. Charged GmD analogues that are unable to cross into the plasma membrane inner leaflet were not toxic to either sensitive or MDR cells. CHO cells transfected with *mdr1* cDNA also displayed cross-resistance to GmD, which directly implicates Pgp as the mediator of resistance. However, GmD was not able to inhibit the photolabeling of Pgp by  $[^3\text{H}]\text{jazidopine}$ . MDR cells are not resistant to other pore-forming ionophores (e.g., alamethicin, melittin, amphotericin B), but show modest levels of cross-resistance to some mobile ionophores (valinomycin, nonactin). Sensitive and MDR cells show no differences in the level of  $^{125}\text{I}$ -GmD uptake. Uptake was low and only a small fraction of GmD in solution was available for uptake. Sensitive cells showed much higher rates of GmD-dependent  $^{86}\text{Rb}^+$  efflux than MDR cells, suggesting that Pgp interferes with formation of ion-conducting GmD dimers. Verapamil sensitized both sensitive and MDR cells to GmD toxicity, and increased GmD-dependent  $^{86}\text{Rb}^+$  efflux in MDR cells. Vinblastine had no effect on cation efflux, and valinomycin had the same effect in both MDR and sensitive cells. We have synthesized a covalently linked GmD dimer, and have shown that MDR cells are highly cross-resistant to this compound. However, while the duration of exposure required for cytotoxicity was similar to that of GmD, dimeric GmD did not increase cation efflux rates in either sensitive or MDR cells. These data argue against a model in which Pgp acts as a flippase to move GmD from the inner to the outer leaflet. [Supported by a grant from the National Cancer Institute of Canada.]

138. Glucocorticoid Stimulation of Ileal  $\text{Na}^+$  Absorptive Cell  $\text{Na}^+/\text{H}^+$  Exchange and Association with an Increase in Message for NHE-3, an Epithelial  $\text{Na}^+/\text{H}^+$  Exchanger Isoform C.-H. CHRIS YUN,\* SARADA GURUBHAGAVATULA,\* SUE LEVINE,\* JAMIE L. M. MONTGOMERY,\* STEVEN BRANT,\* JACQUES POUYSSEGUR, CHUNG-MING TSE,\* and MARK DONOWITZ, *Departments of Medicine and Physiology, The Johns Hopkins University School of Medicine, Baltimore, Maryland; and Department of Biochemistry, University of Nice, Nice, France*

Methylprednisolone (MP) stimulates rabbit ileal neutral NaCl absorption, and aminoglutethimide (AG), which decreases glucocorticoid levels, decreases NaCl absorption (Charney et al. 1975. *J. Clin.*

*Invest.* 56:653; Sellin and Field. 1981. *J. Clin. Invest.* 67:770). Studies were carried out to determine the mechanism of these effects and to determine which member of the gene family of mammalian  $\text{Na}^+/\text{H}^+$  exchangers was involved. Rabbits were treated with either MP (40 mg qd for 24 or 72 h), AG (100 mg q12h for 72 h), or saline as controls. Ileal brush-border membranes were prepared by Mg precipitation and brush-border  $\text{Na}^+/\text{H}^+$  exchange was determined by  $^{22}\text{Na}^+$  uptake over 3–8 s. The  $^{22}\text{Na}^+$  uptake experiments were performed in the presence of PD clamp using either valinomycin/K or TMA/nitrate to eliminate potential contributions by other electrogenic transport processes. MP treatment for 24 and 72 h increased ileal brush-border  $\text{Na}^+/\text{H}^+$  exchange 100%, while AG treatment led to 50% decrease in  $\text{Na}^+/\text{H}^+$  exchange. The effects on  $\text{Na}^+/\text{H}^+$  exchange were specific to the extent that diffusive  $\text{Na}^+$  uptake (no pH gradient), glucose-dependent  $\text{Na}^+$  overshoots, and  $\text{Na}^+$  equilibrium volumes were not affected. To determine whether the increase in  $\text{Na}^+/\text{H}^+$  exchange was associated with an increase in message expression, mRNA levels were measured by ribonuclease protection assay. MP stimulated NHE-3 mRNA levels four- to sixfold at 24 h, and they remained increased at 72 h. In contrast, messages for NHE-1 and NHE-2 were not affected by MP. In summary, (a) MP stimulation of rabbit ileal  $\text{Na}^+$  absorption is due to stimulation of ileal villus cell brush-border  $\text{Na}^+/\text{H}^+$  exchange; (b) basal ileal brush-border  $\text{Na}^+/\text{H}^+$  exchange is dependent on glucocorticoid level; (c) an increase in NHE-3 message, but not in NHE-1 or NHE-2, correlates with the stimulation of ileal brush-border  $\text{Na}^+/\text{H}^+$  exchange. It is likely that NHE-3 is a  $\text{Na}^+/\text{H}^+$  exchanger isoform which is involved in ileal  $\text{Na}^+$  absorption.

139. Evidence for Qualitative Alteration of K-Cl Cotransport in Red Blood Cells with Hemoglobin S NORMA C. ADRAGNA and PETER K. LAUF, *Departments of Pharmacology & Toxicology and Physiology & Biophysics, Wright State University, School of Medicine, Dayton, Ohio*

Erythrocyte K-Cl cotransport is defined as the difference of ouabain-resistant K fluxes in Cl and non-Cl (such as  $\text{NO}_3$ ) media (i.e., the Cl-dependent K flux). A plot of net Cl-dependent K effluxes and Rb influxes as a function of the ratio of external Rb to cellular K,  $\text{Rb}_o/\text{K}_o$ , yields a flux/force diagram with a zero flux intercept or flux reversal point (FRP) (Lauf. 1983. *J. Membr. Biol.* 73:237). For K-Cl cotransport, the FRP is determined by the transmembrane ratio of the ion products of  $\text{K} \times \text{Cl}$  (Delpire and Lauf. 1991. *J. Gen. Physiol.* 97:173). We have determined the FRP of Cl-dependent K/Rb fluxes in red blood cells homozygous for either hemoglobin (Hb) A or Hb S in the presence or absence of Na (methyl-glucamine [MG] replacement) at external pH 7 and at 300 or 200 mosM. At 300 mosM, Cl-dependent Rb influx was present in Hb A but not in Hb S cells, and Cl-dependent K efflux was absent in both. At 200 mosM, the Cl-dependent K efflux was an order of magnitude larger in Hb S than in Hb A cells. In swollen Hb A cells the slopes of the net Cl-dependent fluxes were negative both in Na and MG. The absence of Na induced a left shift of the FRP. In contrast, in swollen Hb S cells the slopes of the net Cl-dependent fluxes were zero in MG, and positive in Na with a FRP at a  $\text{Rb}_o/\text{K}_o$  two orders of magnitude lower than for Hb A cells. We conclude that, under the conditions chosen for the FRP determination, Hb S cells show kinetically not only quantitative (as reported by others) but also, more importantly, qualitative differences with respect to hemoglobin A cells. The relationship of this finding to K-Cl cotransport altered by thiol oxidation is under investigation. [Supported in part by WSU BRSG 661797, American Heart Association, NIH 2R01 37160, and the Cincinnati NIH Sickle Cell Center.]

140. Peptide Transport by Type II Pneumocytes Isolated from Rat Lung D. MEREDITH\* and C. A. R. BOYD,\* *Department of Human Anatomy, University of Oxford, Oxford, United Kingdom*

The type II pneumocyte has the appearance of an actively transporting cell, with microvilli on the free apical surface and numerous intracellular organelles. While probably the best-known function of type II cells is the secretion of pulmonary surfactant, several solute transport systems have been characterized homologous to those in the intestine, with which the lung shares a common embryonic origin. However, the lack of pancreatic-like secretions into the lung suggests that there should be less

proteolytic activity, and thus the possibility of peptide transport as found in the intestine, but without the extensive luminal degradation seen there. This was investigated on type II pneumocytes freshly isolated from rat lung by following the uptake of L-tryptophanyl-L-tyrosine (trp-tyr) by high performance liquid chromatography. The strong UV absorbance of the aromatic rings at 280 nm allows the simultaneous monitoring of both the intact peptide and its breakdown products. In the presence of 30  $\mu$ M amastatin and 60  $\mu$ M bestatin to reduce the endogenous peptidase activity, there is a time-dependent uptake of intact trp-tyr into type II pneumocytes. The presence of the inhibitors also appears to increase the internal trp-tyr concentration above that observed in their absence; this may be due to bestatin entering the cell (Inui et al. 1992. *J. Pharmacol. Exp. Ther.* 260:482), and thus inhibiting intracellular peptidases. The transport of trp-tyr is rapid, with uptake clearly seen after 30 s of incubation in a 2-mM peptide solution. We have not seen any evidence of the intracellular concentration of this neutral dipeptide exceeding that of the external medium. Having demonstrated the presence of intact peptide inside the type II cells, further work is required to characterize the driving force, stoichiometry, kinetics, and specificity of the peptide transporter. In the absence of the degradative enzymes found in the intestine, it remains to be seen whether the peptide transporter described here can be usefully exploited to deliver small peptide drugs that would have little or no oral bioavailability. [Supported by the Medical Research Council and The Wellcome Trust.]

141. Regulation of PKA-activated Cl Conductance in Guinea Pig Ventricular Myocytes: Whole-Cell Studies TZYH-CHANG HWANG,\* MINORU HORIE,\* ATHANASIOS G. DOUSMANIS,\* and DAVID C. GADSBY, *Laboratory of Cardiac/Membrane Physiology, The Rockefeller University, New York*

Cl conductance activated by cAMP-dependent protein kinase (PKA) was studied in myocytes voltage-clamped with wide-tipped ( $\leq 1$  M $\Omega$ ) perfused pipettes. With 100  $\mu$ M GTP and 24 mM Cl in the pipette and 150 mM Cl in the bath, isoproterenol (ISO, 1  $\mu$ M), histamine (10  $\mu$ M), or forskolin (Fsk, 1  $\mu$ M) activated a Cl conductance, which declined rapidly after agonist removal. With pipette GTPyS (40–100  $\mu$ M), ISO- and histamine-, but not Fsk-induced, conductance was persistent. But with GTP or GTPyS in the pipette, addition of a peptide inhibitor (PKI, 100  $\mu$ M) of PKA abolished ISO-induced Cl conductance, indicating that it is activated via PKA and not by direct G protein action. Intrapipette okadaic acid (OA, 1–10  $\mu$ M), an inhibitor of types 1 and 2A phosphatases, had no effect alone, but enhanced the Cl conductance activated by ISO or Fsk by 20–60% and delayed and slowed its decline on washout of agonists, leaving (at maximal [OA]) some 20–60% of the Cl conductance persisting for  $\geq 20$  min. This persistent conductance was insensitive to PKI (150  $\mu$ M). Similar results were obtained with 5  $\mu$ M microcystin, also a 1 and 2A phosphatase inhibitor. Thus, an OA-sensitive phosphatase is essential for full dephosphorylation of the PKA-activated Cl conductance and, hence, at least two functionally distinct phosphorylation sites must be involved. Anion selectivity of the ISO-activated Cl conductance determined, with symmetrical anion concentrations, from the reversal potential shifts on replacing external Cl with test anions indicated the permeability sequence  $P_{Br} > P_{Cl} \geq P_I > P_F$ . With vigorous intracellular dialysis (1–4 M $\Omega$   $R_{access}$ ), the Fsk-induced Cl conductance was insensitive to bath application of diphenyl carboxylic acid (200  $\mu$ M,  $n = 1$ ), or of the stilbene disulfonic acid derivatives DIDS (100  $\mu$ M,  $n = 3$ ) or DNDS ( $\geq 200$   $\mu$ M,  $n = 2$ ), known blockers of some Cl channels. These biochemical, biophysical, and pharmacological properties are very similar to those of the epithelial Cl channel defective in cystic fibrosis (cystic fibrosis transmembrane conductance regulator). [Supported by NIH grant HL-14899 and the New York Heart Association.]

142. High-Field Access Channel to External Binding Sites of the Na/K Pump Demonstrated by Voltage Dependence of Electroneutral Na/Na and K/K Exchanges R. F. RAKOWSKI, PAUL DE WEER, and DAVID C. GADSBY, *Marine Biological Laboratory, Woods Hole, Massachusetts*

Previous measurements of stationary and transient pump currents have shown that, during forward Na/K cycling, interactions of external Na ions ( $Na_o$ ) and (at zero  $[Na]_o$ ) external K ions ( $K_o$ ) with the

sodium pump are voltage sensitive, but could not establish whether binding of extracellular ions, or some subsequent step, was voltage dependent. To make this distinction, we have examined the voltage sensitivity of electroneutral Na/Na and K/K exchanges in voltage-clamped, internally dialyzed squid giant axons by monitoring  $^{22}\text{Na}$  or  $^{42}\text{K}$  efflux over a range of voltages. Experimental conditions were designed to minimize fluxes not mediated by the pump. With saturating  $[\text{Na}]_i$  and at 400 mM  $[\text{Na}]_o$ , pump-mediated electroneutral Na/Na exchange flux was strongly voltage dependent near 0 mV, declining steeply at positive potentials but increasing to saturation at negative potentials. At lower  $[\text{Na}]_i$ , the flux-voltage curve was identical but shifted to more negative potentials. The apparent voltage insensitivity of Na/Na exchange-mediated  $^{22}\text{Na}$  efflux at sufficiently negative voltage, or saturating  $[\text{Na}]_o$ , argues that binding, but not dissociation, at the external Na sites is then the sole voltage-dependent process. The results indicate that the effective  $[\text{Na}]$  at the external binding locus varies with membrane potential, and so provide evidence for a channel-like structure within the external aspect of the Na/K pump molecule. The known competition between  $\text{Na}_o$  and  $\text{K}_o$  suggests that binding of these ions occurs from the same locus and, hence, that electroneutral K/K exchange should also show saturable voltage dependence. Preliminary measurements indeed demonstrate such a voltage sensitivity of K/K exchange. Thus, in the absence of Na and the presence of internal K, ATP, and  $\text{P}_i$ , and at subsaturating  $[\text{K}]_i$ , the  $\text{K}_o$ -activated, or  $\text{H}_2\text{DTG}$ -sensitive,  $^{42}\text{K}$  efflux increases in a saturable manner as the membrane potential is made more negative. [Supported by NIH grants NS-22979, NS-11223, and HL-36783.]

143. Regulation of PKA-activated Cl Conductance in Guinea Pig Ventricular Myocytes: Single-Channel Studies G. A. NAGEL, T.-C. HWANG,\* A. C. NAIRN,\* and D. C. GADSBY, *Laboratories of Cardiac/Membrane Physiology and Molecular and Cellular Neuroscience, The Rockefeller University, New York*

To examine single-channel currents underlying the protein kinase (PKA)-activated Cl conductance, we took advantage of the large membrane area in giant patches (Hilgemann, 1989, *Pflügers Arch.* 415:247) excised from sarcolemmal blebs on guinea pig myocytes, because an earlier study of cell-attached patches with conventional pipettes found the channels in only <5% of patches (Ehara and Ishihara, 1990, *Nature [Lond.]* 347:284). Pipettes contained high (~150 mM) Na- or NMG-Cl; the bath (cytoplasmic) solution usually had low [Cl] and could be exchanged rapidly. Solution pH was 7.4, and the temperature was kept at 25°C. Applying PKA catalytic subunit (c.s.; ~100 nM) with 0.5 mM MgATP induced in ~80% of patches, after a short delay, outward currents of unitary amplitude ~0.4 pA at  $V_{H} = 0$  mV. The single-channel currents remained outward for  $-60 \text{ mV} \leq V_{H} \leq +60$  mV, their amplitude increasing steadily with membrane depolarization. After raising cytoplasmic [Cl] to 144 mM, the magnitude of channel currents varied approximately linearly with  $V_{H}$ , reversed sign close to 0 mV, and gave a single-channel conductance of 10–12 pS. These channels were not activated by either PKA c.s. or ATP alone, nor by PKA c.s. plus ATP in the presence of PKA inhibitor peptide (PKI<sub>5-24</sub>, 4–100  $\mu\text{M}$ ). Once activated by PKA c.s. plus ATP, channel openings could be seen for >15 min after wash-out of PKA c.s., and were then insensitive to PKI<sub>5-24</sub>, indicating that dephosphorylation is very slow in excised patches. But the channels closed rapidly (time constant ~7 s) upon removal of ATP. Reapplication of ATP reopened the channels even more rapidly (time constant ~1 s, close to that for solution exchange). AMP-PNP or ADP could not reopen closed channels; GTP could, but less effectively than ATP. This requirement of hydrolyzable nucleoside triphosphate for channel opening, together with the small ohmic conductance in roughly symmetrical Cl solutions, suggests a strong resemblance between these Cl channels and CFTR (cystic fibrosis transmembrane conductance regulator), the cAMP-dependent, low-conductance Cl channel in epithelial cells. [Supported by NIH grants HL-14899 and HL-36783, the New York Heart Association and the C.F. Foundation.]

144. Signal Transduction Studies in *Escherichia coli* LINDA J. KENNEY and THOMAS J. SILHAVY, *Department of Molecular Biology, Lewis Thomas Laboratory, Princeton University, Princeton, New Jersey*

*Escherichia coli* regulate their outer membrane porins in response to changes in medium osmolarity. At low osmolarity, *ompF* is preferentially expressed, while at high osmolarity *ompC* is expressed. This

regulation is mediated by a pair of proteins, EnvZ, the inner membrane osmosensor, and OmpR, the response regulator. This sensor-regulator protein pair share homology with other two component regulatory systems in *E. coli* which mediate such diverse reactions as chemotaxis, nitrogen utilization, and phosphate regulation, for example. EnvZ is autophosphorylated from ATP and communicates with OmpR via a phosphotransfer reaction. EnvZ also acts as a phosphatase, stimulating dephosphorylation of phospho-OmpR and thereby controlling the concentration of cellular phospho-OmpR. Our current model for porin regulation is as follows: At low phospho-OmpR concentrations, *ompF* expression is activated. As phospho-OmpR concentrations increase, *ompF* is repressed and *ompC* expression is switched on. We are currently studying mutants of both EnvZ and OmpR that have altered enzyme activities in order to understand how these activities regulate porin gene expression. Our recent results on the importance of the phosphorylation-dephosphorylation cycle in signaling will be discussed. [Supported by NIH grant GM-55791.]

145. CFTR: An ATP Channel with Associated Transmembrane ATP Cycle E. H. ABRAHAM, S. T. ZAIDI, L. E. GERWECK, H. F. CANTIELLO, R. J. ARCECI, and D. M. JEFFERSON, *Department of Radiation Oncology and Renal Unit, Massachusetts General Hospital, Boston, Massachusetts; Dana Farber Cancer Institute and Children's Hospital, Boston, Massachusetts; and Department of Physiology, Tufts University School of Medicine, Boston, Massachusetts*

Cystic fibrosis (CF) has a characteristic defect in membrane chloride permeability associated with a mutation in amino acid 508 in the CFTR membrane protein. One of us (EHA) proposed that the CFTR might function as an ATP channel. This model predicts that the 508 mutation would result in altered CFTR ATP conductance. To test this hypothesis, we initially examined immortalized cultured cell lines derived from the airway and biliary epithelia from normal (NL) and CF homozygotes. Using a luciferin-luciferase assay, normal airway cells demonstrated an increased steady-state ATP fraction extracellularly compared with CF airway cells (NL =  $12.7 \pm 1.2\%$  vs. CF =  $3.3 \pm 0.5\%$ ;  $P < 0.001$ ,  $n = 3$ ). Immunofluorescent cell-surface staining revealed increased CFTR and GP170 in CF-derived biliary cells; consistent with this, normal and CF biliary cells show less difference in steady-state ATP release (NL  $7.3 \pm 0.9\%$  vs. CF  $5.3 \pm 0.6\%$ ,  $P = 0.05$ ,  $n = 3$ ). Mouse mammary carcinoma C1271 cells stably transfected with intact CFTR-cDNA (WT2), 508 mutated CFTR-cDNA (508), and mock-transfected (BPV) were a gift of Genzyme Corp. (Cambridge, MA). The steady-state fraction of total cellular ATP detected extracellularly was measured by luminometry; WT2:  $11.4 \pm 1.1\%$ ,  $n = 6$ ; 508:  $8.2 \pm 1.0\%$ ,  $n = 6$ ; BPV:  $5.3 \pm 0.8\%$ ,  $n = 6$ . CFTR-specific ATP release was determined as the difference of release rates from WT2 and BPV cells;  $4.8 \pm 0.5$  fmol ATP min<sup>-1</sup> cell<sup>-1</sup>. Extracellular ATP is reabsorbed via hydrolysis to ADP, AMP, and subsequently adenosine by action of ectoATPases and ecto-5' nucleotidases. The cycle is completed with uptake by Na<sup>+</sup>-adenosine cotransporters. The effect of extracellular adenylates on intracellular ionic content was investigated with electron probe microanalysis. The addition of extracellular adenosine and ATP results in a large decrease in intracellular chloride/phosphorus ratios in cells containing the intact or mutated CFTR but not in the mock-transfected cells. Intracellular potassium/phosphorus ratios remained constant in the presence of extracellular adenylate additions:

	Control	+Adenosine	+ADP	+ATP
BPV, no CFTR	$0.64 \pm 0.04$	$0.93 \pm 0.08$	$0.68 \pm 0.03$	$0.90 \pm 0.04$
508, mutant	$0.87 \pm 0.04$	$0.37 \pm 0.03$	$0.78 \pm 0.07$	$0.54 \pm 0.03$
WT2, intact	$0.79 \pm 0.03$	$0.39 \pm 0.03$	$0.52 \pm 0.03$	$0.46 \pm 0.03$

These results indicate that the CFTR is associated with ATP release, and that resultant extracellular adenylates can modulate cellular chloride content, probably through direct action on the CFTR.

**146. Intramolecular Fusion of the  $\alpha$  and  $\beta$  Subunits of the Na,K-ATPase: A Simplification for Cell-biological Analysis** MARK C. EMERICK,\* and DOUGLAS M. FAMBROUGH, *Department of Biology, The Johns Hopkins University, Baltimore, Maryland*

We have constructed coding DNA for a complete, single-subunit chicken Na,K-ATPase molecule by joining the amino terminus of the  $\beta_1$ -subunit to the carboxyl terminus of  $\alpha_3$  through a 17-residue linker. Expression of this construct in mammalian cells yields an unclipped ( $\sim 145$  kD)  $\alpha$ - $\beta$  fusion protein. The conformation-dependent monoclonal antibody (mAb)  $\beta_{21}$  binds to the expressed protein, demonstrating that the  $\beta$ -subunit domain can still fold properly while attached to the  $\alpha$ -domain (Tamkun and Fambrough, 1986, *J. Biol. Chem.* 261:1009). This suggests that the normal transmembrane topology of  $\beta$  is maintained in the fusion protein, with the segment corresponding to the  $\text{NH}_2$  terminus of  $\beta$  being cytoplasmic, and makes us optimistic that the  $\alpha$  domain is properly folded as well. The  $\alpha$ - $\beta$  protein is targeted to the surface membrane, further evidence for proper folding of  $\alpha$  as well as  $\beta$ . We are currently testing the ion-transport and ATPase functions of  $\alpha$ - $\beta$ . The single-subunit form simplifies the analysis of mutations in either the  $\alpha$  or  $\beta$  subunits. First, both  $\alpha$  and  $\beta$  mutants can be detected directly on the cell surface with antibodies to the chicken  $\beta$ -subunit without permeabilizing the membrane. Second, by preventing the formation of interspecies hybrids (Takevasu et al. 1987, *J. Biol. Chem.* 262:10733; Takevasu et al. 1988, *J. Biol. Chem.* 263:4347) between endogenous subunits from the host cell and modified avian subunits introduced by transfection, we have control of the exact subunit composition of the test molecules. We will use mutant single-subunit forms to screen for variants with disrupted targeting to the surface membrane and to investigate the role of ankyrin in directing Na,K-ATPase molecules to the basolateral membrane of confluent cultured epithelial cells. [Supported by NIH grant NS-23241.]

**147. cAMP-dependent Control of the Expression of GLUT5 in Caco-2 Cells** EDITH BROT-LAROCHE,\* LAHCEN MAHRAOUI,\* ELISABETH DUSSAULX,\* MONIQUE ROUSSET,\* and ALAIN ZWEIBAUM,\* *INSERM U178, Villejuif France*

The human cancer cell line Caco-2 expresses the Na/D-glucose cotransporter (SGLT1) and two members of the facilitative hexose transporter family, GLUT1 and GLUT5. The expression of GLUT5 which has recently been shown to be a fructose transporter (Burant et al. 1992, *J. Biol. Chem.* In press) was shown to be related to the differentiation of Caco-2 cells after confluence. The level of GLUT5 mRNA increases with the number of cell passages like other proteins involved in the absorption of sugars, i.e., sucrase-isomaltase and SGLT1. GLUT5 was shown to be located at the brush-border membrane of Caco-2 cells and adult human and fetal small intestine by means of both Western blot analysis and indirect immunofluorescence studies using an anti-rabbit antibody directed against the 15-amino acid COOH terminus peptide of GLUT5 deduced from the cDNA sequence (Mahraoui et al. 1992, *Am. J. Physiol.* In press). Treatment of Caco-2 cells by forskolin strongly increases the level of GLUT5 mRNA. This effect was not obtained with dideoxyforskolin, an analogue of forskolin that does not affect adenylate cyclase. The same effect was obtained with dibutyryl-cAMP. These results indicate that cAMP is involved in the metabolic control of the expression of GLUT5 in Caco-2 cells.

**148. Maltose Transport in *Salmonella typhimurium*: Large-Scale Purification, Nucleotide-binding Properties, and ATPase Activity of MalK** K. HÖNER ZU BENTRUP, C. WALTER, and E. SCHNEIDER, *Universität Osnabrück, Fachbereich Biologie/Chemie, Arbeitsgruppe Mikrobiologie, Osnabrück, Germany*

MalK, the membrane-associated nucleotide-binding component of the *Salmonella typhimurium* maltose transport system was overproduced from strain ES1(pCW14) upon temperature shift to 42°C. The overproduced protein was sequestered in inclusion bodies as revealed by electron microscopy. MalK was purified to homogeneity on a large scale by disrupting the cells with a passage through a Ribi press, solubilizing the inclusion bodies with 8 M urea, and subsequent chromatography on red

agarose. The purified MalK, as the wild-type MalK protein, could be covalently modified by 8-azido-ATP and was demonstrated to bind ATP with a dissociation constant of 150  $\mu$ M (Walter et al. 1992. *J. Biol. Chem.* In press). Furthermore, MalK exhibited an intrinsic ATPase activity which was stimulated by  $\text{Me}_2\text{SO}$  and inhibited by ADP. The preparation of milligram quantities of MalK, functional in binding and hydrolyzing ATP, from an overproducing strain by a one step procedure, enables us to begin with crystallization attempts.

149. Regulation of Swelling-induced [K-Cl] Cotransport in Dog Red Cells G. CRAIG COLCLASURE\* and JOHN C. PARKER, Department of Medicine, The University of North Carolina at Chapel Hill, Chapel Hill, North Carolina

[K-Cl] cotransport in dog red cells is activated by hypotonic or isotonic swelling, the latter achieved by the nystatin technique. In this respect dog red cells differ from those of the rainbow trout, in which hypotonic swelling activates chloride-independent K movements while isotonic swelling activates [K-Cl] cotransport (Motaïs et al. 1991. *Biochim. Biophys. Acta.* 1075:169). Swelling-induced [K-Cl] cotransport is demonstrable in resealed ghosts from dog red cells and correlates with cytosolic protein concentration rather than ghost volume. The critical ghost cytosolic protein concentration below which swelling-induced [K-Cl] cotransport is activated (300 g/kg wet weight) is close to that above which shrinkage-induced Na/H exchange occurs (Parker and Colclasure. 1991. *J. Gen. Physiol.* 98:881). The "set point" for both transporters can be shifted to a lower volume (higher cytosolic protein concentration) by incubating cells in 0.2–0.5 M urea. Thus, cells with a normal volume behave as if swollen when equilibrated with urea. Swelling-induced [K-Cl] cotransport in dog ghosts requires the incorporation of an ATP regenerating system that includes creatine phosphate, but added creatine kinase is unnecessary because dog red cells appear to possess this enzyme. An excess of ATP in the ghosts inhibits swelling-activated [K-Cl] cotransport, and this can be overcome by increasing the magnesium concentration in the cytosol. We conclude that dog red cells detect perturbations in their volume via the mechanism of macromolecular crowding, in which small changes in ambient protein concentration can influence the kinetics and thermodynamics of enzyme-catalyzed reactions (Minton. 1990. *Int. J. Biochem.* 22:1063). The signal is transmitted to the membrane transporters by processes that have not yet been described but probably involve changes in the phosphorylation state of regulatory proteins (Jennings and Schulz. 1991. *J. Gen. Physiol.* 97:799; Kaji and Tsukitani. 1991. *Am. J. Physiol.* 260:C178). The requirement for an ATP regenerating system in the resealed ghosts may be to activate the protein phosphatase-1 recently implicated in regulation of swelling-induced [K-Cl] cotransport (Shenolikar and Nairn. 1991. *Adv. Second Messenger Phosphoprotein Res.* 23:1).

150. Inhibitory Effects of Intracellular Ions on  $\text{Na}^+, \text{K}^+, \text{Cl}^-$  Cotransporter-mediated  $\text{Cl}^-$  Influx G. E. BREITWIESER, A. A. ALTAMIRANO, and J. M. RUSSELL, Johns Hopkins School of Medicine, Baltimore, Maryland; and University of Texas Medical Branch, Galveston, Texas

Influx mediated by the  $\text{Na}^+, \text{K}^+, \text{Cl}^-$  cotransporter requires the simultaneous presence of all three cotransported ions on the extracellular side of the membrane. Although the  $\text{Na}^+, \text{K}^+, \text{Cl}^-$  cotransporter is reversible, the kinetic effects of intracellular substrate ions on unidirectional influx cannot be predicted. We have previously shown that intracellular  $\text{Cl}^-$  inhibits cotransporter-mediated influx with an apparent  $K_{0.5}$  of 100 mM (1990. *Am. J. Physiol.* 258:C749). We pursued this finding by studying the effects of other intracellular ions on cotransporter-mediated influx in squid giant axons. Using intracellular dialysis, we are able to independently vary and control the intracellular concentrations of inorganic ions while measuring bumetanide-sensitive (B-S) unidirectional (not net) influx of  $^{36}\text{Cl}$ . Axons were dialyzed free of  $\text{Na}^+$  and  $\text{Cl}^-$  ( $[\text{K}^+]_i = 200$  mM) in order to prevent unidirectional cotransporter-mediated efflux. In one series of experiments, we tested the effects of intracellular  $\text{SCN}^-$  or  $\text{Br}^-$ . Both anions inhibit B-S influx in a concentration-dependent manner with the following  $K_{0.5}$ 's:  $\text{SCN}^- = 17$  mM;  $\text{Br}^- = 35$  mM. In addition, we found that 150 mM  $\text{NO}_3^-$  and  $\text{SO}_4^{2-}$  inhibited

B-S influx by 30–40%. In a second series of experiments, we varied  $[\text{Na}^+]_i$  at  $[\text{Cl}^-]_i = 0$  mM and  $[\text{K}^+]_i = 200$  mM. Intracellular  $\text{Na}^+$  inhibited B-S  $\text{Cl}^-$  influx in a concentration-dependent manner with low affinity. Thus, in the absence of at least one of the substrate ions, both intracellular  $\text{Cl}^-$  and  $\text{Na}^+$  can inhibit unidirectional B-S  $\text{Cl}^-$  influx. Other anions, including  $\text{SCN}^-$  (which does not support cotransport), can also inhibit cotransport influx. These data are consistent with either (a) partial occupancy of intracellular transport sites being inhibitory for cotransporter-mediated influx or (b) the existence of separate intracellular  $\text{Na}^+$  and/or  $\text{Cl}^-$  inhibitory binding sites. [Supported by NIH grant NS-11946.]

## INDEX TO AUTHORS OF ABSTRACTS

*Abstract number follows name*

- |                                 |                                   |
|---------------------------------|-----------------------------------|
| Abraham, E. H., 67, 68, 69, 145 | Brady, M. J., 53                  |
| Adair, B. D., 2                 | Brant, S. R., 107, 122, 138       |
| Adragna, N. C., 139             | Breitwieser, G. E., 150           |
| Agre, P., 127                   | Brot-Laroche, E., 147             |
| Alfonzo, M., 43                 | Browning, K. S., 73               |
| Allen, P., 43                   | Brugnara, C., 95                  |
| Alper, S. L., 95                | Brunger, A., 2                    |
| Altamirano, A. A., 150          | Budding, M., 76                   |
| Altenberg, G. A., 75            | Burdett, E., 108                  |
| Amara, J., 67                   | Caressa, M., 40                   |
| Ambudkar, S. V., 65, 127        | Cantiello, H. F., 67, 68, 69, 145 |
| Ani, M., 33                     | Cardarelli, C. O., 65             |
| Anwer, M. S., 82                | Carlson, D., 105                  |
| Arceci, R. J., 68, 69, 145      | Caron, M. G., 99                  |
| Arreola, J., 54                 | Carrasco, N., 31                  |
| Ausiello, D. A., 67             | Cass, C. E., 85                   |
| Babnigg, G., 53                 | Chalfant, M. L., 62               |
| Bankston, L. A., 13             | Chang, E. B., 53                  |
| Barthelson, R. A., 116          | Chang, N.-B., 36                  |
| Bashan, N., 108                 | Chen, D., 18                      |
| Bauer, P. J., 83                | Chipperfield, A. R., 110          |
| Bayle, D., 48                   | Chiu, M. L., 76                   |
| Bear, C. E., 21                 | Chow, D., 57                      |
| Beckwith, J., 3                 | Civan, M., 62                     |
| Beechev, R. B., 33, 34          | Cochran, M., 118                  |
| Begenisich, T., 54, 55          | Cohen, B. N., 120                 |
| Belcher, T. S., 124             | Colclasure, G. C., 149            |
| Belli, J., 75                   | Collins, F. S., 71                |
| Benz, E., Jr., 27, 80           | Cook, B. J., 132                  |
| Berkower, C., 11                | Cook, J. S., 98                   |
| Bernstein, M., 107              | Copello, J. A., 75                |
| Berson, H., 12                  | Counillon, L., 41                 |
| Biber, T. U. L., 124            | Coupaye-Gerard, B., 62, 63        |
| Bibi, E., 56                    | Cremaschi, D., 92                 |
| Biemesderfer, D., 27            | Croop, J. M., 76                  |
| Blakely, R. D., 12, 88, 99      | Culham, D. E., 94                 |
| Blank, M. E., 59                | Davidson, N., 120                 |
| Blazer-Yost, B. L., 119         | Davis, B. M., 59                  |
| Borgese, F., 25                 | Davis, J. P. L., 110              |
| Botta, G., 92                   | Dawson, D. C., 70, 71, 72         |
| Boulpaep, E. L., 103            | Dawson, M. A., 104                |
| Boyd, C. A. R., 140             | DeFelice, L. J., 88               |
| Boyd, D., 3                     | De Franceschi, L., 95             |

- Deisenhofer, J., 4  
Delpire, E., 112  
Devine, S. E., 77, 142  
De Weer, P., 142  
Diedrich, D. F., 59  
Doige, C. A., 136  
Donowitz, M., 25, 107, 130, 138  
Dousmanis, A. G., 141  
Drumm, M. L., 71  
Dussault, E., 147  
Dyer, J., 33  
Eisenberg, R., 18  
Ellison, M., 85  
Emerick, M. C., 146  
Emma, F., 100  
Emmerson, K. S., 94  
Engel, A., 6  
Engelman, D. M., 2  
Erdmann, A., 129  
Fafournoux, P., 25  
Fambrough, D. M., 146  
Ferro-Luzzi Ames, G., 19  
Fitz, J. G., 117  
Flanagan, J. M., 2  
Forbush, B., III, 27, 66, 79, 80  
Forte, J. G., 57  
Foskett, J. K., 96  
Foskett, K., 36  
Franchi, A., 41  
Frank, J. S., 26  
Freneau, R. T., Jr., 99  
Gadsby, D. C., 141, 142, 143  
Galloway, P. J., 98  
Gamba, G., 14  
Gatto, C., 86  
Gerweck, L., 68, 69, 145  
Goldstein, L., 134  
Gottesman, M. M., 65  
Gregory, R. J., 67, 126  
Griffith, J. K., 8  
Grinstein, S., 36  
Groelle, H., 46  
Gros, P., 20, 56  
Gruenert, D. C., 116  
Grüne, S., 82  
Guidotti, G., 13, 44, 68, 69, 135  
Gullans, S. R., 112  
Guma, A., 108  
Gunn, F. J., 8  
Gunn, R. B., 74  
Gurubhagavatula, S., 138  
Gyles, C., 94  
Haas, M., 27  
Hall, S. K., 64  
Hallows, K. R., 123  
Handler, J. S., 91  
Harper, A. A., 110  
Harris, H. W., 100  
Harris, S. P., 70  
Hart, P. J., 97  
Harvey, B. J., 37  
Haspel, H. C., 106  
Hazama, A., 38  
He, X., 49  
Hebert, S. C., 14  
Hediger, M. A., 15, 61  
Henderson, P. J. F., 8  
Hilgemann, D. W., 16, 26  
Hirayama, B. A., 39  
Hoefner, D. M., 59  
Hoffman, J. F., 115  
Hogue, D., 85  
Höner zu Bentrup, K., 148  
Horie, M., 141  
Horowitz, B., 97  
Hume, J. R., 97  
Hundal, H., 108  
Huppertz, B., 83  
Hwang, T.-C., 141, 143  
Ismail-Beigi, F., 114  
Jabs, E. W., 107  
Jander, G., 3  
Jefferson, D. M., 145  
Jennings, M. L., 32, 42  
Jensen, T. J., 21  
Johnstone, R. M., 47  
Kaback, H. R., 1, 56  
Kaji, D., 113  
Kaminsky, S., 31  
Kanai, Y., 15, 61  
Kanner, B. I., 30, 50  
Kartner, N., 21, 36  
Kavanaugh, M. P., 78  
Kennedy, H. J., 93  
Kenney, L. J., 144  
Kenyon, J. L., 97  
Keynan, S., 30  
Khademazad, M., 111  
Klein, J. D., 45  
Kleyman, T. R., 62, 63

- Klingenberg, M., 10  
 Klip, A., 108  
 Knauf, P. A., 123  
 Kopito, R. R., 9  
 Kramer, R., 68, 69, 76  
 Kronauge, J. F., 76  
 Kwon, H. M., 91  
 Landolt, C., 84  
 Lauf, P. K., 129, 139  
 Leblanc, G., 28  
 Lee, C. H., 109  
 Lee, C., 3  
 Lee, W.-S., 15, 61  
 Lelong, I., 65  
 Lemmon, M. A., 2  
 Lester, H. A., 120  
 Levesque, P. C., 97  
 Levine, S., 122, 130, 138  
 Levy, O., 31  
 Lewin, M., 48  
 Li, X., 107  
 Li, Z., 26  
 Liang, W.-J., 8  
 Lidofsky, S. D., 117, 118  
 Lieberman, M., 64  
 Liedtke, C. M., 52  
 Lin, G., 47  
 Linares, N., 43  
 Ling, V., 35, 109, 121  
 Liu, J. Y., 135  
 Liu, K., 74  
 Loe, D. W., 137  
 Loeb, J. N., 114  
 Logsdon, C. D., 70  
 Lombardi, M., 14  
 London, E., 5  
 Loo, D. D. F., 38  
 Lopez, J., 43  
 Lukacs, G. L., 36  
 Lyall, V., 124  
 Lytle, C., 27, 66, 79, 80  
 Mabjeesh, N., 30, 50  
 Mager, S., 120  
 Mahraoui, L., 147  
 Mairbäurl, H., 115  
 Maloney, P. C., 23  
 Mamelak, D., 94  
 Mansoura, M. K., 71  
 Marcus, D. C., 131  
 Martin, G. E. M., 8  
 Matsuoaka, S., 16  
 McCormick, J. I., 47  
 McDonald, T. P., 8  
 McGeoch, J. E. M., 44  
 McKinney, L. C., 51  
 McManus, M., 90  
 McSwine-Kennick, R. L., 53  
 Melera, P. W., 77  
 Melvin, J. E., 49  
 Meredith, D., 140  
 Meyer, G., 92  
 Michaelis, S., 11  
 Milanick, M. A., 86  
 Miyanoshita, A., 14  
 Montgomery, J. L. M., 138  
 Montrose, M., 122, 130  
 Moore, K., 12  
 Moran, A., 51  
 Morielli, A., 44  
 Morrison, R., 101  
 Motaïs, R., 25  
 Mrsny, R. J., 116  
 Muallem, S., 111  
 Mullins, J. G. L., 34  
 Musch, M. W., 53, 134  
 Naeve, J., 120  
 Nagel, G. A., 143  
 Nairn, A. C., 143  
 Namboodiripad, A. N., 32  
 Nicoll, D. A., 26  
 North, R. A., 78  
 O'Neill, W. C., 45  
 Oesterheld, D., 7  
 Ortiz, P. A., 106  
 Padan, E., 58  
 Pajor, A. M., 133  
 Parent, L., 17  
 Parker, J. C., 149  
 Pastan, I., 65  
 Payne, J., 27  
 Perez, C., 43  
 Perez, G. P., 55  
 Perry, P. B., 45  
 Philipson, K. D., 26  
 Piwnica-Worms, D., 76  
 Pontremoli, R., 40  
 Porta, C., 92  
 Post, M. A., 72  
 Pourcher, T., 28  
 Pouyssegur, J., 25, 41, 70, 107, 122, 130, 138

- Prat, A. G., 67, 68, 69  
Preston, A. S., 91  
Putnam, R. W., 89, 90, 101  
Quick, M., 120  
Rakowski, R. F., 142  
Ramjeesingh, M., 21  
Ramlal, T., 108  
Rasmusson, R. L., 64  
Ravel, J. M., 73  
Reisin, I. L., 67  
Reithmeier, R. A. F., 24, 84  
Renfro, J. L., 104  
Restrepo, D., 123, 128  
Reuss, L., 75  
Riccardi, D., 92  
Rich, D. P., 126  
Richards, N. W., 70  
Riordan, J. R., 21, 36  
Risso, S., 88  
Rivera, A., 40  
Robert, J. C., 48  
Roepe, P. D., 105  
Rohr, S., 87  
Rousset, M., 147  
Rudnick, G., 30, 102  
Ruetz, S., 9  
Russell, J. M., 150  
Salvador, C., 31  
Salzberg, B. M., 87  
Sardet, C., 25  
Scharschmidt, B. F., 117, 118  
Schneider, E., 148  
Schuldiner, S., 58  
Scott, H., 105  
Sen, A. K., 66  
Seneveratne, T., 68, 69  
Shapiro, A. B., 121  
Sharom, F. J., 136, 137  
Shen, B.-Q., 116  
Sheppard, D. N., 126  
Shetty, M., 114  
Shiga, N., 131  
Shirazi-Beechey, S., 33, 34  
Shrode, L. D., 90, 101  
Sigal, E., 116  
Silhavy, T. J., 144  
Skach, W., 116  
Smit, L. S., 71  
Smith, A. E., 126  
Smith, B. L., 127  
Smith, C. D., 39  
Smith, P., 74  
Snyder, R. B., 128  
Soltoff, S. P., 81  
Soumarmon, A., 48  
Souza, D. W., 126  
Spires, S., 34  
Starke, L. C., 32  
Steer, B., 94  
Strange, K., 100, 101  
Strong, T. V., 71  
Strumwasser, F., 46  
Suh, Y.-J., 30  
Supplisson, S., 38  
Tabak, L. A., 49  
Thomas, R. C., 93  
Timmer, R. T., 73  
Torchia, J., 66, 79  
Traxler, B., 3  
Treutlein, H., 2  
Tse, C.-M., 107, 122, 138  
Tse, M., 25, 130  
Turk, E., 38  
Turner, T. J., 81  
Uchida, S., 91  
Uhler, M. D., 71  
Urbach, V., 37  
Vanah, P., 52  
Vikstrom, K., 114  
Villereal, M. L., 53  
Wakabayashi, S., 25  
Walker, S., 107, 122  
Wall, S. C., 102  
Walmsley, A. R., 8  
Walter, C., 148  
Wang, K., 125  
Wangemann, P., 131  
Wasmuth, J., 107  
Weber, M. R., 103  
Weill, L., 73  
Wei, L.-Y., 105  
Wells, R. G., 15  
Welsh, M. J., 22, 126  
Whisenant, N., 111  
Widdicombe, J. H., 116  
Wilkinson, A. D. J., 71  
Willis, J. S., 60  
Wilson, T. H., 23  
Wondergem, R., 125  
Wong, D., 96

- |                               |                      |
|-------------------------------|----------------------|
| Wood, J. M., 94               | Yun, C.-H. C., 138   |
| Wright, E. M., 17, 29, 38, 39 | Zaidi, S. T., 145    |
| Wu, X., 49                    | Zani, M. L., 28      |
| Xie, M.-H., 117, 118          | Zeidel, M. L., 127   |
| Xu, J.-C., 27, 80             | Zerbini, G., 40      |
| Xu, W., 60                    | Zhang, J., 2, 64, 65 |
| Yamauchi, A., 91              | Zhang, J.-T., 35     |
| Yost, R. W., 119              | Zhang, Y., 75        |
| You, G., 61                   | Zhu, T., 80          |
| Yu, X.-H., 136                | Zweibaum, A., 147    |